Order Number 8822417

Design, synthesis, conformation and biological activities of cyclic α-melanotropin and related compounds

Ahmed, Al-Obeidi Fahad, Ph.D.

The University of Arizona, 1988

U·M·I
300 N. Zeeb Rd.
Ann Arbor, MI 48106

PLEASE NOTE:

In all cases this material has been filmed in the best possible way from the available copy. Problems encountered with this document have been identified here with a check mark __√__.

1. Glossy photographs or pages _____
2. Colored illustrations, paper or print _____
3. Photographs with dark background _____
4. Illustrations are poor copy _____
5. Pages with black marks, not original copy __√__
6. Print shows through as there is text on both sides of page _____
7. Indistinct, broken or small print on several pages __√__
8. Print exceeds margin requirements _____
9. Tightly bound copy with print lost in spine _____
10. Computer printout pages with indistinct print _____
11. Page(s) _____ lacking when material received, and not available from school or author.
12. Page(s) _____ seem to be missing in numbering only as text follows.
13. Two pages numbered _____. Text follows.
14. Curling and wrinkled pages _____
15. Dissertation contains pages with print at a slant, filmed as received __✓__
16. Other _____

_____

_____

DESIGN, SYNTHESIS, CONFORMATION AND BIOLOGICAL ACTIVITIES OF CYCLIC α-MELANOTROPIN AND RELATED COMPOUNDS

by

Al-Obeidi Fahad Ahmed

A Dissertation Submitted to the Faculty of the

DEPARTMENT OF CHEMISTRY

in Partial Fulfillment of the Requirements

For the Degree of

DOCTOR OF PHILOSOPHY

in the Graduate College

THE UNIVERSITY OF ARIZONA

1988

THE UNIVERSITY OF ARIZONA
GRADUATE COLLEGE

As members of the Final Examination Committee, we certify that we have read the dissertation prepared by Al-Obeidi Fahad Ahmed Danouk

entitled DESIGN, SYNTHESIS, CONFORMATION AND BIOLOGICAL ACTIVITIES OF CYCLIC α-MELANOTROPIN AND RELATED COMPOUNDS

and recommend that it be accepted as fulfilling the dissertation requirement for the Degree of Ph.D.

Dr. Victor J. Hruby	Victor J. Hruby	12/4/87 Date
Dr. Henry K. Hall	Henry K. Hall	12/4/87 Date
Dr. Michael Barfield	Michael Barfield	12/4/87 Date
Dr. Cornelius Steelink	Cornelius Steelink	12/4/87 Date
Dr. Michael Cusanovich		Date

Final approval and acceptance of this dissertation is contingent upon the candidate's submission of the final copy of the dissertation to the Graduate College.

I hereby certify that I have read this dissertation prepared under my direction and recommend that it be accepted as fulfilling the dissertation requirement.

Victor J. Hruby
Dissertation Director

12/4/87
Date

STATEMENT BY AUTHOR

This dissertation has been submitted in partial fulfillment of requirements for an advanced degree at The University of Arizona and is deposited in the University Library to be made available to borrowers under rules of the Library.

Brief quotations from this dissertation are allowable without special permission, provided that accurate acknowledgment of source is made. Requests for permission for extended quotation from or reproduction of this manuscript in whole or in part may be granted by the head of the major department or the Dean of the Graduate College when in his or her judgment the proposed use of the material is in the interests of scholarship. In all other instances, however, permission must be obtained from the author.

SIGNED: Jehad al-Obeidi

PREFACE

This work was supported in part by National Science Foundation Grant No. All optically active amino acids are of L variety unless otherwise stated. Symbols and abbreviations are in accord with the recommendations of the IUPAC-IUB Commission on Biochemical Nomenclature.

The author expresses highest gratitude to Dr. Victor J. Hruby, Dr. Mac E. Hadley and Dr. Tomi K. Sawyer for their friendship, enthusiastic support and keen insights which they have contributed to him during this research project.

The author thanks Dr. Henry K. Hall, Dr. Victor J. Hruby, Dr. Michael Barfield, Dr. Cornelius C. Steelink and Dr. Richard S. Glass and Dr. Michael A. Cusanovich for their support and advice in his graduate study. The author thanks all graduate students and post doctorals in Victor J. Hruby's laboratory during the period 1977 to 1988 for their excellent cooperation and encouragement. The author thanks his family for their encouragement. Also, the author would like to thank Dr. Hashim A. Yousif and Dr. Kais T. Almarzouk for their excellent friendship.

The author thanks the University of Arizona Society of Sigma Xi for the Travel Scholarship (1980) granted to him. The author thanks Mr. Constantin Job for his excellent help in the NMR and the computer works. The author thanks Ms. Karen Burgan for the excellent typing of this dissertation. Finally, the author expresses special gratitude to his parents and his brothers and sister for their encouragement and help.

TABLE OF CONTENTS

TABLE OF CONTENTS--Continued

TABLE OF CONTENTS--Continued

LIST OF TABLES

LIST OF TABLES--Continued

LIST OF ILLUSTRATIONS

LIST OF ILLUSTRATIONS--Continued

ABSTRACT

This research initiated an investigation of the structural relationships between melanocyte stimulating hormone (α-MSH) and its melanin dispersion on lizard (Anolis carolinensis) and frog (Rana pipiens) skins bioassays as representing models for mammalian and amphibian melanocytes, respectively.

From previous extensive structure-activity relationships of α-MSH together with the theoretical modeling we were able to design a group of linear and cyclic peptides related to "4-10" fragment analogues of α-MSH.

The solid phase synthesis of α-MSH and its related analogues using the p-methylbenzhydrylamine resin was accomplished. The C-terminal carboxamide and the N-terminal acetylamide were maintained in all peptides synthesized. The cyclic peptides were prepared in solution phase using the linear peptides generated by solid phase. All the cyclization were done by using the hydrochloride salts of the peptide and DMF as a solvent with diphenylphosphoryl azide (DPPA) as a coupling reagent in the presence of K_2HPO_4 as a base. The yeilds of the cyclic peptides were in the range of 30-40%.

In all the synthesized peptides the replacement of D-Phe^7 with L-Phe^7 causes a reduction in the potency of the peptide on lizard or frog skins bioassays. Also, the reduction or increase in ring size in the cyclic peptide from 23 membered ring diminishes the biological effect of the peptide under testing.

CHAPTER ONE

INTRODUCTION

α-MSH is a tridecapeptide (Ac-Ser-Tyr-Ser-Met-Glu-His-Phe-Arg-Trp-Gly-Lys-Pro-Val-NH_2) which is secreted by the pars intermedia lobe of the pituitary gland. Since its discovery at the beginning of this century (Smith, 1916; Allen, 1916) and its full characterization in the mid-fifties (Lerner et al., 1955; Benfey et al., 1955; Porath et al., 1955; Harris et al., 1957), it has been the subject of extensive studies (Hruby et al., 1984; Cody, et al., 1988). α-MSH shares the first thirteen amino acids with adrenocorticotropic hormone (ACTH). Recently it has been shown that α-MSH and related peptides are derived from a large molecular weight precursor protein, pro-opiomelanocortin (Herbert et al., 1980; Mains et al., 1980) (POMC) in vertebrate pituitary and hypothalamus. All the peptides related to α-MSH isolated thus far from the pituitary gland show conservation of the sequence Met-Glu-His-Phe-Arg-Trp-Gly in their active core structure throughout evolution (Hruby.et al., 1984). In an attempt to correlate the structure of α-MSH to its biological activity, classical structure-activity relationships have been carried out by numerous workers (Hruby et al., 1984). Results of these studies showed that the minimal active sequence for this peptide hormone is the tetrapeptide His-Phe-Arg-Trp (Hruby et al., 1987). Another approach in studying the relationship between the hormone structure and its biological activity is through the correlation of the 3-dimensional structure to the biological activity

Several techniques have been used to understand the topographical structure of α-MSH and its effect on the biological response (Sawyer, 1981; Cody, 1985 and references therein), but the conclusions from these studies are still unclear. Some workers believed that α-MSH has a β-turn type of conformation centered around the Phe^7 amino acid residue. This hypothesis was tested by synthesizing an analogue where L-Phe was substituted by D-Phe as a β-turn stabilizer. The result of that study showed a 60-fold enhancement in the biological potency of the resulting analogues (Sawyer et al., 1980). Another approach to test the hypothesis was by stabilization of the β-turn through side chain to side chain pseudoisosteric cyclization via a disulfide bridge (Hruby, 1982). This molecule was prepared by replacing the Met^4 and Gly^{10} by Cys residues and closing the disulfide. The resulting analogue was a superpotent agonist in the frog skin bioassay (Sawyer et al., 1982). Extensive studies were carried out along these lines to correlate the primary, secondary and tertiary structure of MSH to its biological activity (Wilkes, 1985; Cody, 1985). NMR and CD studies suggested that these compounds had no distinct secondary or tertiary structure with the possibility of β-like conformations (Cody, 1985; Sugg et al., 1986; Ikeda et al., 1971, Higuchi et al., 1981; Rawson et al., 1982).

As previously indicated, conformational studies led to the synthesis of cyclic [Cys^4, Cys^{10}]α-MSH and its fragment analogues. Conformational calculations were carried out on three of these cyclic analogues: Ac-[Cys^4, Cys^{10}]α-MSH_{4-10}-NH_2, Ac-[Cys^4, Cys^{10}]α-

MSH_{4-13}-NH_2 and Ac-[Cys^4, Cys^{10}]α-MSH_{4-13}-NH_2. The same type of calculations were performed on α-MSH. The results of these calculations have suggested that the conformation of α-MSH and its superagonist analogues is either a β-turn or a helical form (Nikiforovich et al., 1981; Nikiforovich et al., 1984). All these studies were made using the rigid body approach (Ramachandran and Sasisekharan, 1968; Scheraga, 1968) in which the bond lengths and angles were kept "frozen" at their "equilibrium" values. Furthermore, since the peptide bond has a rotational barrier of ~20 Kcal/Mol owing to its partial double-bond character, it was assumed that this torsion angle could be kept fixed at 180°, corresponding to a trans conformation. Finally, in these calculations the possible side-chains conformations were assumed to be either gauche or trans (±60, 180, respectively), and selection of conformers was based on using differences of 10 Kcal/Mol as a criterion for keeping or neglecting that conformer.

Peptides such as α-MSH are not static, fixed structures, but rather dynamic entities. Thus, they constantly vibrate with characteristic frequencies and undergo conformational fluctuations and transitions (Hagler et al., 1985). It has been hypothesized that the dynamic properties of peptide hormones are integrally involved in the transduction of the biological messages (Hruby and Mosberg, 1982; Hruby and Hadley, 1986). Also, these molecules exist in a variety of media which may effect their conformations to a considerable extent. Finally, entropic contributions to the free energy, which are not

considered in rigid-geometry calculations, may be very important in determining the conformational equilibria. These facts have led to new approaches to study peptide systems, including the use of molecular dynamics (Karplus and McCammon, 1981) and Monte Carlo (Hagler and Moult, 1978) techniques.

In this study, we have used synthetic, biophysical and theoretical approaches in an integrated manner to develop analogues of α-melanotropin with high agonistic potency and specificity. These results from these studies may provide a compound or compounds with a potential medical applications for treatment of certain diseases (Hadley et al., 1987).

CHAPTER TWO

DESIGN AND SYNTHESIS OF LINEAR POTENT ANALOGUES OF α-MELANOTROPIN MODIFIED IN POSITIONS 5 AND 10

The ability of tadpoles, frogs, chameleans, certain fishes, and other animals to change color is under the control of the melanocyte-stimulating hormone (α-MSH). The existence of substances in the pituitary that affect skin darkening in frogs and tadpoles was discovered in the early part of this century (Smith, 1916; Allen, 1916). The isolation, structure, determination, synthesis and bioassay of α-MSH were accomplished in the 1950's by several workers (Lerner, et al., 1955; Benfey, et al., 1955; Porath, et al., 1955; Root, 1956; Lee et al., 1956; Harris, 1959; Harris, et al., 1957; Lerner, et al., 1960; Shizume et al., 1954; Hadley, et al., 1975). They defined the structure of α-melanotropin as the tridecapeptide (Ac-Ser-Tyr-Ser-Met-Glu-His-Phe-Arg-Trp-Gly-Lys-Pro-Val-NH_2), which represents the first thirteenth amino acids of adrenocorticotropin hormone (ACTH). Recently it has been shown that α-MSH and related peptides are derived from a large molecular weight precursor protein, pro-opiomelanocortin (Herbert, et al., 1980; Mains et al., 1980) (POMC) in the vertebrate pituitary and hypothalamus. Invesitigation of all of the peptides related to α-MSH which are isolated from the pituitary gland showed a conservation of the sequence Met-Glu-His-Phe-Arg-Trp-Gly in their active core structure throughout evolution (Hruby et al., 1984). This heptapeptide sequence

has been suggested to be the active site of the hormones that are generated from the biological processing of the POMC in the biological system (Hofmann, et al., 1974; van Nispen, et al., 1982).

Based on the structural relationship to the biological potency of α-MSH and its analogues and fragments (Hofmann, et al., 1974; van Nispen, et al., 1982) using in vitro frog skin bioassay system (Shizume, et al., 1954), the active site of α-MSH has been shown to be the heptapeptide in position 4 to 10 which includes Met-Glu-His-Phe-Arg-Trp-Gly. This fragment (α-MSH_{4-10}) has been synthesized and tested for its melanocyte expanding activity in frog skin and showed to be a weak agonist in comparison to the native hormone (Hruby et al., 1984). The effects of amino acid exchange in positions 5 (Glu) and 10 (Gly) were not fully and systematically investigated (Medzihradszky, 1982). From our previous studies and other investigations (Medzihradszky, 1982; Hruby, et al., 1984) it was found that replacement of Met^4 with Nle in the active site heptapeptide gave a potent analogue of α-MSH. In addition, substitution of Phe in position 7 with its enantiomer D-Phe resulted in a more potent analogue with prolonged activity in both systems of bioassay (frog and lizard skins bioassay) (Sawyer, 1981; Cody, 1985; Wilkes, 1985). Table I shows the summary of some of the results of these studies.

These structural-activity relationships showed two important results. Firstly, the replacement of the Met amino acid with its oxidizable side chain with the oxidatively stable amino acid Nle, which is also an isosteric for Met, resulted in about a 10 fold enhancement of

Table I

Selective Fragments of α-MSH and Their Biological Activities on Frog (Rana pipiens) Skin and Lizard (Anolis carolinensis)

Peptide	Relative Potency		Reference
	Frog	Lizard	
1. α-MSH	1.0	1.0	
2. Ac-[Nle^4, D-Phe^7]-α-MSH$_{1-13}$NH$_2$	60.0	5.0	a,b
3. Ac-α-MSH$_{4-10}$NH$_2$	0.0003	0.004	c
4. Ac-[Nle^4]-α-MSH$_{4-10}$NH$_2$	0.002	0.06	c
5. Ac-[Nle^4]-α-MSH$_{4-11}$NH$_2$	0.002	1.0	d
6. Ac-[Nle^4, D-Phe^7]-α-MSH$_{4-10}$NH$_2$	0.02	10.0	c
7. Ac-[Nle^4, D-Phe^7]-α-MSH$_{4-11}$NH$_2$	0.16	8.0	d

a Hadley, et al., 1981

b Sawyer, et al., 1980

c Sawyer, et al., 1982

d Wilkes, et al., 1983

the biological potency of the peptide fragment. Secondly, replacement of L-Phe in position 7 with D-Phe and adding Lys in position 11 further enhances the biological potency of the α-MSH fragment. To further investigate the structure-potency relationship of α-MSH_{4-10} fragments, we have systematically investigated the structural requirement for melanotropic activity of a number of α-MSH_{4-10} analogues with emphasis on the effect of substitutions in positions 5 and 10. In this section we will report the synthesis of these α-MSH_{4-10} fragments; some of them display a potency higher than the native hormone in a number of bioassay systems.

Results and Discussion

The Ac-α-MSH_{4-10}-NH_2 analogues listed in Table II were synthesized by solid-phase peptide synthetic methods (Stewart, et al., 1976; Hruby, et al., 1977; Hruby, et al., 1973) using p-methylbenzhydrylamine resin (pMBHA) as a solid support (Yang, et al., 1980), and purified by methods related to those used previously for α-melanotropin and analogues (Yajima, et al., 1974; Huntington, et al., 1970). The details of the synthetic methods are given in the Experimental Section, and the analytical results are given in Tables III and IV. The *in vitro* biological activities of the peptides were determined in both the frog (*Rana pipiens*) (Shizume, et al., 1954) and lizard (*Anolis carolinensis*) skin assays (Huntington, et al., 1970) over the full range of the log dose-response curves for the peptides. The results of the

latter studies are shown in Figure I, and the relative potencies for both assays are summarized in Table V. Previously, it was reported that the addition of Lys-11 to the Ac-[Nle^4, D-Phe^7]-α-MSH$_{4-10}$-NH$_2$ peptide resulted in an analogue with about one-tenth the potency of the native hormone α-MSH in frog skin bioassay (Wilkes, et al., 1983) and about 8 times the potency of the native hormone in lizard skin assay. Also, it has been shown that replacement of Glu in position 5 with either Gln or Gly amino acids resulted in equipotent or slightly less potent α-MSH analogues (Medzihradszky, 1982; Hruby, et al., 1984). Replacement of Gly in position 10 by β-alanine reduces the potency of the peptide (Medzihradszky, 1982).

However, in this study we found that the exchange of Glu in position 5 with the shorter side chain amino acid aspartic acid causes slight enhancement in the biological potency, as in comparison of peptides 2, 6, 9 with peptides 3, 7, 10 in Table V. In addition, exchanging Gly in position 10 with the basic amino acids Lys, Orn, Dab, or Dpr gave analogues with enhanced activity in comparison to the native hormone, α-MSH or Ac-[Nle^4, D-Phe^7]-α MSH$_{4-10}$-NH$_2$ (see Table V). The effect of Glu substitution with Asp is more pronounced in compounds 2 and 3 (Table I). This result may be attributed to the potentiation of the effect of shorter side chain amino acids in the full length hormone α-MSH. The synthesis of compounds 2, 3, 4 and 5 was done to complete the comparison, and to study the effect of exchange of amino acids in position 5, 10 and 11. The biological potency of these four compounds clearly showed the effect of those sites (5 and 10) on the biological

response which resulted in compounds with up to 9 times the potency of the native α-MSH as in compound 3. In addition to the enhanced potency, some of these analogues showed prolonged activity in the frog skin and lizard skin bioassays. There is a clear effect of the first three N-terminal amino acids on the prolongation of these peptides in lizard skin bioassay, as in compounds 2 and 3 (Table II). This phenomenon could be related to the enhanced hydrophilicity of the peptides because of the hydrophilic side chains of these three amino acids (Ser-Tyr-Ser). This phenomenon was not noticed in all previous studies.

In previous work (Hruby, et al., 1984) it had been reported that the Ac-[Nle^4, D-Phe^7]α-MSH_{4-10}-NH_2 was prolonged on lizard but not on frog. This property of prolongation on one system and not on the other is very interesting because it had been shown that the response in lizard skin bioassay goes in parallel with the response in the melanoma adenylate cyclase system (Hruby, et al., 1984). However, the latter two systems appear to have quite similar structural requirements for hormone-receptor binding and signal transduction, at least based on our results and the previous work done by other groups (Medzihradszky, 1982; Hruby, et al., 1984).

Substitution of Gly^{10} in compound 6 by Lys^{10} resulted in an analogue (7) with one-tenth the potency of α-MSH in the frog skin assay, but 8 times more potency in the lizard skin assay. There was no prolongation of activity in either bioassays. This pattern of reactivity was retained in the series of compounds 7 through 12 (Table II) with

clear effect of enhancement of the potency upon substitution of Glu^5 with Asp^5 and Lys^{10} with shorter side chain basic amino acids Orn, Dab, and Dpr. The effect of the length of the side chain of the basic amino acids on the biological activity is manifested in going from Lys (4 CH_2[5]) to Dpr (1 CH_2) with the maximum at compound 11 where we have potentiation of both effects of Asp at 5 position with Dab (2 CH_2[4]) in position 10. Compound 11 has equipotency to α-MSH in the frog assay but is 50 times more potent in the lizard assay system.

This tremendous change in biological potency cannot be explained on the basis of the lipophilicity-hydrophilicity of this analogue since it has the same residual charge in comparison with the other homologues. The possible reason for such a high potency for 12 may be due to the topological relationships of the side chain groups in such a way that it forms a strong ionic bond between basic side chain of Dab^{10} (NH_2) with the acidic side chain of Asp^5 (COOH). This ionic bonding may force the molecule to assume a proper topological conformation which fits the peptide-hormone receptor. Modification in position 7 by replacement D-Phe with L-Phe gave an analogue with reduced potency in confirmation with the previously reported effect of this substitution on the potency of α-MSH and its analogues (Medzihradszky, 1982; Hruby, et al., 1984). As a result, compounds 14 and 15 (Table II) were less active than their D-Phe^7 analogues with a noticeable difference of prolongation in the frog skin assay. These results confirmed what has previously been reported by our laboratory (Sawyer, et al., 1982). In conclusion, this systematic structure-function investi-

gation provides the first extensive correlation between stereostructural and amino acids replacement to comparative melanotropic potency within the primary active site of α-MSH (Met-Glu-His-Phe-Arg-Trp-Gly). The potency range for the active-site heptapeptide analogue of α-MSH tested was four orders of magnitude. Structural modification at the Glu^5 and Gly^{10} of Ac-[Nle^4, D-Phe^7]α-MSH_{4-10}-NH_2 resulting in markedly increased (>45-fold) melanotropic potency for the resultant peptide, Ac-[Nle^4, Asp^5, D-Phe^7, Dab^{10}]α-MSH_{4-10}-NH_2. Furthermore, substitution of Gly-10 by basic amino acids (Lys, Orn, Dab, Dpr) resulted in more potent analogues in both lizard and frog skin bioassays. These results are very important for the future use of these analogues as drug carriers to target melanoma cells. Conjugation of drugs active against melanoma cells using these acidic or basic side chains may prove very important for medicinal use of α-MSH and its analogues (Hruby, et al., 1984). Also the length of side chain groups in position 10 is very important for the biological activity of these α-MSH_{4-10} analogues. Further studies in this direction are under investigation in our laboratory.

Experimental Section

General Methods. Amino acid analysis was performed on a Beckman Model 120C amino acid analyzer after acid hydrolysis in sealed vials, using either 4M methanesulfonic acid or 6 M HCl:propionic acid containing 0.5% phenol, at 110°C for 22 h in vacuo. Ascending TLC was

performed on Baker 250 nm analytical silica gel glass plates in the following solvent systems: (A) 1-butanol/acetic acid/pyridine/water (5:5:1:4); v/v (B) 2-propanol/25% aqueous ammonia/water (3:1:1) v/v; (C) ethyl acetate/pyridine/acetic acid/water (5:5:1:3) v/v; (D) 1-butanol/acetic acid/water (4:1:5, upper phase) v/v peptides were visualized by ninhydrin, fluorescamine, and iodine vapor. Optical rotations were performed at the mercury green line (546 nm) in a Rudolph Research Polarimeter (autopol). Carboxymethyl cellulose (CMC) cation exchange fine mesh resin with 0.72 meg/g capacity was purchased from Sigma Chemical Co., St. Louis, MO. HPLC was performed on Perkin-Elmer series 313 chromatograph, equipped with a Model LCI 100 laboratory computing integrator using a Vydac 218TP15-16 C_{18}RP column (25 cm x 4.6 mm for analytical and 25 cm x 25 mm for preparative purposes), with a 0.1% trifluoroacetic acid/CH_3CN gradient (80:20 to 50:50) over 20 minutes with flow rate of 3 mL/min. Peaks were monitored at 223 nm and 280 nm. HPLC solvents (Burdick and Jackson) were purchased from American Scientific Products (Phoenix, AZ.). In the solid phase synthesis, N^{α}-Boc protected amino acids were N^{α}-deprotected with 48% TFA in methylene chloride containing 2% anisole for 5 and 20 min each. After completion of coupling of all amino acids, the amino terminal end of each peptide was acetylated with a 6-fold excess of N-acetylimidazole or a 2-fold excess of a 1:1 mixture of acetic anhydride: pyridine in methylene chloride. The protected peptides were deprotected and removed from the resin with anhydrous liquid HF (10 mL/g of peptide resin) containing 10% anisole and 6% of 1,2-dithioethane

(Hruby, et al., 1977; Mitsueda, 1982) at 0°C for 30-45 min. After removal of the HF in vacuo, the peptides with the resin were washed with ether or ethyl acetate (3 x 30 ML) and the free peptide extracted with 30% aqueous acetic acid and lyophilized. The finished analogues were purified by ion-exchange chromatography on CMC; the eluting peptides were monitored at 280 nm.

p-Methylbenzhydrylamine Resin. The synthetic resin was prepared and purified according to the procedure previously reported (Hruby, et al., 1977). All syntheses were performed on a semiautomatic peptide synthesizer, or on a Vega Coupler Model 1000 or 250 Peptide Synthesizer (Vega Biochemicals, Tucson, AZ).

Ac-[Nle^4, D-Phe^7, Lys^{10}, Gly^{11}]α-MSH_{1-13}-NH_2, Ac-Ser-Tyr-Ser-Nle-Glu-His-D-Phe-Arg-Trp-Lys-Gly-Pro-Val-NH_2 (2). The title compound was prepared by coupling N^{α}-Boc-Val to p-methylbenzhydrylamine resin (2.0 g pMBHA resin, 0.7 mmol NH_2/g of resin) using a 3 fold excess of the amino acid and solid-phase methods of peptide synthesis. After 90 min the resin was washed with dichloromethane, neutralized and the terminal amino group was acetylated with the acetic anhydride-pyridine mixture. No reactive amino groups on the resin were detected by the ninhydrin test (Kaiser, et al., 1970) after 30 min. A cycle for coupling of each amino acid residue into the growing peptide chain consisted of the following: 1) Washing with four 30-mL portions of CH_2Cl_2, 2 min/wash; 2) Cleavage of the Boc group by 30 mL of 48% trifluoroacetic acid in dichloromethane containing 2% anisole, one

treatment for 5 min, and a second for 20 min; 3) Washing with four 30-mL portions of dichloromethane, 2 min/wash; 4) neutralization by addition of two 30-mL portions of 10% diisopropylethylamine in dichloromethane and shaking for 2 min each; 5) Washing with four 30-mL portions of dichloromethane, 2 min/wash; 6) Addition of 3 fold excess of the N^{α}-Boc amino acid derivative (in this case 2.1 mmol) in 5 mL of dichloromethane, 2.4 mL of N-hydroxybenzotriazole of 1 mmol/mL in DMF (except in the case of N^{α}-Boc-N^{im}Tos-His), followed by 2.4 mL of DCC of 1 mmol/mL solution of DCC in DMF. The mixture then shook for 2-3 h (in case of Trp, Arg, and His, DMF was used as the coupling solvent); 7) After completion of the coupling (ninhydrin negative) washing with three 30-mL portions of dichloromethane, 2 min/wash; 8) Washing with three 30-mL portions of 100% ethanol, 2 min/wash; 9) Washing with four 30-mL portions of dichloromethane, 1 min/wash. The protected peptide resin corresponding to the title compound was obtained after stepwise coupling of the following N^{α}-Boc amino acids (or derivatives) was performed (in order of addition): N^{α}-Boc-Pro, N^{α}-Boc-Gly, N^{α}-Boc-Lys(N^{ε}-2-ClZ); N^{α}-Boc-Trp(N^{i}-For), N^{α}-Boc-Arg, N^{α}-Boc-D-Phe, and N^{α}-Boc-His(N^{im}-Tos). The resulted Boc-His(N^{im}-Tos)-D-Phe-Arg-(N^{g}-Tos)-Trp(N^{i}-For)-Lys(N^{ε}-2-ClZ)-Gly-Pro-Val-p-MBHA resin was divided into four portions. One-quarter (1.0 g, ~ 0.35 mmol) of the protected peptide-resin was converted to the protected title peptide resin after coupling N^{α}-Boc-Glu(γ-Bzl), N^{α}-Boc-Nle, N^{α}-Boc-Ser(O-Bzl), N^{α}-Boc-Tyr(O-2 Brz); N^{α}-Boc-Ser(O-Bzl). After coupling the last amino

acid, the N^{α}-Boc protecting group was removed, the amino group neutralized, and the protected peptide was N^{α}-acetylated with a 10-fold excess of N-acetylimidazole in 20 mL of dichloromethane and the resulting protected peptide resin, Ac-Ser-(O-Bzl)-Tyr(O-2-Brz)-Ser-(O-Bzl)-Nle-Glu(γ-Bzl)His(N^{im}-Tos)-D-Phe-Arg(N^{g}-Tos)-Trp(N^{i}-For)-Lys-(N^{ε}-α-ClZ)-Gly-Pro-Val-p-MBHA resin, dried *in vacuo*. The protected peptide resin (1.0 g) was cleaved from the resin by liquid HF (*vide supra*). After evaporation of the volatile materials *in vacuo* at 0°C, the dried product was washed with ethyl ether (3 x 30 mL), extracted with 30% aqueous HOAc (3 x 30 mL), and lyophilized. The peptide powder (530 mg) was divided into two portions (260 mg each) and one portion was dissolved in 1.5 mL of ammonium acetate buffer (pH 4.5) and filtered through a cartridge filter into the top of a CMC column (2.0 x 30.0 cm) and eluted using 250 mL each of 0.01 (pH 4.5), 0.1 (pH 6.8), and 0.2 (pH 6.8) M NH_4OAc. The major peak detected at 280 nm, was eluted between the end of the 0.1 and the first half of the 0.2 M NH_4OAc fraction and was lyophilized to give 142.3 mg of white powder. Then 80.0 mg of the peptide powder was purified by preparative HPLC using 0.1% trifluoroacetic acid/CIBCN gradient (80:20 to 50:50) over 20 minutes with flow rate of 3 mL/min on Vydac semipreparative column, and the major peak was collected and lyophilized to give 63 mg of the title peptide. The analytical data for the purified compound are given in Tables III and IV and the biological activities are given in Table V.

Ac-[Nle^4, Asp^5, D-Phe^7, Lys^{10}, Gly^{11}]α-MSH$_{1-13}$-NH$_2$, Ac-Ser-Tyr-Ser-Nle-Asp-His-D-Phe-Arg-Trp-Lys-Gly-Pro-Val-NH$_2$ (3). The title compound was prepared from 1.0 g (~0.35 mmol) of Boc-His(N^{im}-Tos)-D-Phe-Arg(N^g-Tos)-Trp-(N^i-For)-Lys(N$^\epsilon$-2-ClZ)-Gly-Pro-Val-p-MBHA resin (prepared above), by stepwise coupling of N$^\alpha$-Boc-Asp(β-Bzl), N$^\alpha$-Boc-Nle, N$^\alpha$-Boc-Ser(O-Bzl), N$^\alpha$-Boc-Tyr(O-2-BrZ), and N$^\alpha$-Boc-Ser(O-Bzl). Each coupling was achieved as mentioned previously. Acetylation of the protected tridecapeptide-resin was carried out by using a 10-fold excess of N-acetylimidazole in dichloromethane (5 h) after deprotection and neutralization of N-terminal Boc group. The Ac-Ser(O-Bzl)-Tyr-(O-2-Brz)-Ser(O-Bzl)-Nle-Asp(β-Bzl)-His(N^{im}-Tos)-D-Phe-Arg(N^g-Tos)-Trp(N^i-For)-Lys(N$^\epsilon$-2-ClZ)-Gly-Pro-Val-p-MBHA resin was dried in vacuo to give 1.8 g of protected peptide resin. A 1.0 g of the protected peptide resin was cleaved by liquid HF and upon evaporation of the volatile materials, washing the resin material with diethyl ether (3 x 30 mL), extraction of the peptide with 30% aqueous HOAc (3 x 30 mL) and lyophilization a 600 mg of powder peptide was obtained. A portion of the crude tridecapeptide (200 mg) was dissolved in 1.5 mL of NH$_4$OAc buffer (pH 4.5) and filtered through a cartridge filter into the top of the CMC column (2.0 x 30.0 cm) and eluted with the same discontinuous gradient of aqueous NH$_4$OAc as outlined under the previous peptide. After lyophilization, 152 mg was obtained. A 100 mg sample of this crude peptide was further purified by HPLC to give 67 mg of the title peptide. The analytical data for this peptide are given in Tables III

and IV, and a summary of the biological potencies is given in Table V.

Ac-[Nle^4, D-Phe^7, Lys^{10}, Gly^{11}]α-MSH$_{4-13}$-NH$_2$, Ac-Nle-Glu-His-D-Phe-Arg-Trp-Lys-Gly-Pro-Val-NH$_2$ (4). From 1.0 g (~0.35 mmol) of Boc-His(N^{im}-Tos)-D-Phe-Arg(N^g-Tos)-Trp(N^i-For) Lys(N$^\varepsilon$-2-ClZ)-Gly-Pro-Val-p-MBHA resin (prepared above), the title peptide was synthesized by the solid-phase method after stepwise coupling of N$^\alpha$-Boc-Glu(γ-Bzl) and N$^\alpha$-Boc-Nle. Each coupling reaction was achieved by the same way previously reported for 2, except that the acetylation of the N-terminous was achieved by 2-fold excess of 1:1 acetic anhydride-pyridine in dichloromethane for 1 h. The peptide 4 was obtained in purified form as outlined for compound 3 to give a white powder of 4, yield 22%; the analytical data for the compound 4 are given in Tables III and IV, and the biological activities are given in Table V.

Ac-[Nle^4, Asp^5, D-Phe^7, Lys^{10}, Gly^{11}]α-MSH$_{4-13}$-NH$_2$, Ac-Nle-Asp-His-D-Phe-Arg-Asp-Lys-Gly-Val-NH$_2$ (5). From 1.0 g (~0.35 mmol) of Boc-His(N^{im}-Tos)-D-Phe-Arg(N^g-Tos)-Trp(N^i-For)-Lys(N$^\varepsilon$-2-ClZ)-Gly-Pro-Val-p-MBHA resin prepared as in 2, the title peptide was prepared by stepwise coupling of N$^\alpha$-Boc-Asp(β-Bzl), and N$^\alpha$-Boc-Nle. The same technique was used as for compound 2 in processing the resulting protective peptide resin. The peptide 5 was obtained as mentioned previously for compound 3 to give 53 mg of HPLC pure peptide starting with 130 mg of crude peptide purified previously with CMC chromotography as outlined in compound 2. The analytical data for compound 5 are given in Tables

III and IV, and an outline of the biological activities is given in Table V.

Ac-[Nle^4, Asp^5, D-Phe^7]α-MSH$_{4-10}$NH$_2$, Ac-Nle-Asp-His-D-Phe-Arg-Trp-Gly-NH$_2$ (6). A 1.0 g of p-methylbenzhydrylamine-resin (0.7 mmol NH$_2$/g resin) was suspended in dichloromethane, washed, neutralized, swelled and washed with dichloromethane. The swelled p-MBHA resin was coupled with the following amino acid derivatives: N$^\alpha$-Boc-Gly, N$^\alpha$-Boc-Trp(N^i-For), N$^\alpha$-Boc-Arg(N9-Tos), N$^\alpha$-Boc-D-Phe, N$^\alpha$-Boc-His(N^{im}-Tos), N$^\alpha$-Boc-Asp(β-Bzl) and N$^\alpha$-Boc-Nle. Each coupling reaction was achieved with a 3-fold excess of N$^\alpha$-Boc amino acid (or derivative), a 2.4-fold excess of DCC, and a 2.4-fold excess of HOBt following the same technique mentioned above. After coupling the last amino acid, the N$^\alpha$-Boc protection group was removed, the amino group neutralized, and the N$^\alpha$-amino group acetylated with 2-fold excess of 1:1 mixture of acetic anhydride-pyridine in dichloromethane for 1 h. The finished peptide-resin weighed 1.8 g after overnight drying under vacuum. Cleavage of 1 g of the peptide-resin by HF gave 250 mg of crude peptide. Purification by CMC of this crude peptide using discontinuous gradient of NH$_4$OAC (0.01-0.2M) with pH 4.5 to pH 6.8, gave 180 mg of partially purified peptide. Then, 100 mg of CMC purified peptide was subjected to HPLC purification to give 52 mg of pure peptide. The analytical data for the compound are given in Tables II and IV, and the biological potencies are given in Table V.

Ac-[Nle^4, D-Phe^7, Lys^{10}]α-MSH$_{4-10}$-NH$_2$, Ac-Nle-Glu-His-D-Phe-

Arg-Trp-Lys-NH_2 (7). A 2.7 g portion of p-methylbenzhydrylamine-resin (0.7 mmol NH_2/g resin) was suspended in dichloromethane and washed three times with 30 mL-portions of dichloromethane. The washed resin was shaken for 2 h in dichloromethane before filtering off the solvent. The swollen p-MBHA resin was neutralized the amino acids were coupled successively as outlined for compound 2. The following amino acid derivatives were coupled onto the resin (in order of their coupling): N^{α}-Boc-D-Lys(N^{ε}-2-ClZ), N^{α}-Boc-Trp(N^{i}-For), N^{α}-Boc-Arg(N^{g}-Tos), N^{α}-Boc-D-Phe, N^{α}-Boc-His(N^{im}-Tos). The resulting Boc-His(N^{im}-Tos) D-Phe-Arg(N^{g}-Tos)-Trp(Ni-For)-Lys(N^{ε}-2-ClZ)-p-MBHA resin was divided into two portions. One part of the resin was coupled stepwise with: N^{α}-Boc-Glu(γ-Bzl) and N^{α}-Boc-Nle. This peptide-resin was N^{α} deprotected and the N-terminal acetylated with 2-fold excess of 1:1 mixture of acetic anhydride-pyridine in dichloromethane for 1 h. The finished protected peptide resin was washed with dichloromethane and dried in vacuo to give 2.1 g. A 1.7 g of the protected peptide resin was cleaved by anhydrous liquid HF-anisole-dithioethane (17 ml HF, 2 mL anisole, 1 mL dithioethane). After evaporation of the volatile materials, the dried, peptide and resin mixture was washed with 3 x 30 mL of anhydrous diethylether and extracted with 3 x 30 mL of 30% aqueous HOAc. The aqueous extract of the peptide lyophilized to give 700 mg of crude peptide. A 300 mg portion of the crude peptide was dissolved in 2 mL of NH_4OAc buffer (pH 4.5), filtered through a

cartridge filter on the top of CMC column as outlined under compound 2. The major peak was collected and lyophilized to give 172 mg of white powder peptide. Then, 110 mg of the crude peptide was purified on HPLC to give 58 mg of pure title peptide. The analytical data for the compound are given in Tables III and IV, and the biological potencies are given in Table V.

Ac-[Nle^4, Asp^5, D-Phe^7, Lys^{10}]α-MSH$_{4-10}$-NH$_2$, Ac-Nle-Asp-His-D-Phe-Arg-Trp-Lys-NH$_2$ (8). The protected peptide resin to the title compound was prepared from 1.8 g of Boc-His(N^{im}-Tos)-D-Phe-Arg(N^g-Tos)-Trp(N^i-For)-Lys(N$^\varepsilon$-2-ClZ)-p-MBHA (prepared above) by stepwise coupling of N$^\alpha$-Boc-Asp(β-Bzl) and N$^\alpha$-Boc-Nle. Each coupling reaction was achieved with a 3-fold excess of N$^\alpha$-Boc amino acid (or derivative), a 2.4-fold excess of DCC, and a 2.4-fold excess of HOBt following the same strategy outlined above. After coupling the last amino acid, the N$^\alpha$-Boc protection group was removed, the amino group neutralized, and the N$^\alpha$-amino group acetylated with 2-fold excess of 1:1 mixture of acetic anhydride-pyridine in dichloromethane for 1 h. The Ac-Nle-Asp(β-Bzl)-His(N^{im}-Tos)-D-Phe-Arg(N^g-Tos)-Trp(N^i-For)-Lys(N$^\varepsilon$-2-ClZ)-p-MBHA resin was washed with dichloromethane and dried in vacuo to give 2.1 g. A 1.5 g portion of the protected peptide resin was cleaved by liquid HF and processed as in 7 to give 64 mg of the title peptide after HPLC purification of 112 mg of CMC chromotographically pure peptide. The analytical data for the compound are given in Tables III and IV, and the biological potencies are given in Table V.

Ac-[Nle^4, D-Phe^7, Orn^{10}]α-MSH$_{4-10}$-NH$_2$, Ac-Nle-Glu-His-D-Phe-Arg-Phe-Arg-Trp-Orn-NH$_2$ (9). The protected peptide resin to the title compound was synthesized as reported for 7, except the N$^\alpha$-Boc-Orn(N$^\delta$-Z) was used instead of N$^\alpha$-Boc-Lys(N$^\varepsilon$-2-ClZ) in the coupling scheme to give Ac-Nle-Glu(γ-Bzl)-His(N^{im}-Tos)-D-Phe-Arg(N^g-Tos)-Trp(N^i-For)-Orn-(N$^\delta$-Z)-p-MBHA resin. The peptide was cleaved from the resin, the protecting groups removed, and the title compound purified as reported for 7 to give the product 9 as a white powder: the yield 38%; the analytical data for the compound are given in Tables III and IV, and the biological potencies are given in Table V.

Ac-[Nle^4, Asp^5, D-Phe^7, Orn^{10}]α-MSH$_{4-10}$-NH$_2$, Ac-Nle-Asp-His-D-Phe-Arg-Trp-Orn-NH$_2$ (10). The protected peptide resin to the title compound was synthesized as reported for 9, except the N$^\alpha$-Boc-Asp(β-Bzl) was used instead of N$^\alpha$-Boc-Glu(γ-Bzl) in the coupling scheme to give Ac-Nle-Asp(β-Bzl)-His(N^{im}-Tos)-D-Phe-Arg(N^g-Tos)-Trp(N^i-For)-Orn(N$^\delta$-Z)-pMBHA resin. The peptide was cleaved from the resin, the protecting groups removed, and the title compound purified as reported for 7 to give the product 10 as a white powder: the yield 41%; the analytical data for the compound are given in Tables III and IV, and the biological potencies are given in Table V.

Ac-[Nle^4, D-Phe^7, Dab^{10}]α-MSH$_{4-10}$-NH$_2$, Ac-Nle-Glu-His-D-Phe-Arg-Trp-Dab-NH$_2$ (11). The protected peptide resin to the title compound was synthesized as reported for 7, except the N$^\alpha$-Boc-Dab(N$^\gamma$-Z)

was used instead of N^{α}-Boc-Lys(N^{ε}-2-ClZ) in the coupling scheme to give Ac-Nle-Glu(γ-Bzl)-His(N^{im}-Tos)-D-Phe-Phe-Arg(N^{g}-Tos)-Trp(N^{i}-For)-Dab(N^{γ}-Z) pMBHA resin. The N^{α}-Boc-Dab(N^{α}-Z) was synthesized as reported in literature (London, et al., 1984; Waki, et al., 1981). The peptide was cleaved from the resin, the protecting groups removed, and the title compound purified as reported for 7 to give the product 11 as a white powder: yield 42%. The analytical data for the compound are given in Tables III and IV, and the biological potencies are given in Table V.

Ac-[Nle^{4}, Asp^{5}, D-Phe^{7}, Dab^{10}]α-MSH_{4-10}-NH_2, Ac-Nle-Asp-His-D-Phe-Arg-Trp-Dab-NH_2 (12). The protected peptide resin to the title compound was synthesized as reported for 7, except the N^{α}-Boc-Dab(N^{γ}-Z) and N^{α}-Boc-Asp(β-Bzl) were used, instead of N^{α}-Boc-Lys(N^{ε}-2ClZ) and N^{α}-Boc-Glu(γ-Bzl), respectively, in the coupling scheme to give Ac-Nle-Asp(β-Bzl)-His(N^{im}-Tos)-D-Phe-Arg(N^{g}-Tos)-Trp(N^{i}-For)-Dab(N^{γ}-Z)-p-MBHA resin. Upon cleaving and processing the peptide resin as reported for 7, the peptide 12 was obtained as a white powder in 36% yield. The anlaytical data for the compound are given in Tables III and IV, and the biological potencies are given in Table V.

Ac-[Nle^{4}, Asp^{5}, D-Phe^{7}, Dpr^{10}]α-MSH_{4-10}-NH_2, Ac-Nle-Asp-His-D-Phe-Arg-Trp-Dap-NH_2 (13). The protected peptide resin to the title compound was synthesized as reported for 7, with the exception that N^{α}-Boc-Dap(N^{β}-Z) was used instead of N^{α}-Boc-Lys(N^{ε}-2-ClZ) and N^{α}-Boc-Asp(β-Bzl) for N^{α}-Boc-Glu(γ-Bzl) in the coupling scheme to give

Ac-Nle-Asp(β-Bzl)-His(N^{im}-Tos)-D-Phe-Arg(N^{g}-Tos)-Trp(N^{i}-For)-Dpr(N^{β}-Z)-p-MBHA resin. The N^{α}-Boc-Dpr(N^{β}-Z) was synthesized as reported in the literature (Waki, et al., 1981; London, et al., 1984). The peptide was cleaved from the resin, and purified as reported for 7 to give the peptide 13 as a white powder: yield 36%; the analytical data for the compound are given in Tables III and IV, and the biological potencies are given in Table V.

Ac-[Nle^{4}, Lys^{10}]α-MSH_{4-10}-NH_2, Ac-Nle-Glu-His-Phe-Arg-Trp-Lys-NH_2 (14). The protected peptide resin to the title compound was synthesized as reported for 7, with the exception that N^{α}-Boc-Phe was used instead of N^{α}-Boc-D-Phe in the coupling scheme to give Ac-Nle-Glu(γ-Bzl)-His(N^{im}-Tos)-Phe-Arg-Arg(N^{g}-Tos)-Trp(N^{i}-For)-Lys-(N^{ε}-2-ClZ)-p-MBHA resin. The peptide was cleaved from the resin and purified as reported for 7 to give the title compound with 40% yield. The analytical data for the compound are given in Tables III and IV, and the biological potencies are given in Table V.

Ac-[Nle^{4}, Asp^{5}, Lys^{10}]α-MSH_{4-10}-NH_2, Ac-Nle-Asp-His-Phe-Arg-Trp-Lys-NH_2 (15). The protected peptide resin to the title compound was synthesized as reported for 7, with the exception that N^{α}-Boc-Phe was used instead of N^{α}-Boc-D-Phe and N^{α}-Boc-Asp(β-Bzl) replaced N^{α}-Boc-Glu(γ-Bzl) in the coupling scheme to give Ac-Nle-Asp(β-Bzl)-Phe-Arg(N^{g}-Tos)-Trp(N^{i}-For)-Lys(N^{ε}-2-ClZ)-p-MBHA resin. The peptide was cleaved from the resin, the protecting groups removed, and the

title compound purified as previously reported to give the product 15 as a white powder in 37% yield. The analytical data for the compound are given in Tables III and IV, and the biological potencies are given in Table V.

Table II(a). Structure of α-Melanotropin Analogues Prepared During This Study

No.	Primary Sequence
	1 2 3 4 5 6 7 8 9 10 11 12 13
1	Ac-Ser-Tyr-Ser-Met-Glu-His-Phe-Arg-Trp-Gly-Lys-Pro-Val-NH_2
2	Ac-Ser-Tyr-Ser-Nle-Glu-His-D-Phe-Arg-Trp-Lys-Gly-Pro-Val-NH_2
3	Ac-Ser-Tyr-Ser-Nle-Asp-His-D-Phe-Arg-Trp-Lys-Gly-Pro-Val-NH_2
4	Ac-Nle-Glu-His-D-Phe-Arg-Trp-Lys-Gly-Pro-Val-NH_2
5	Ac-Nle-Asp-His-D-Phe-Arg-Trp-Lys-Gly-Pro-Val-NH_2
6	Ac-Nle-Asp-His-D-Phe-Arg-Trp-Gly-NH_2
7	Ac-Nle-Glu-His-D-Phe-Arg-Trp-Lys-NH_2
8	Ac-Nle-Asp-His-D-Phe-Arg-Trp-Lys-NH_2
9	Ac-Nle-Glu-His-D-Phe-Arg-Trp-Orn-NH_2
10	Ac-Nle-Asp-His-D-Phe-Arg-Trp-Orn-NH_2
11	Ac-Nle-Glu-His-D-Phe-Arg-Trp-Dab-NH_2
12	Ac-Nle-Asp-His-D-Phe-Arg-Trp-Dab-NH_2
13	Ac-Nle-Asp-His-D-Phe-Arg-Trp-Dpr-NH_2
14	Ac-Nle-Glu-His-Phe-Arg-Trp-Lys-NH_2
15	Ac-Nle-Asp-His-Phe-Arg-Trp-Lys-NH_2

Table II(b). Structure of α-Melanotropin Analogues Prepared During This Study

No.	Analogue
1.	α-MSH
2.	Ac-[Nle^4, D-Phe^7, Lys^{10}, Gly^{11}]α-MSH$_{1-13}$NH$_2$
3.	Ac-[Nle^4, Asp^5, D-Phe^7, Lys^{10}, Gly^{11}]α-MSH$_{1-13}$NH$_2$
4.	Ac-[Nle^4, D-Phe^7, Lys^{10}, Gly^{11}]α-MSH$_{4-13}$NH$_2$
5.	Ac-[Nle^4, Asp^5, D-Phe^7, Lys^{10}, Gly^{11}]α-MSH$_{4-13}$NH$_2$
6.	Ac-[Nle^4, Asp^5, D-Phe^7]α-MSH$_{4-10}$NH$_2$
7.	Ac-[Nle^4, D-Phe^7, Lys^{10}]α-MSH$_{4-10}$NH$_2$
8.	Ac-[Nle^4, Asp^5, D-Phe^7, Lys^{10}]α-MSH$_{4-10}$NH$_2$
9.	Ac-[Nle^4, D-Phe^7, Orn^{10}]α-MSH$_{4-10}$NH$_2$
10.	Ac-[Nle^4, Asp^5, D-Phe^7, Orn^{10}]α-MSH$_{4-10}$NH$_2$
11.	Ac-[Nle^4, D-Phe^7, Dab^{10}]α-MSH$_{4-10}$NH$_2$
12.	Ac-[Nle^4, Asp^5, D-Phe^7, Dab^{10}]α-MSH$_{4-10}$NH$_2$
13.	Ac-[Nle^4, Asp^5, D-Phe^7, Dpr^{10}]α-MSH$_{4-10}$NH$_2$
14.	Ac-[Nle^4, Lys^{10}]α-MSH$_{4-10}$NH$_2$
15.	Ac-[Nle^4, Asp^5, Lys^{10}]α-MSH$_{4-10}$NH$_2$

Table III. Analytical Data of α-Melanotropin Analogues Synthesized in This Study

Compound	Thin-Layer Chromatography R_f Values in Different Solvents					$[\alpha]_{546}^{23}$ in 10% acetic acid	HPLC K'^{a}
	A	B	C	D	E		
2	0.34	0.62	0.0	0.0	0.39	-51.6 (c=0.31)	1.86
3	0.32	0.63	0.0	0.0	0.38	-52.3 (c=0.33)	1.82
4	0.43	0.67	0.0	0.0	0.42	-49.14 (c=0.35)	3.05
5	0.41	0.69	0.0	0.0	0.40	-50.0 (c=0.32)	2.98
6	0.01	0.76	0.74	0.29	0.62	-44.8° (c=0.25)	3.32
7	0.35	0.39	0.01	0.05	--	-50.0° (c=0.12)	2.56
8	0.36	0.40	0.0	0.07	--	-28.0° (c=0.05)	2.25
9	0.37	0.40	0.0	0.08	--	-12.5° (c=0.04)	2.24
10	0.34	0.41	0.0	0.07	--	-20.0° (c=0.03)	2.14
11	0.44	0.65	0.03	0.0	--	-30.0° (c=0.05)	2.12
12	0.43	0.64	0.03	0.0	--	-32.7° (c=0.11)	2.21
13	0.41	0.63	0.02	0.0	--	-53.7° (c=0.033)	2.18
14	0.34	0.38	0.0	0.1	0.0	-25.0 (c=0.02)	2.20
15	0.32	0.39	0.0	0.08	0.0	-24.6 (c=0.16)	2.17

[a]Solvent system was 15% acetonitrile in 0.1% trifluoroacetic acid; isocratic for 5 min, then, gradient to 45% acetonitrile (65% 0.1 FTA) over 15 min. Then, 5 min to 90% acetonitrile and 5 min to go to initial conditions.

Table IV(a). Amino Acid Analysis of α-Melanotropin Analogues Prepared in This Study

Compound	Ser	Tyr	Nle	Glu	Asp	His	Phe	Arg
2	1.92	0.93	0.98	1.01	--	0.91	0.98	1.03
3	1.94	0.96	0.97	--	0.98	0.97	1.01	1.1
4	--	--	0.96	1.0	--	0.96	1.0	0.98
5	--	--	0.99	--	0.96	0.98	1.01	0.97
6	--	--	1.0	--	1.10	0.92	1.0	1.10
7	--	--	1.0	0.97	--	0.90	1.1	0.96
8	--	--	1.1	--	1.1	0.90	0.97	1.0
9	--	--	1.10	1.10	--	0.99	1.0	1.10
10	--	--	1.10	--	1.10	0.99	1.0	1.10
11	--	--	1.10	0.90	--	0.92	1.10	1.10
12	--	--	1.10	--	1.10	0.91	1.10	0.96
13	--	--	1.10	--	1.0	1.1	0.90	0.94
14	--	--	1.10	0.98	--	0.96	1.10	0.95
15	--	--	1.10	--	0.98	0.99	1.10	0.96

Table IV(b). Amino Acid Analysis of α-Melanotropin Analogues Prepared in This Study

Compound	Trp	Gly	Lys	Pro	Val	Orn	Dab	Dpr
2	0.90	1.03	0.99	0.92	1.03	--	--	--
3	0.91	1.01	1.02	0.91	1.01	--	--	--
4	0.90	1.02	0.98	0.90	1.02	--	--	--
5	0.91	1.01	0.96	0.89	1.01	--	--	--
6	0.91	1.1	--	--	--	--	--	--
7	1.10	--	0.90	0.90	--	--	--	--
8	0.90	--	0.93	--	--	--	--	--
9	0.90	--	--	--	--	0.90	--	--
10	0.90	--	--	--	--	0.90	--	--
11	1.0	--	--	--	--	--	0.90	--
12	1.10	--	--	--	--	--	0.91	--
13	0.95	--	--	--	--	--	--	0.91
14	0.90	--	0.94	--	--	--	--	--
15	0.93	--	0.97	--	--	--	--	--

Table V. Biological Activities of α-Melanotropin Analogues Studied in This Research

Analogue	Biological Potency		Residual Activity	
	Frog	Lizard	Frog	Lizard
1	1.0	1.0	P(-)	P(-)
2	6.0	8.0	P(+)	P(-)
3	9.0	8.0	P(+)	P(-)
4	0.8	8.0	P(+)	P(+)
5	1.0	10.0	P(+)	P(+)
6	0.1	8.0	P(-)	P(-)
7	0.2	8.0	P(-)	P(-)
8	0.7	8.0	P(-)	P(-)
9	0.6	8.0	P(-)	P(-)
10	0.9	10.0	ND	P(-)
11	0.9	10.0	P(+-)	P(+-)
12	0.9	50.0	P(-)	P(-)
13	0.2	8.0	P(-)	P(-)
14	0.001	0.08	P(+)	P(-)
15	0.004	0.08	P(+)	P(-)

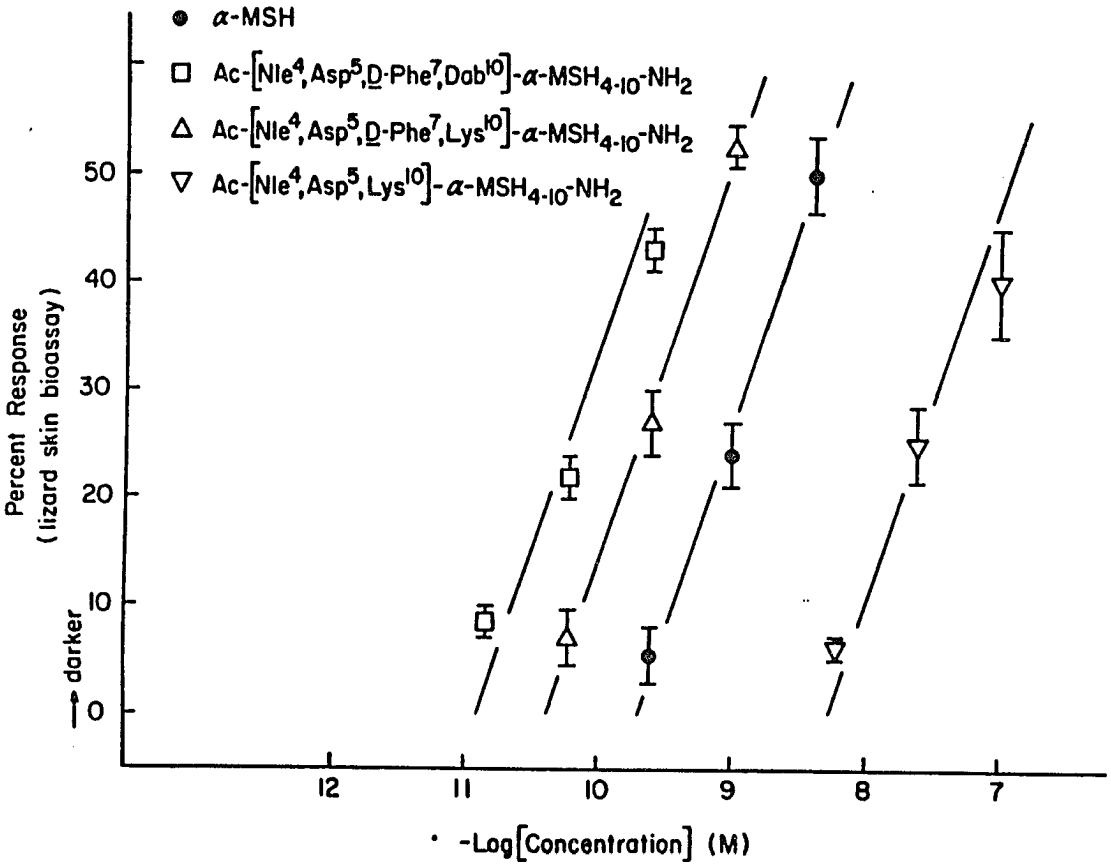

Fig. 1. Biological potencies of different analogues of Ac-[Nle^4, Asp^5, D-Phe^7, Lys^{10}]α-MSH$_{4-10}$-NH$_2$ in lizard skin.

CHAPTER THREE

DESIGN AND SYNTHESIS OF CONFORMATIONALLY RESTRICTED CYCLIC α-MSH WITH HIGH POTENCY

Peptide hormones and their analogues are one of the most important tools for studing the physico-chemical basis of biological information transfer at specific target tissues. α-Melanocyte stimulating hormone (α-MSH) is a linear tridecapeptide, Ac-Ser-Tyr-Ser-Met-Glu-His-Phe-Arg-Trp-Gly-Lys-Pro-Val-NH_2, that is synthesized and secreted by the pars intermedia of the vertebrate pituitary (Hadley et al., 1975). The hormone, along with other melanotropins, is derived from a large protein precursor, pro-opiomelanocortin, within cells of the pars intermedia and the brain tissue (Herbert et al., 1980; Mains et al., 1980). α-MSH has vital physiological roles in the control of vertebrate pigment cell melanogenesis (Hadley et al., 1981), neural functioning related to learning and behavior (O'Donohue et al., 1980; Tilders et al., 1977), fetal development (Tilders et al., 1977), and human skin coloration (Lerner et al., 1960).

While the physiological role of α-MSH in regulating hair and skin coloration in vertebrate seems well-established (Medzihradszky, 1981; Hruby et al., 1984), its role in other animals and other systems, especially in CNS (Hruby, 1984) and human, is less well defined. One such interaction is that in coloration of human skin and hair (Lerner et al., 1960). For this purpose, we have utilized various structural considerations in conjunction with conformational constraints (Hruby,

1984; Hruby, 1985) to modify the Ac-[Nle^4, D-Phe^7]α-MSH$_{4-10}$-NH$_2$ structure in a manner which enhances melanocyte dispersions in mammalian type of receptor (lizard skin). In our previous investigations toward these goals (Cody et al., 1987), conformationally constrained α-MSH compounds were synthesized and tested for their biological potency. The first synthesized analogues in this series was [Cys^4, Cys^{10}]α-MSH$_{1-13}$-NH$_2$ which had over 20 times the activity of the native α-MSH hormone in frog skin bioassay over the linear portion of the dose-response curve, and about two to four fold the potency of α-MSH in the lizard skin bioassay (Sawyer et al., 1982). The design and synthesis of those cyclic α-MSH analogues were based on the consideration of the β-turn structure at the center of the active site (-His^6-Phe^7-Arg^8-Trp^9-) of α-MSH and the importance of this conformational property for the biological activity. From the structure activity studies of this class of α-MSH analogues, several conclusions can be drawn: 1) cyclization between positions 4 (Met^4) and 10 (Gly^{10}) by isosteric replacement of Met^4 and Gly^{10} with cysteine amino acids enhanced the melanocyte dispersion activity by not less than 20 times in frog skin bioassay and two times in the lizard skin bioassay; 2) replacement of Phe^7 with D-Phe^7 in these cyclic analogues results in a 2-fold increase in potency in the frog skin bioassay and a 4-fold increase in the lizard skin bioassay; 3) the presence of Lys in position 11 always gave more active analogues than those without it; 4) reduction or expansion of the ring size of disulfide bridge from 23-membered ring caused severe

reduction in the biological potency of the resulted analogue. The results of these studies are summarized in Table VI.

In considering these results with the results we reported in Chapter 2 of this research, we undertook a study to examine the possibility for a different kind of conformationally restricted α-MSH analogue. To simplify the picture, we concentrated on 4-10 fragments of α-MSH with the following general structure, Ac-[Nle^4, Xxx^5, D-Phe^7, Yyy^{10}]α-MSH$_{4-10}$-NH$_2$ where the Xxx amino acid was either Glu or Asp and the Yyy amino acid was a basic amino acid, e.g. Lys, Orn, Dab, or Dpr. Theoretical studies of a member of these linear peptides using energy minimization and molecular dynamics simulation (see Chapter 5) suggested that they share a general conformational pattern characterized by the proximity of the charged side chains of Xxx and Yyy amino acids. Using these facts, we synthesized a group of cyclic α-MSH analogues, and evaluated their biological activities. The results of these studies are reported in this chapter.

Results and Discussion

The protected linear decapeptide Ac-[Nle^4, D-Phe^7, Lys^{10}, Gly^{11}]α-MSH$_{4-13}$-NH$_2$ and the other heptapeptide Ac-[Nle^4, Yyy^5, D-Phe^7, Xxx]α-MSH$_{4-10}$-NH$_2$ analogues were prepared in a stepwise manner on a p-methylbenzhydrylamine resin (substitution = 0.7 mmol NH$_2$/g resin) using the regular solid phase methodology (see Experimental Section). The Yxy amino acids in the heptapeptides were Glu or Asp and the Xxx amino

acid residues were Lys, Orn, Dab or Dpr. The synthesized analogues are listed in Table VII. All the syntheses were carried out in dichloromethane or in a mixture of dichloromethane/dimethylformamide (1:1) using a threefold excess of the N^{α}-t-butyloxycarbonyl-amino acid derivatives (N^{α}-Boc-amino acid). The side chains of the functional amino acids were properly protected as will be discussed in the Experimental Section. After completion of the linear peptide synthesis, they were cleaved and purified. The homogenous peptides were characterized by quantitative amino acid analysis, thin layer chromatography and HPLC.

Before cyclization, the linear peptides were converted to their trihydrochloride salts on a diethylaminoethylcellulose column (hydrochloride form) (Donzel et al., 1977) and lyophilized to a glassy powder. Cyclizations to a cyclic lactam involving the side chain groups of positions 5 and 10 were then accomplished according to procedures documented in the literature with little modification (Bradley et al., 1983; Christensen, 1979; Halstrom et al., 1968; Bradley et al., 1979). Cyclization using diphenyl phosphoryl azide and solid potassium phosphate dibasic in DMF was the method of choice in comparison to the one using triethylamine as a base. The latter was used in cyclization of Ac-[Nle^4, Asp^5, D-Phe^7, Lys^{10}]α-MSH. In comparison with the general cyclization procedure followed by us, the triethylamine methods gave more polymer and thus lower yields of the compounds of interest in comparison were the K_2HPO_4 procedure (25% vs. 50%). The progress of the cyclization reaction was followed by analytical HPLC together with the

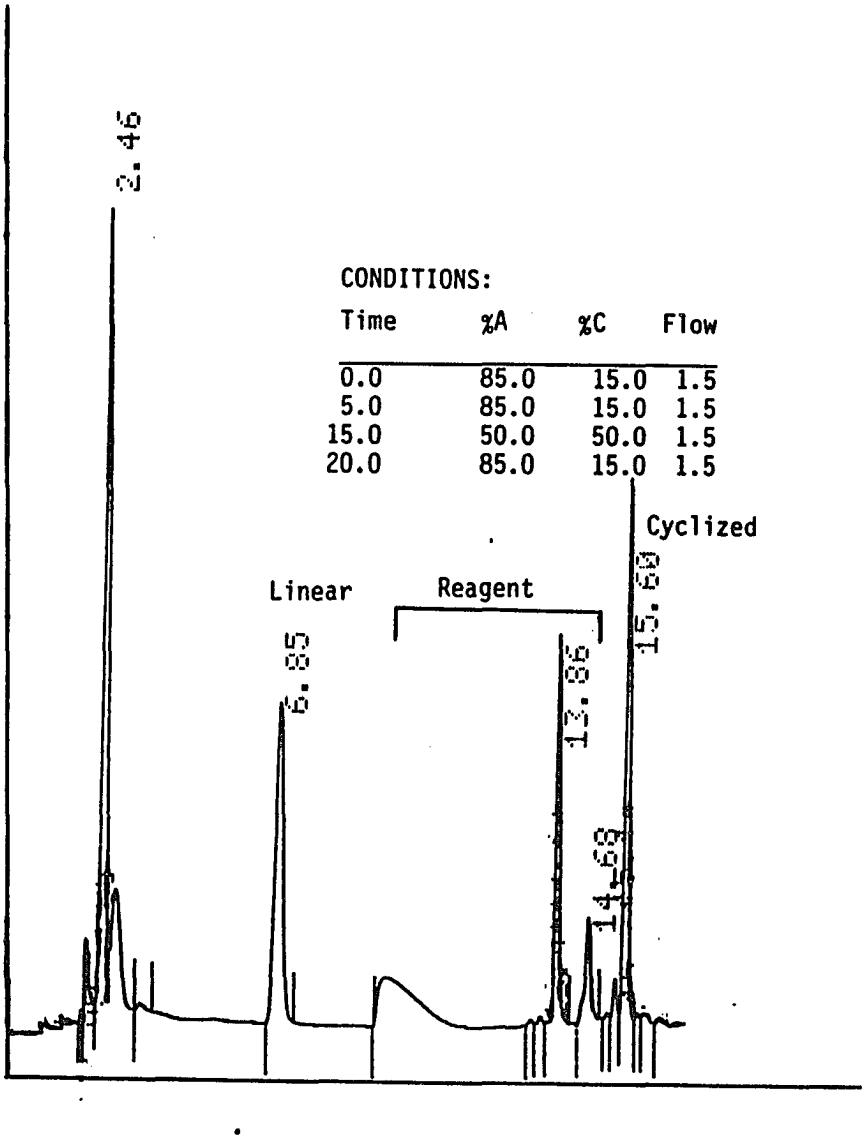

Fig. 2. Chromotogram of the reaction mixture of Ac-[Nle^4, D-Phe^7, Lys^{10}, Gly^{11}]α-MSH$_{4-13}$-NH$_2$ after 2h of mixing with DPPA at 0°C. A; 0.1% trifluoroacetic acid buffer, B; Acetonitrile.

ninhydrin test. The completion of the reaction was reflected by the complete disappearance of the starting material (the linear precursor) shown in Figure 2 for Ac-[Nle^4, Asp^5, D-Phe^7, Lys^{10}]α-MSH$_{4-13}$-NH$_2$ as a prototype for the other analogues. From these studies we did not notice any major difference in the rate of cyclization of different heptapeptide analogues. Thus, it seems to be that the ring size of the final products which range from 20 to 24-membered rings, did not appreciably affect the progress of cyclization in this series of peptides. This phenomenon may be attributed to the fact that these analogues all fall into a conformation which brings the side chain groups of positions 5 and 10 in a proper position for interaction with each other. This conclusion will be further discussed in Chapter 5.

The cyclization reaction was achieved using the fully deprotected linear decapeptides and heptapeptides. In order to minimize the possibilities of side reactions, the linear peptide was first converted to its trihydrochloride salts and then cyclized in the presence of five-fold excess of K_2HPO_4 as a base. Under those conditions, the arginine side-chain should remain protonated and thus protected. However, it had been reported that when cyclization was attempted on a linear peptides in its triacetate form, the cyclization failed, leading primarily to acetylation of the basic amino acid side-chains (Donzel et al., 1977; Kopple, 1972). The characterization of the cyclic peptides was of primary importance. The negative ninhydrin test is, of course, a

necessary condition for the cyclic structure. However, all the experiments of cyclization we carried out did not give a completely ninhydrin negative, but instead gave a very weak positive response. As a matter of fact, cyclization using triethylamine as a base gave a product which was complete ninhydrin negative but with more polymeric material (HPLC and mass spectrometry). In spite of the residual ninhydrin positive response, the HPLC showed more than 95% conversion of the starting material (linear peptide) to the product (cyclic peptide). Since the most likely side reaction that could occur during the cyclization step would involve a cyclodimerization (or oligomerization), we investigated this possibility for each compound we prepared. The testing for dimers and polymer products was carried out by looking at the FAB mass spectrometry of the HPLC purified cyclic peptides. The physical data are found in Table VIII.

Our previous studies, together with the results of the others (Hruby et al., 1984; Liepkaula et al., 1983, 1984), pointed to the importance of conformational restriction for the active site of α-MSH or ACTH. Cyclization constraints of α-MSH at positions 4 and 10 using pseudoisosteric replacement of Met-4 and Gly-10 with Cys resulted in many fold enhancements in melanocyte dispersions activity of the synthesized analogue as reported in Table VII. The potency enhancement of the cyclic analogues compared to that of their linear precursor is clearly dependent on the bioassay system we used. Our major interest here was to get analogues with high potency at the lizard skin bioassay

since the activity on the latter bioassay is well correlated to the activity in mammalian systems (Hruby et al., 1984). The major characteristics of [Cys^{4}, Cys^{10}]α-MSH cyclic analogues were that they showed low activity in lizard skin bioassay and high potency in the frog skin bioassay, and also a 500-fold reduction in potency upon ring size reduction (22-membered ring) or increase (24-membered ring) in comparison with the optimized ring size (23-membered ring) as reported in Table VI. The conformational constraints imposed by a cyclic lactam ring formation using the side chain groups of the amino acids in positions 5 and 10 resulted in a group of compounds shown in Table VII, with the relative biological potencies shown in Table IX. Compound 4, which possesses a 23-membered ring, gave the highest biological potency in the lizard skin assay system. No large changes in potency were seen in the frog skin assay. The enhancement in potency between the cyclic and its linear ancestor is on the order of ten times (see Chapter 2). The potency of cyclic analogue 3 is not much affected in comparison to the linear analogue, but one important change does occur with the appearance of prolonged activity for this cyclic analogue. The C-terminal tripeptide, Gly-Pro-Val has no effect on the potency of these analogues as is demonstrated in compound 2. There is one important factor in these cyclic lactam peptides, which is the prolongation in activity of the cyclic analogue in comparison to the linear analogue as shown in Figure 3. The prolongation phenomenon was observed previously

and it was reported that it may require different conformational and structural features which are not parallel with those related to the potency of the analogues (Hruby et al., 1984). In addition, the loss in prolongation and potency reduction as the ring size goes down from 23-membered ring is very clear for compounds 5, 6, and 7. This change in biological activity may be attributed to the effect of the ring constraint on the active conformation of these peptides (see Hruby et al., 1986 for a general discussion). The correlation of ring size with biological activity was reported in other cases of peptides like oxytocin (20-membered ring). This ring effect which is directly related to the conformation of the peptide hormone will be further examined in Chapters 4 and 5 for some of these analogues.

In conclusion, it appears that positions 13, 12, and 11 in α-MSH are not important for full biological activity of the cyclic compounds. This is parallel to previously reported results (Hruby, et al., 1984, 1987). The correlation of biological activity of melanotropin is related to conformational constraints imposed by the lactam bond which may be closely related to the bioactive conformation. It is also clear that in this group of peptides, the 4-10 sequence retains all the structural components necessary for superpotency and prolongation. The critical ring size effect on biological potency appeared again in the lactam type of peptide which indicates that this ring-size-effect is not dependent on the bridge type of cyclic peptide.

Experimental Section

General Methods. Capillary melting points were determined on a Thomas-Hoover melting point apparatus and are reported uncorrected. R_f values on thin-layer chromatograms of silica gel were observed in the following solvent systems: (A) 1-butanol/HOAc/H_2O (4:1:5 upper phase only), (B) 1-butanol/HOAc/pyridine/H_2O (15:3:10:12), (C) 1-butanol/pyridine/HOAc/H_2O (5:5:1:4), (D) 25% ammonium hydroxide/isopropanol/H_2O (1:3:1). Spots were revealed by U.V. absorption, ninhydrin, and iodine vapor. Amino acid analyses were obtained using a Beckman 120C amino acid analyzer following hydrolysis for 22 h at 120° with 4 M methanesulfonic acid containing 0.2% 3-(2-aminoethyl) indole and subsequent neutralization with 4 N NaOH to pH 3.5. Also mixtures of HCl:propionic acid containing 0.5% w/v phenol were used for hydrolysis of the peptide sample under the same conditions. No corrections were made for destruction of amino acids during hydrolysis. Fast atom bombardment mass spectra were obtained on a Varian 311A spectrometer equipped with an Ion Tech Ltd. Source with Xenon as the bombarding gas. Optical rotations were obtained on a Rudolph Research Autopol III polarimeter at the mercury green line (546 nm). HPLC was performed with the following solvent systems: 0.1% trifluoroacetic acid/CH_3CN as organic modifier; Vydac 218TP15-16 C_{18}RP columns (25 cm × 4.6 mm)(and (25 cm × 25 mm) were used. The eluted peaks were monitored at 223 nm and 280 nm.

N^{α}-Boc-protected amino acids and amino acid derivatives were

purchased from Bachem (Torrance, CA) or were prepared by published methods. N^{α}-Boc-Dab (N^{γ}-Z) and N^{α}-Boc-Dpr(N^{β}-Z) were prepared according to the literature procedure (see CH. 2). The p-methylbenzhydrylamine resin (p-MBHA) was prepared from 1% divinylbenzene cross-linked polystyrene resin by previously reported methods with an amine substitution of 0.7 mmol/g (see CH. 2).

Solid-Phase Peptide Synthesis of Cyclic Melanotropin Peptides. Analogues were prepared by standard solid-phase synthetic techniques used in our laboratory (Sawyer et al., 1982; Upson et al., 1976; Yang et al., 1980). In summary, N^{α}-tert-butyloxycarbonyl(N^{α}-Boc) protected amino acids and their derivatives were coupled to a p-methylbenzhydrylamine resin with a 3-fold excess of the Boc-protected amino acid derivative, a 2.4-fold excess of N-hydroxybenzotriazole (HOBt) of 1 mmol/mL solution in DMF (except in case of His) (Fujii et al., 1974), and a 2.4-fold excess of 1 mmol/mL solution of dicyclohexylcarbodiimide (DCC) in DMF. The coupling reaction was carried out in dichloromethane for a 1 to 3 hour period, which were monitored by ninhydrin (Christensen, 1979) and/or chloranil (Yamashiro, 1964) tests and repeated as necessary. Reactive side chains of amino acids were protected as follows: Lys, 2,4-dichlorobenzyloxycarbonyl; Orn, Dab, and Dap, N^{ε}-benzyloxycarbonyl; Trp, formyl; Arg, tosyl; His, tosyl; Glu and Asp, benzyl ester. Cleavage of the N^{α}-Boc protecting group was performed by treatment with 48% trifluoroacetic acid containing 2% anisole in dichloromethane for 5 and 20 min each.

A cycle for the incorporation of each amino acid residue into the growing peptide chain consists of the following: 1) washing with CH_2Cl_2 (4 x 30 mL, 1 min/wash); 2) Boc protection was removed at each step by two treatments with 48% TFA in CH_2Cl_2 containing 2% anisole for 5 and 20 min each; 3) washing with CH_2Cl_2 (4 x 30 mL, 1 min/wash); 4) neutralizing with 10% diisopropylethylamine in CH_2Cl_2 (2 x 30 mL, 3 min/wash); 5) washing with CH_2Cl_2 (3 x 30 mL, 2 min/wash), 6) adding the Boc-protected amino acid derivative in 20 mL CH_2Cl_2 (except in the cases of Trp, Arg, and His, where DMF was substituted for CH_2Cl_2 because of the solubility problem), followed by HOBt, followed by DCC and shaking for 1-3 h; 7) washing with CH_2Cl_2 (3 x 30 mL, 2 min/wash), 8) washing with 100% EtOH (3 x 30-mL, 2 min/wash). Completion of coupling was monitored as mentioned above. After coupling the last amino acid, the N^{α}-Boc protecting group was removed, the amino group neutralized, and acetylated with a 10-fold excess of N-acetylimidazole in CH_2Cl_2 or using 1:1 mixture of acetic anhydrided:pyridine in CH_2Cl_2 (2-fold excess for 1 h).

Peptides were deprotected and removed from the resin with anhydrous liquid HF (10 ml 1 g of resin) containing 10% anisole and 8% 1,2-dithioethane (Matsueda, 1982) at 0°C for 45 min. After evaporation of the volatile materials in vacuo, the free peptides were washed with diethyl-ether or ethyl acetate (3 x 30-mL) and then extracted with 30% aqueous solution of acetic acid (3 x 30-mL), and distilled water (3 x 30 mL). The combined aqueous extract was lyophilized to give a white

powder of the crude peptide. Each peptide was purified by column chromatography on cation-exchange carboxymethyl cellulose (CMC) resin, using a discontinuous gradient of ammonium acetate buffer as follows: 250 mL of 0.01 M NH_4OAc, pH4.5; 250 mL of 0.01 M NH_4OAc, pH 6.8, 250 mL of 0.1 M NH_4OAc, pH 6.8; and 250 mL of 0.2 M NH_4OAc, pH 6.8. The major peak (280 nm detection) eluted during the last part of 0.01 M NH_4OAc (pH 6.8) and the first half of the 0.1 M NH_4OAc (pH 6.8) buffer was lyophilized to give a white powder. A certain amount of this peptide was then purified further by using semipreparative HPLC column (Vydac 218 TP 15-16 C_{18}RP 25 cm x 25 mm) and the amino acids analyses was determined together with the other physical constants as shown in Table I.

Ac-[Nle^4, Glu^5, D-Phe^7, Lys^{10}, Gly^{11}]α-MSH_{4-13}-NH_2 (1).

Starting with 1.0 g of N^{α}-Boc-Val-p-MBHA resin (0.7 mmol of N^{α}-Boc-Val), the protected peptide resin for the title compound was prepared after stepwise coupling of the following N^{α}-Boc-protected amino acids (in order of addition): N^{α}-Boc-Pro; N^{α}-Boc-Gly; N^{α}-Boc-Lys(N^{ε}-2,4-ClZ); N^{α}-Boc-Trp(N^{i}-For); N^{α}-Boc-Arg(N^{g}-Tos); N^{α}-Boc-D-Phe; N^{α}-Boc-His(N^{im}-Tos); N^{α}-Boc-Glu(γ-Bzl); N^{α}-Boc-Nle. After coupling the last amino acid, the N^{α}-Boc protecting group was removed, the amino group neutralized, and acetylated with either 10-fold excess of N-acetylimidazole in dichloromethane (6-8 h) or with 2-fold excess of 1:1 mixture of acetic anhydride:pyridine in dichloromethane (1-2 h), and the resulting protected peptide resin Ac-Nle-Glu(γ-Bzl)-His(N^{im}-Tos)-D-Phe-Arg(N^{g}-Tos)-Trp(N^{i}-For)-Lys(N^{ε}-

2,4-ClZ)-Gly-Pro-Val-p-MBHA. A 1.0 g (~0.6 mmol) portion of the protected peptide resin was treated with 10 mL anhydrous HF in presence of 1 mL anisole and 0.8 mL 1,2-dithioethane for 45 min at 0°C. After the HF, anisole, and 1,2-dithioethane were evaporated in vacuo, the dried product mixture was washed with three 30-mL portions of diethylether, and the peptide was extracted with three 30-mL portions of 30% acetic acid. Then, upon lyophilization of the aqueous extract of the peptide, a 325 mg of crude Ac-Nle-Glu-His-D-Phe-Arg-Trp-Lys-Gly-Pro-Val-NH_2 peptide, as a white powder, was obtained. A 150 mg of crude Ac-[Nle^4, D-Phe^7, Lys^{10}, Gly^{11}]α-MSH_{4-13}-NH_2 was subjected to the purification scheme which included dissolving the crude peptide in 2-4 mL of 0.01 M NH_4OAc, pH 4.5, and chromatographed on carboxymethylcellulose column (2.0 x 25.0 cm) with a discontinuous gradient (250 mL each) of 0.01 (pH 4.5), 0.01, 0.1, and 0.2 M NH_4OAc (pH 6.8). The major peak detected at 280 nm was eluted during the first half of the 0.1 M NH_4OAc (pH 6.8) buffer and was lyophilized to give 104 mg of a white powder. The CMC pure Ac-[Nle^4, D-Phe^7, Lys^{10}, Gly^{11}]α-MSH_{4-13}-NH_2 was further purified by HPLC, using 0.1% trifluoroacetic acid buffer and acetonitrile as organic modifier on Vydac 218TP15-16 C_{18}RP (25 cm x 25 mm) semipreparative column. A 100 mg of the peptide was HPLC purified to give 74 mg pure Ac-[Nle^4, D-Phe^7, Lys^{10}, Gly^{11}]α-MSH_{4-13}-NH_2 peptide. The analytical data of the compound are reported in Tables III and IV. A 40 mg sample of pure Ac-[Nle^4, D-Phe^7, Lys^{10}, Gly^{11}]α-MSH_{4-13}-NH_2 was dissolved in 1 mL of 5% HCl aqueous solution and chromatographed on

diethylaminoethylcellulose (Donzel et al., 1977) (of hydrochloric acid form) column (1.0 x 15.0 cm) with 100 mL of 5% HCl aqueous solution and the eluted peak monitored at 280 nm. Lyophilization of the collected peptide peak gave 35 mg of the Ac-[Nle, D-Phe^{7}, Lys^{10}, Gly^{11}]-α-MSH$_{4-13}$-NH$_2$ • HCl salt. Then the peptide salt was dissolved in 3 mL of dry DMF and secondary amine free (distilled from ninhydrin under reduced pressure) (Stewart et al., 1985). To the peptide solution in DMF was added 120 mg of anhydrous K_2HPO_4 (Bradley et al., 1983). Then the reaction mixture was cooled in an ice-salt bath to 0°C and 17 μL of diphenylphosphorylazide added and the reaction mixture stirred at 0°C and then the whole reaction flask transferred to the cold room with 12°C. The reaction mixture was stirred overnight at 12°C and the completion of the reaction was monitored by HPLC (Vydac column, 25.0 cm x 4.6 mm) with 0.1% trifluoroacetic acid/CH_3CN as shown in Figure 2. Also, the ninhydrin test was used to detect the completion of the cyclization. The Ac-[Nle^{4}, Glu^{5}, D-Phe^{7}, Lys^{10}, Gly^{11}]-α-MSH$_{4-13}$-NH$_2$ was purified, after quenching the reaction with 10% aqueous HOAc solution, by desalting on a P$_4$ polyacrylamide column (80.0 cm x 1.0 cm) using 30% HOAc, followed by semipreparative HPLC to give 16 mg of cyclic peptide Ac-[Nle^{4}, Glu^{5}, D-Phe^{7}, Lys^{10}, Gly^{11}]-α-MSH$_{4-13}$-NH$_2$. The physical data of the compound are reported in Table VIII, and the biological potencies are given in Table IX.

Ac-[Nle^{4}, Glu^{5}, D-Phe^{7}, Lys^{10}]α-MSH$_{4-10}$-NH$_2$ (2). The title

compound was prepared starting with 2.0 g of N^{α}-Boc-Lys(N^{ϵ}-2,4-Cl_2Z)-p-MBHA resin (~1.0 mmol of N^{α}-Boc-Lys(N^{ϵ}-2,4-Cl_2Z), the protected peptide resin to the title compound was prepared after stepwise coupling of the following N^{α}-Boc-protected amino acids (in order of addition): N^{α}-Boc-Trp(N^{i}-For); N^{α}-Boc-Arg(N^{g}-Tos); N^{α}-D-Phe; N^{α}-Boc-His(N^{im}-Tos). The resulting protected peptide resin, Ac-His(N^{im}-Tos)-D-Phe-Arg(N^{g}-Tos)-Trp(N^{i}-For)-Lys(N^{ϵ}-2,4-Cl_2Z)-p-MBHA resin was split into two halves. A 1.4 g (~0.5 mmol) portion of the protected pentapeptide-resin was converted to the protected title peptide resin after coupling N^{α}-Boc-Glu(γ-Bzl), and N^{α}-Boc-Nle. After coupling the last amino acid, the N^{α}-Boc protecting group was removed, the amino group neutralized, and acetylated as reported for compound 1, to give the protected peptide resin Ac-Nle-Glu(γ-Bzl)-His(N^{im}-Tos)-D-Phe-Arg(N^{g}-Tos)-Trp(N^{i}-For)-Lys(N^{ϵ}-2,4-Cl_2Z)-p-MBHA resin. A 1.0 g of the protected peptide resin was subjected to liquid HF cleavage and the peptide processed as reported for 1, to give 356 mg of the crude Ac-[Nle^{4}, D-Phe^{7}, Lys^{10}]α-MSH_{4-10}-NH_2 peptide as a white powder. A 100.0 mg of the crude peptide was subjected to the purification scheme as outlined for 1, to give 65 mg of HPLC pure Ac-[Nle^{4}, D-Phe^{7}, Lys^{10}]α-MSH_{4-10}-NH_2 peptide. The analytical data of the compound are listed in Tables III and IV. A 40.0 mg of pure Ac-[Nle^{4}, D-Phe^{7}, Lys^{10}]α-MSH_{4-10}-NH_2 was cyclized by the same approach used for 1 to give 13 mg of HPLC pure Ac-[Nle^{4}, $\overline{Glu^{5}}$, $\overline{D\text{-}Phe^{7}}$, Lys^{10}]-α-$MSH_{4-10}NH_2$. The physical data for 2 are listed in Table VIII, and the biological potencies are summarized in Table IX.

Ac-[Nle^4, Asp^5, D-Phe^7, Lys^{10}]α-MSH$_{4-10}$-NH$_2$ (3). From 1.4 g (~0.5 mmol) of Boc-His(N^{im}-Tos)-D-Phe-Arg(N^g-Tos)-Trp(N^i-For)-Lys(N$^\varepsilon$-2,4-Cl$_2$Z)-p-MBHA resin (prepared in II), the protected peptide resin of the title compound was prepared by stepwise coupling of N$^\alpha$-Boc-Asp-(β-Bzl) and N$^\alpha$-Boc-Nle. Each coupling reaction was achieved by following the same coupling scheme reported under the general solid-phase peptide methodology. After coupling the last amino acid, the N$^\alpha$-Boc protecting group was removed, the amino group neutralized and acetylated as reported for compound I, to give the protected peptide resin Ac-Nle-Asp(β-Bzl)-His(N^{im}-Tos)-D-Phe-Arg(N^g-Tos)-Trp(N^i-For)-Lys(N$^\varepsilon$-2,4-Cl$_2$Z)-p-MBHA resin. A 1.0 g of the vacuum dried peptide resin was cleaved and processed as mentioned for I to give 370 mg of the crude Ac-[Nle^4, Asp^5, D-Phe^7, Lys^{10}]α-MSH$_{4-10}$-NH$_2$. A portion of the crude heptapeptide (110 mg) was purified by the same procedure used for I to give 82 mg of white powder of the linear title peptide. The analytical data of the compound are listed in Tables III and IV. A 40.0 mg of the pure Ac-[Nle^4, Asp^5, D-Phe^7, Lys^{10}]α-MSH$_{4-10}$-NH$_2$ was subjected to the cyclization scheme as reported for 1, to give after processing and HPLC purification, 12 mg of pure Ac-[Nle^4, Asp^5, D-Phe^7, Lys^{10}]α-MSH$_{4-10}$-NH$_2$. The physical data for 3 are given in Table VIII, and the biological potencies are given in Table IX.

Ac-[Nle^4, Asp^5, D-Phe^7, Orn^{10}]α-MSH$_{4-10}$-NH$_2$ (4). A 1.0 g of p-MBHA resin (0.7 mmol/g) was loaded with N$^\alpha$-Boc-Orn(N$^\gamma$-Z) using the coupling scheme reported in the general solid-phase procedure. After 1

h coupling the reaction stopped, the resin washed, neutralized and the free amino group on the resin acetylated with 2-fold excess of 1:1 mixture of acetic anhydride:pyridine in dichloromethane for 1 h. Then the following amino acids were successfully coupled to the resin by stepwise coupling: N^{α}-Boc-Trp(N^{i}-For); N^{α}-Boc-Arg(N^{g}-Tos); N^{α}-Boc-D-Phe; N^{α}Boc-His(N^{im}-Tos); N^{α}-Boc-Asp(β Bzl); N^{α}-Boc-Nle. Each coupling reaction was achieved by following the same coupling scheme outlined under the general solid-phase peptide methodology. After coupling the last amino acid, the N^{α}-Boc protecting group was removed, the N-terminal amino group neutralized, and acetylated as reported for compound 1, to give the protected peptide resin Ac-Nle-Asp(β-Bzl)-His-(N^{im}-Tos)-D-Phe-Arg(N^{g}-Tos)-Trp(N^{i}-For)-Orn(N^{γ}-Z)-p-MBHA resin. A 1.0 g of the vacuum dried peptide resin was cleaved and processed as outlined under I to give 332 mg of the crude Ac-[Nle^{4}, Asp^{5}, D-Phe^{7}, Orn^{10}]α-MSH_{4-10}-NH_2. A 105 mg of the crude heptapeptide was purified by the method used for I to give 78 mg of white powder of the linear peptide. The analytical data of the compound are listed in Tables III and IV. A 40.0 mg of the pure Ac-[Nle^{4}, Asp^{5}, D-Phe^{7}, Orn^{10}]α-MSH_{4-10}-NH_2 was exposed to the cyclization procedure used for 1, to give, after proper workup, a 15 mg of pure Ac-[Nle^{4}, $\overline{Asp^{5}, D\text{-}Phe^{7}, Orn^{10}}$]α-$MSH_{4-10}$-$NH_2$. The physical data for 4 are given in Table VIII, and the biological potencies are given in Table IX.

Ac-[Nle^{4}, $\overline{Asp^{5}, D\text{-}Phe^{7}, Dab^{10}}$]α-$MSH_{4-10}$-$NH_2$ (5). A 1.0 g of p-MBHA resin (0.7 mmol/g) was coupled with N^{α}-Boc-Dab(N^{γ}-Z) using the

coupling scheme reported in the general solid-phase procedure. After 1 h coupling the reaction stopped, the resin washed, neutralized and the unreacted amino group on the resin acetylated with 2-fold excess of 1:1 mixture of acetic anhydride:pyridine in dichloromethane for 1 h. Then, the following amino acids were successively coupled to the resin by stepwise coupling: N^{α}-Boc-Trp(N^{i}-For); N^{α}-Boc-Arg(N^{g}-Tos); N^{α}-Boc-D-Phe; N^{α}-Boc-His(N^{im}-Tos); N^{α}-Boc-His(N^{im}-Tos); N^{α}-Boc-Asp(β-Bzl); N^{α}-Boc-Nle. After coupling the last amino acid, the N^{α}-Boc protecting group was removed, the N-terminal amino group neutralized, and acetylated as reported for compound 1, to give the protected peptide resin Ac-Nle-Asp(β-Bzl)-His(N^{im}-Tos)-D-Phe-Arg(N^{g}-Tos)-Trp(N^{i}-For)-Dab(N^{γ}-Z)-p-MBHA resin. A 1.0 g of the vacuum dried peptide resin was cleaved and processed as outlined under I to give 318.2 mg of the crude Ac-[Nle^{4}, Asp^{5}, D-Phe^{7}, Dab^{10}]α-MSH_{4-10}-NH_2. A 100.0 mg of the crude heptapeptide was purified according to the procedure used for 1 to give 78.2 mg of white powder of the linear peptide. The analytical data of the compound are reported in Tables III and IV. A 45.0 mg of the pure Ac-[Nle^{4}, Asp^{5}, D-Phe^{7}, Dab^{10}]α-MSH_{4-10}-NH_2 was cyclized and purified as previously discussed to give 13.2 mg of pure Ac-[Nle^{4}, $\overline{Asp^{5}, D\text{-}Phe^{7}, Dab^{10}}$]α-$MSH_{4-10}$-$NH_2$. The physical data for 5 are given in Table VIII, and the biological potencies are given in Table IX.

Ac-[Nle^{4}, $\overline{Asp^{5}, D\text{-}Phe^{7}, Dpr^{10}}$]α-$MSH_{4-10}$-$NH_2$ (6). A 1.0 g of p-MBHA resin (0.7 mmol/g) was coupled with N^{α}-Boc-Dpr(N^{β}-Z) using the

coupling scheme reported in the general solid-phase procedure. After 1 h coupling the reaction stopped, the resin washed, neutralized and the unreacted amino group on the resin acetylated with 2-fold excess of 1:1 mixture of acetic anhydride:pyridine in dichloromethane for 1 h. Then the following amino acids were successively coupled to the resin by stepwise coupling: N^{α}-Boc-Trp(N^{i}-For); N^{α}-Boc-Trp(N^{i}-For); N^{α}-Boc-Arg(N^{g}-Tos); N^{α}-Boc-D-Phe; N^{α}-Boc-His(N^{im}-Tos); N^{α}-Boc-Asp(β-Bzl); N^{α}-Boc-Nle. After coupling the last amino acid, the N^{α}-Boc protecting group was removed, the N-terminal amino group neutralized, and acetylated as reported for compound 1 to give the protected peptide resin Ac-Nle-Asp(β-Zl)-His(N^{im}-Tos)-D-Phe-Arg(N^{g}-Tos)-Trp(N^{i}-For)-Dpr(β-Z)-p-MBHA resin. A 1.0 g of the vacuum dried peptide resin was cleaved and processed as outlined under 1 to give 310.8 mg of the crude Ac-[Nle^{4}, Asp^{5}, D-Phe^{7}, Dpr^{10}]α-MSH_{4-10}-NH_2. A 115.0 mg of the crude heptapeptide was purified according to the procedure used for 1 to give 82.5 mg of white powder of the linear peptide. The analytical data for the compound are reported in Tables III and IV. A 38.3 mg of the pure Ac-[Nle^{4}, Asp^{5}, D-Phe^{7}, Dap^{10}]α-MSH_{4-10}-NH_2 was cyclized and purified as previously discussed to give 11.3 mg of pure Ac-[Nle^{4}, $\overline{Asp^{5}}$, D-Phe^{7}, $\overline{Dpr^{10}}$]α-MSH_{4-10}-NH_2. The physical data for 6 are given in Table VIII, and the biological potencies are given in Table IX.

Frog and Lizard Skin Bioassays. The biological potencies of α-MSH and the cyclic analogues were determined by their ability to sti-

mulate melanosome dispersion in vitro in the frog and lizard bioassays as previously described (Shizume, et. al., 1954; Huntington, et al., 1970). This in vitro assay provides clear cut dose response curves (between 2.5×10^{-11} and 4×10^{-10} M) and can detect minimal concentration of α-MSH of about 10^{-11} M. The assay is based upon the centrifugal dispersion of melanosomes (melanin granules) within the dendritic processes of integumental dermal melanophores leading to darkening of the skin. All the test solutions were prepared via serial dilutions from a stock solution (10^{-4} M). The frogs (Rana pipiens) used in these evaluations were obtained from Kons Scientific, Germantown, WI, and the lizards (Anolis carolinensis) were from the Snake Farm, La Place, LA.

Table VI

Relative in Vitro Potencies of Cyclic α-MSH Analogues in the Frog (Rana pipiens) and Lizard (Anolis carolinensis) Skin Bioassays

Peptide Analogue	Rel. Ptcy. to α-MSH[a] Frog	Lizard	Ref.
Part A. Amino Acids substitution effect			
1. α-MSH	1.0	1.0	
2. [Cys^{4}, Cys^{10}]-α-MSH$_{1-13}$NH$_2$	10.0	2.0	Sawyer, 1984
3. Ac-[Cys^{4}, Cys^{10}]-α-MSH$_{4-13}$NH$_2$	30.0	0.6	Cody, 1984
4. Ac-[Cys^{4}, D-Phe^{7}, Cys^{10}]-α-MSH$_{4-13}$NH$_2$	2.0	6.0	Cody, 1984
5. Ac-[Cys^{4}, Cys^{10}]-α-MSH$_{4-12}$NH$_2$	10.0	1.5	Cody, 1984
6. Ac-[Cys^{4}, D-Phe^{7}, Cys^{10}]-α-MSH$_{4-12}$NH$_2$	20.0	6.0	Cody, 1984
7. Ac-[Cys^{4}, Cys^{10}]-α-MSH$_{4-11}$NH$_2$	0.16	0.07	Cody, 1984
8. Ac-[Cys^{4}, D-Phe^{7}, Cys^{10}]-α-MSH$_{4-11}$NH$_2$	2.5	3.0	Hruby, 1984
9. Ac-[Cys^{4}, Cys^{10}]-α-MSH$_{4-10}$NH$_2$	0.06	0.003	Knittel, 1983
10. Ac-[Cys^{4}, D-Phe^{7}, Cys^{10}]-α-MSH$_{4-10}$NH$_2$	0.75	0.5	Cody, 1984
Part B. Ring Size effect (ring size)[b]			
1. α-MSH	1	1	
2. Ac-[Cys^{4}, Cys^{10}]-α-MSH$_{4-13}$NH$_2$ (23)	30.0	0.60	Knittel, 1983
3. [Mpa, Cys]-α-MSH$_{4-13}$NH$_2$	30.0	1.0	Knittel, 1983
4. [Maa^{4}, Cys^{10}]-α-MSH$_{4-13}$NH$_2$ (22)	0.06	0.06	Lebl, 1984
5. Ac-[Hcy^{4}, Cys^{4}]-α-MSH$_{4-13}$NH$_2$ (24)	0.06	0.70	Lebl, 1984

[a]Biological potencies are measured relative to α-MSH over the linear portion of the dose-response curve.

[b]Ring size = Number of bonds forming the ring of the peptide
Maa = 2-Mercaptoacetic acid
Mpa = 3-Mercaptopropionic acid
Hcy = Homocysteine

Table VII(a). Structure of Cyclic α-Melanotropin Analogues Prepared During This Study

No.	Primary Sequence
	1 2 3 4 5 6 7 8 9 10 11 12 13
1	Ac-Ser-Tyr-Ser-Met-Glu-His-Phe-Arg-Trp-Gly-Lys-Pro-Val-NH_2
2	Ac-Nle-Glu-His-D-Phe-Arg-Trp-Lys-Gly-Pro-Val-NH_2
3	Ac-Nle-Glu-His-D-Phe-Arg-Trp-Lys-NH_2
4	Ac-Nle-Asp-His-D-Phe-Arg-Trp-Lys-NH_2
5	Ac-Nle-Asp-His-D-Phe-Arg-Trp-Orn-NH_2
6	Ac-Nle-Asp-His-D-Phe-Arg-Trp-Dab-NH_2
7	Ac-Nle-Asp-His-D-Phe-Arg-Trp-Dap-NH_2

Table VII(b). Structure of Cyclic α-Melanotropin Analogues Prepared During This Study

1	α-MSH
2	Ac-[Nle^4, Glu^5, D-Phe^7, Lys^{10}, Gly^{11}]-α-MSH$_{4-13}$NH$_2$
3	Ac-[Nle^4, Glu^5, D-Phe^7, Lys^{10}]-α-MSH$_{4-10}$NH$_2$
4	Ac-[Nle^4, Asp^5, D-Phe^7, Lys^{10}]-α-MSH$_{4-10}$NH$_2$
5	Ac-[Nle^4, Asp^5, D-Phe^7, Orn^{10}]-α-MSH$_{4-10}$NH$_2$
6	Ac-[Nle^4, Asp^5, D-Phe^7, Dab^{10}]-α-MSH$_{4-10}$NH$_2$
7	Ac-[Nle^4, Asp^5, D-Phe^7, Dap^{10}]-α-MSH$_{4-10}$NH$_2$

Table VIII. The Analytical Data of Cyclic α-Melanotropin Analogues Synthesized in This Study

Compound	Thin-Layer Chromatography R_f Values in Different Solvent				$[\alpha]_{546}^{23}$ in 10% acetic acid	K	MH^+ Found Calculated
	A	B	C	D			
2	0.76	0.79	0.89	---	-57.8 (c=0.045)	4.01	1291 1290.7
3	0.89	---	0.65	0.18	-13.3 (c=0.015)	5.87	1040.0 1040.1
4	0.65	0.73	0.80	0.29	-54.28 (c=0.07)	6.02	1025.0 1026.1
5	0.66	0.71	0.79	0.28	-37.14 (c=0.07)	5.76	1011.0 1012.1
6	0.77	0.80	0.88		-54.5 (c=0.01)	4.33	997.0 998.08
7	0.77	0.78	0.87		-33.3 (c=0.045)	3.45	983.0 984.05

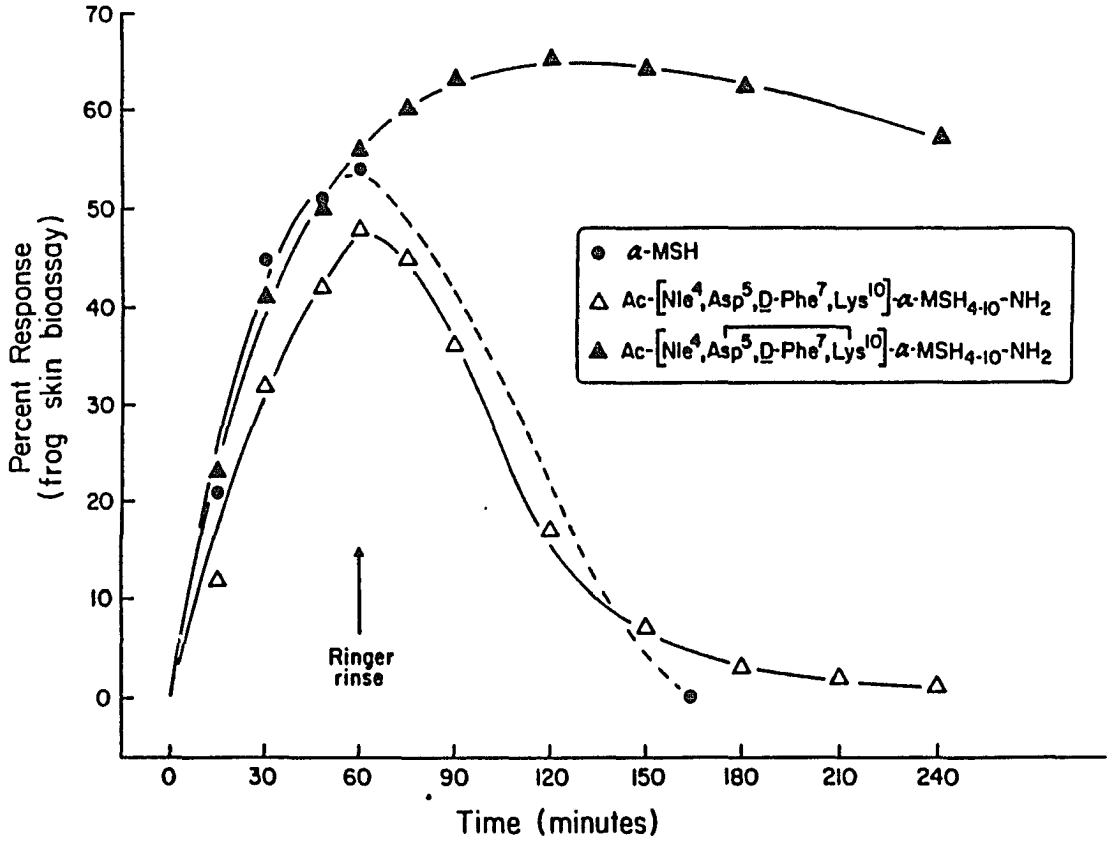

Fig. 3. Demonstration of prolongation effect of linear vs. cyclic analogous Ac-[Nle^4, Asp^5, D-Phe^7, Lys^{10}]α-MSH$_{4-10}$-NH$_2$ in lizard skin.

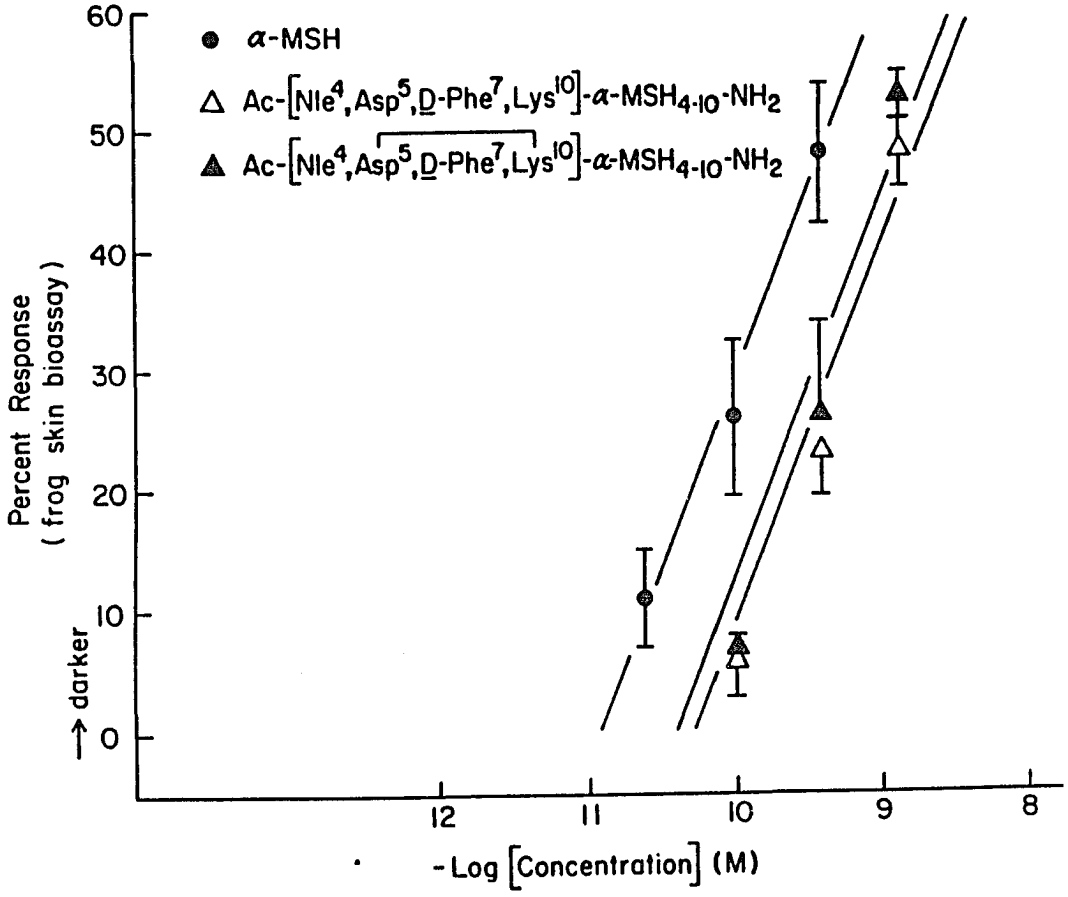

Fig. 4. Comparison of the biological potencies of cyclic and linear analogues of Ac-[Nle^4, Asp^5, D-Phe^7, Lys^{10}]α-MSH$_{4-10}$-NH$_2$ in frog skin.

Table IX. Biological Activities of Cyclic α-Melanotropin Analogues Studied in This Research

	Relative Potency		Prolonged Activity	
Analogue	Frog	Lizard	Frog	Lizard
1	1.0	1.0	p(-)	p(-)
2	1.0	6.0	p(+)	p(+)
3	0.5	9.0	p(+)	p(+)
4	0.5	90.0	p(+)	p(+)
5	1.0	20.0	p(-)	p(-)
6	1.0	5.0	p(-)	p(-)
7	0.01	5.0	p(-)	p(-)

CHAPTER FOUR

CONFORMATIONAL STUDY OF LINEAR AND CYCLIC FRAGMENTS OF MELANOTROPIN BY NMR

To understand the relationships of structure to biological activities of peptides, knowledge of their conformational properties is an important prerequisite (Farmer, 1980; Vida and Gordon, 1984; Hruby, 1981). The importance of peptide conformation in determining the chemical-physical properties which initiate molecular recognition in hormone-receptor interactions, cell differentiation, active transport, and other biological regulatory mechanisms is now generally accepted. Transduction of the signal is then achieved via conformational changes in the receptor-peptide complex which are caused by the complexation (Hruby, 1981; Hruby and Hadley, 1986). Thus far no 3-dimensional structural method is available to study the structure of the complex or the bound hormone at the receptor level. As a result of these limitations, the most reliable approach to understanding the hormone-receptor interaction is via the extensive analysis of the isolated ligand (peptide), especially if conformationally constrained. Although the most popular method of analysis of a single crystalline compound is the X-ray, it is restricted to crystalline samples and gives only information related to the solid state. Many reports have shown the large difference in conformation of a small molecule in solution relative to solid state conformation (Kessler et al., 1981). In addition to the difficulty in getting a pure crystal for small peptides,

the crystal structure often is strongly determined by intermolecular hydrogen bonds, whereas the solution structure is determined primarily by intramolecular interactions. However, it has been shown that in the cases where the energy barrier between the solid-state and solution conformation is high enough, the conformational changes can be followed directly by NMR after dissolution of the crystalline compound (Kessler et al., 1981; Bats et al., 1980). Thus the transfer of X-ray information to the solution conformation as a representative of the bioactive structure should be carried out with care. The best representation of solution conformation can be obtained via NMR studies using as many different media as possible (Kessler, 1982), including micells (Bosch et al., 1980; Thompson and Gierasch, 1984) and artificial membranes (Higashijima et. al., 1987). The best link between X-ray analysis and NMR spectroscopy is provided by solid-state NMR (Opella and Gierasch, 1985). The main advantages of the NMR technique over others with respect to the study of the peptide conformations can be summarized as follows:

1. Single atoms (^{1}H, ^{13}C, ^{15}N) within a molecule can be detected separately in the same sample. The correlation between the spectra of these atoms and their surroundings can be investigated, and hence their analysis permits the determination of the spatial arrangements of the peptide components.

2. The presence of a set of different spectral parameters are available which depend in different ways on molecular conformations, e.g. chemical shifts (δ), coupling constants (J), nuclear Overhauser enhancement (NOE) effects, and relaxation times (T_1, T_2, T_ρ) (Poole and Farach, 1971).

3. The revolution in making assignments of individual signals to the atoms within the molecules as well as the extraction of the relevant spectral parameters, by the application of two-dimensional NMR techniques (Aue et al., 1976; Freeman and Morris, 1979; Bax, 1982, 1984; Benn and Funther, 1983; Wider et al., 1984; Kessler and Bermel, 1985; Bax and Lerner, 1986).

The description of the conformation of peptide is based on certain defined parameters (IUPAC-IUB Commission on Biochemical Nomenclature, 1972) which includes the backbone dihedral angles ϕ, ψ and ω and side chain torsion angles χ. The definition of these angles is illustrated in Fig. 5. The rotational freedom about several bonds in the peptide chain as well as in the side chains leads to the occurrence of a number of different conformations in solution, which normally are in rapid equilibrium with each other on the NMR time scale ($<10^{-4}$ sec). The detection of a distinct rotamer will be possible if the energy barrier for that rotamer to rotate about ψ or ϕ bonds is equal or higher than 4 Kcal/Mol (Kessler, 1970). In addition, free enthalpies of 15 to 17 Kcal/Mol are observed for rotations about amide bonds (Kessler, 1970;

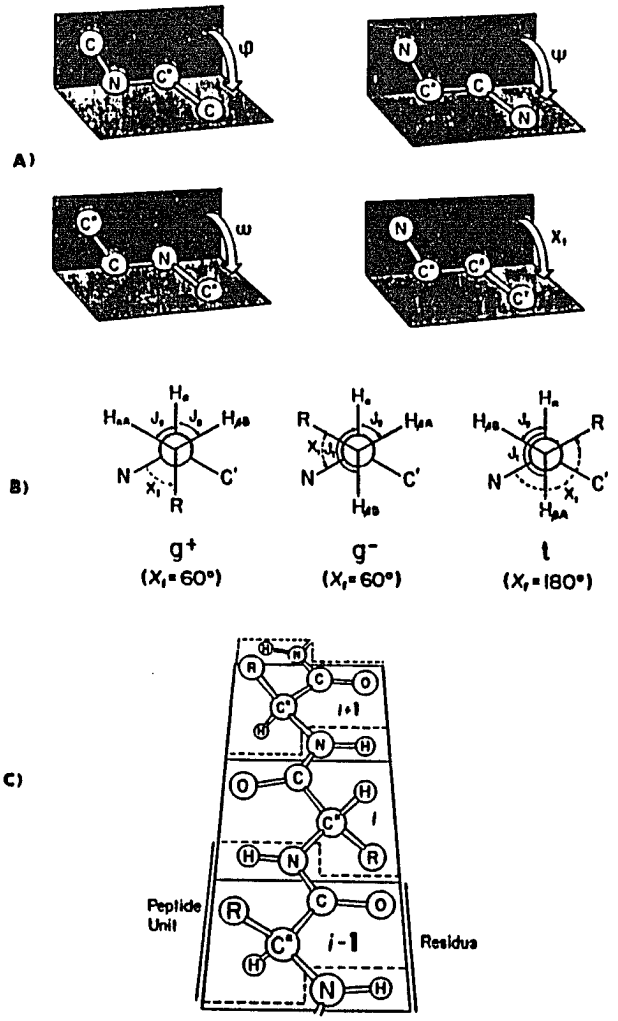

Fig. 5. A. Standard convention for the description of torsion angles in main and side chains. B. Rotation states χ^1 about Cα - Cβ single bond in amino acid side chains and vicinal spin-spin coupling constants $^3J_{CH\alpha - CH\beta}$. C. Standard conventions for the description of residues (broken lines) and peptide units (broken lines) recommended by the IUPAC-IUB commission on Biochemical Nomenclature (1970).

Ackman, 1975). To study such flexible molecules, conformational restriction by either a synthetic approach or via intramolecular hydrogen bonding will be indespensible tools. These approaches will reduce the space available to the large number of conformations that the peptide molecule could attain. Hydrogen bonding is a weak constraining force but it may increase the preferrence of one conformer over the others. Further reduction in the conformational space available to the molecule can be achieved by cyclization of peptides via side chain to side chain or backbone to backbone or any combination of these (Hruby, 1982). Another approach to constraint in peptide can be achieved via proper amino acid substitution or backbone modification (Spatola, 1985).

The full recognition of the importance of cyclic restrictions in designing a biologically active peptides as an approach for the development of peptidic drug is nowadays getting more popular (Hruby, 1985; Vida and Gordon, 1984). The major advantages of the conformational constraint approach can be summarized as follows:

1. The reduction in the number of conformations that are available compared to most linear analogues.

2. Higher selectivity for specific receptor is often found for cyclic structures over the linear analogue (Mosberg et al., 1982, 1983a,b).

3. The in vivo stability can be enhanced several thousands fold over the linear against enzymatic degredation (Akiyama et. al., 1984).

4. Conformationally restriction makes the experimental access to the solution conformation much easier than in the case of linear analogues.

There are several requirements in the NMR study for conformational homogeneity (Kessler, 1982; Jardetzky, 1980; Bundi and Wuthrich, 1979). The most important factors are:

1. Strong differentiation of chemical shifts and coupling constants values of the same amino acid in different position in the same sequence.

2. Strong differentiation of NH chemical shifts and their temperature dependence.

3. Pronounced splitting of the diastereotopic protons of the side-chain moieties.

4. Deviation of $^{3}J_{NH-CH\alpha}$ from its mean value of ~7.5 Hz in the random coil conformation.

5. A linear correlation between the NH chemical shift and the temperature.

6. Independence of coupling constants from solvent or temperature.

The use of these factors as a probe to test whether the molecule is rigid or not, or whether there is a predominant conformer or not, is not absolutely conclusive in most of the cases. Nonetheless they generally are necessary criteria for a predominant conformer. In our study of a prototype fragment of melanotropin using NMR techniques, consideration of these criteria will be referred to most of the time.

Some of the inherent problems which still frustrate the use of NMR technique in peptide conformational study include: (1) in most cases, a larger sample is required than for most other physical methods; (2) the requirement to run several different experiments to remove the ambiguity from some of the results, e.g. in the cases where an overlapping between certain protons occurs. Running these experiments sometimes requires a highly skilled operator, even though the NMR technique is still one of the best ways to examine the structure and conformation of peptides and proteins. In the synthetic peptide case, the availability of large samples does not represent a problem in most cases, so the required experiments can be done on the peptide under study. In this chapter the investigation of proton NMR of four selected peptide analogues will be represented. The selection of these peptides was based on the highly active and least active analogues of the cyclic and linear series. Also, the fact that the cyclic peptides have a different ring size (23 vs 20) was another consideration in their selection. The structures of these peptides are:

I. Ace-[Nle^4, Asp^5, D-Phe^7, Lys^{10}]α-MSH$_{4-10}$NH$_2$.

II. Ace-[Nle^4, Asp^5, D-Phe^7, Dpr^{10}]α-MSH$_{4-10}$NH$_2$.

III. Ace-[Nle^4, $\overline{\text{Asp}^5, \text{D-Phe}^7, \text{Lys}^{10}}$]α-MSH$_{4-10}NH_2$.

IV. Ace-[Nle^4, $\overline{\text{Asp}^5, \text{D-Phe}^7, \text{Dpr}^{10}}$]α-MSH$_{4-10}NH_2$.

Methodology:

In studying any one of the peptide fragments, the following series of experiments were carried out.

1. 1D Spectra:

Here the simple spectra of each peptide (~4 mg/0.3 ml solvent) under study were recorded. The following parameters were used during the study; solvent, DMSO-d_6, D_2O, and H_2O with 10% D_2O were used; the suppression of HOD peak in the case of water solvent was carried out by selective irradiation before data aquisition. Usually 16K spectral points were collected. TSD was used as a reference in aqueous solution, and the DMSO methyl proton was used in the case of DMSO-d_6 as a solvent. Each sample was bubbled for 5-10 min with dry N_2 before use. Conventional 1D spectra were obtained in the Fourier transform mode and the resolution was enhanced with a Gaussian multiplication routine (resolution was 0.36 Hzl point).

2. Temperature Study:

All the temperature studies were done on samples dissolved in DMSO-d_6. The samples were equilibrated for 15-25 min at each temperature before recording the spectra. Usually, at least four different temperatures were used for each sample.

3. 2D Spectra:

The COSY spectra (Jeener experiment $90°-t_1-90°-FID(t_2)$; 256 increments in t_1 and 1024 points in t_2 were recorded) in DMSO and D_2O were used as a tool to assist in the assignment of various peaks in the spectra. Due to the overlapping of the aromatic β and α protons of His, D-Phe and Trp residues, a long range COSY in D_2O was used to remove those ambiguities.

4. Homodecoupling (Double-Resonance):

To further improve the assignment of different protons, the homodecoupling technique was used. The solution of the peptide in D_2O was used in most of these studies.

5. Nuclear Overhauser Enhancement Correlation Spectroscopy (NOESY):

This technique was used to study each of the four peptides in DMSO as a solvent at 25°C. Variations of mixing time were used in the range of 150 millisecond (ms) to 800 ms in 100 ms intervals, in an effort to find the proper mixing times. In all the experiments that were done on linear peptides, we were unable to detect NOEs, so the data from this study will not be discussed in this chapter.

All the NMR spectra were recorded on a Bruker AM 250 Spectrometer equipped with an Aspect 3000 data system and a standard temperature control unit. Figures 5-11 are representative examples of various types of spectra recorded for the different peptides.

Results and Discussion

Peptide I: Ac-[Nle^4, Asp^5, D-Phe^7, Lys^{10}]α-MSH$_{4-10}$-NH$_2$.

The assignments of the various peaks in different solvents were compared with the literature data (Sugg et al., 1986; Rawson et al., 1982; Higuchi et al., 1981). Several attempts have been made previously to study fragments of ACTH$_{4-10}$ or α-MSH$_{4-10}$, which share the same sequence of amino acids, using NMR techniques (Rawson et al., 1982; Higuchi et al., 1981; Cody, 1985; and Sugg et al., 1986). The general conclusion from these studies was that the α-MSH$_{4-10}$ fragments can exist in either a random coil or an extended β-sheet conformation. In our previous extensive structure activity studies of α-MSH, the presence of a β-turn centered around the Phe in position 7 was proposed. This idea was tested by substitution of L-Phe^7 with its enantiomer D-Phe^7 as a way to stabilize the β-turn at that position. The biological data supported that suggestion (Hruby et al., 1984). From the NMR investigation of peptide I, the formation of certain β-turn structures was indicated by the involvement of His^4 in intramolecular hydrogen bonding ($\delta NH/\Delta T$ = 1.4). In addition, the amide NH of D-Phe^7 and Lys^8 were clearly suggested to be hydrogen bonded to some part of the peptide backbone or side chain (Table X). This conclusion came from the fact that the temperature coefficients ($\delta NH/\Delta T$) of amide hydrogen involved in some type of intramolecular hydrogen bonding will be below 3 (Kessler, 1982; Hruby, 1974). The involvement of Trp is also possible since its temperature coefficient is small compared to those

Table (X). Proton NMR parameters in DMSO at 27°C for Ace-[Nle^4, Asp^5, D-Phe^7, Lys^{10}]α-MSH$_{4-10}$NH$_2$. Chemical Shifts Are Relative to TMS.

Amino Acid	Proton Chemical Shifts (ppm)						10^{-3} x δNH/ΔT	
	αCH	βCH$_2$	γCH$_2$	δCH$_2$	Others	NH	NH	Others
Ace	---	---	---	---	1.85			
Nle	4.02	(1.44)	(1.22)	(1.27)	εCH$_3$ 0.83	7.93	3.7	
Asp	4.28	2.60	---	---	---	8.33	4.0	
His	4.42	2.72	---	---	C$_2$H 8.91	7.96	1.4	
					C$_4$H 6.97			
D-Phe	4.35	3.00	---	---	φH 7.25	8.10	2.9	
Arg	4.20	(1.64)	(1.27)	(2.67)	δNH 7.5	8.26	4.2	δNH1.6
Trp	4.50	3.15			Indole	8.19	3.3	Indole
					NH 10.76			NH2.4
					C$_4$H 7.6			
					C$_7$H 7.3			
					C$_2$H 7.17			
					C$_5$H 7.03			
					C$_6$H 7.09			
							4.0	
Lys	4.26	(1.50)	(1.24)	(1.34)	εCH$_2$ 2.53	8.10	2.85	εNH$_2$
								7.73

of NH protons which are exposed to solvent (4 to 7.5). The Arg δ NH protons for this peptide show, also, little temperature dependence. This can be interpreted to result from either intramolecular hydrogen bonding through side-chain to backbone or backbone to backbone interactions.

The Arg $^{\varepsilon}NH_2$ was not clearly identified in the NMR spectra because it was hidden underneath the aromatic protons. Raising the temperature shifted the Arg $^{\varepsilon}NH_2$ out of the aromatic region toward the higher field. The Arg $^{\varepsilon}NH_2$ showed a high temperature dependence. This result was in contradiction to the reported result in the case of the C-terminal-protected peptide H-His-Phe-Arg-Trp-Gly-OMe (Higuchi et al., 1981).

The Trp indole NH was temperature insensitive which was the case in other melanotropin fragments studied by the others (Higuchi et al., 1981). The Lys^8 amide protons showed little dependence on temperature, which may indicate its involvement in an intramolecular hydrogen bonding network. These results clearly indicate that some kind of secondary structure exists for peptide I in DMSO solution. The chemical shift ranges for the NH proton extended over about 0.4 ppm (Table X). This range is wider than that reported for a random coil arrangement, which is within 0.3 ppm (Bundi and Wuthrich, 1979), suggesting the presence of ordered structure in peptide I. Investigation of Table X showed that the N-terminal amino acids Nle^4 and Asp^5 both are exposed to solvent. This fact may indicate that this dipep-

tide tail is flexible with respect to the other part of the peptide. Another amino acid which is highly exposed to solvent is Arg^8. This exposure results from steric hindrance between the side chains of D-Phe^7 and Arg^8, which apparently leads to a slight bending in the peptide backbone in order to relieve this strain. Further investigation of this point is necessary.

Another important factor which can give information about the spatial arrangement of the backbone and side chains in peptide I is the $^3J_{NH-CH\alpha}$ and $^3J_{CH\alpha-CH\beta}$. From investigation of Table XI, the $^3J_{NH-CH\alpha}$ values ranged from 6.9 to 8.13 Hz. This range of amide coupling constants is different than that reported for random coil (6~7Hz) or α-helix (~3Hz) (Bunchi and Wuthrich, 1979; Tonelli and Bovey, 1970; Ferretti and Padillo, 1969). However, this deviation of NH-CHα coupling constant is not very large in comparison to the mean value of ~7.5Hz reported by others (Kessler, 1985). The latter value of $^3J_{NH-CH\alpha}$ is the one which was used in comparison of a fully rigid peptide to a flexible one. In the case of peptide I, the results indicated that this peptide is between the two extreme cases. The empirical relationship between the coupling constant and the dihedral angle (Pardi et al., 1984) (eq. 1) was used to calculate the different possibilities for ϕ angles for each residue (Table XI).

$$^3J(\theta) = 6.4 \cos^2\theta - 1.4 \cos\theta + 1.9 \quad (1).$$

In proteins, however, the dihedral angles ϕ for all amino acid residues except glycine are concentrated in the range from -30° to -180° (Richardson, 1981). In a regular α-helix, ϕ = -57°, and from

Table (XI). Proton NMR Generated Conformational Parameters for Ace-[Nle^4, Asp^5, D-Phe^7, Lys^{10}]αMSH$_{4-10}$NH$_2$ in DMSO

Amino Acids	$^3J_{NH-CH\alpha}$ (Hz)	[a]Possible Torsion Angles (deg)				[b]$^3J_{CH\alpha-CH\beta1}$ $^3J_{CH\alpha-CH\beta2}$ (Hz)	[c]Possible Rotation States of χ^1 (deg)		
		ϕA	ϕB	ϕC	ϕD		g^+	t	g^-
Nle	7.7	60	60	-87	-153	7.6 8.0	0.0	0.59	0.41
Asp	7.4	60	60	-87	-153	9.7 10.7	0.0	0.89	0.11
His	7.8	60	60	-90	-150	6.15 8.45	0.0	0.64	0.36
D-Phe	6.9	-60	60	81	159	5.0 6.95	0.30	0.46	0.24
Arg	7.9	60	60	-90	-150	7.5 6.4	0.06	0.42	0.52
Trp	8.13	60	60	-92	-148	8.2 6.2	0.0	0.39	0.61
Lys	7.5	60	60	-87	-153	7.6 7.7	0.0	0.57	0.43

[a]Calculated according to Bundi and Wuthrich, 1984.

[b]Digital resolution was 0.36 Hzl point.

[c]Calculated according to deLeeuw and Altona, 1982.

equation (1) the corresponding value for $^3J_{HN-CH\alpha}$ = 3.9Hz. For a regular, anti-parallel β-sheet, ϕ = -139° and $^3J_{HN-CH\alpha}$ = 8.9Hz; for a parallel β-sheet, ϕ = -119° and $^3J_{HN-CH\alpha}$ = 9.7Hz. These numbers indicate that $^3J_{HN-CH\alpha}$ should be a useful parameter for distinguishing between α-helical and β-sheet structures. However, it is well-established that the secondary structure elements in globular proteins are usually somewhat distorted (Richardson, 1981), so that they include sizeable deviations in their individual spin-spin couplings from the standard values. In addition to that, the ϕ angles in tight turns and random coil peptide segments are crowded into the same general region as those occupied by helices and β-sheets (Richardson, 1981). However, for peptides deviation in the secondary structure should be even greater, since in general they are more flexible than the globular proteins and their backbone is more exposed to the surrounding environments. Thus, the range of the coupling constants in the case of peptide I is within the region between α-helix and a parallel β-sheet. The possible range of ϕ angles is -87° to -92° for L-amino acids and 81° for D-Phe. This range of values was in a good agreement with the values obtained from the theoretical calculations (Ch. 5). These numbers also are consistent with the distorted type of β-or γ-turn (Rose et al., 1985; Smith and Pease, 1980).

The conformation of the side-chains of amino acid components of peptide have been reported to be essential in receptor recognition and

transduction of peptide hormones (Rose et al., 1985). Thus, from the analysis of the side chain coupling constant, $^3J_{CH\alpha-CH\beta}$, we can deduce the relative population of different conformations. Such treatments are analogous to those used for substituted ethane, where the conformational state at the Cα-Cβ bond is represented in the form of three energetically-stable staggered rotamers g^-, t, g^+ (Fig. 5) corresponding to minimal energy conformation about this bond. The relative conformer populations are determined by differences in their free energies:

$$g^-/t = \exp(-\Delta Fg^-t/RT)$$

$$t/g^+ = \exp(-\Delta Ftg^+/RT)$$

where $\Delta Fg^-t = Fg^- - Ft$ and $\Delta Ftg^+ = Ft - Fg^+$. Since the rotations around the ordinary C-C bond usually are very rapid on a proton NMR time scale ($<10^{-5}$sec) the observed constants are the averaged weighted values for the rotamers (Bystrov, 1976). To determine $H\beta_1$ and $H\beta_2$ is difficult in most of the cases. Without the correct assignment of those protons only the relative population of rotamer g^+ for which both β-protons are gauche to the α-proton, can be estimated. Under such circumstances each of the two other rotamer populations can't be evaluated alone, since the transposition of $H\beta_1$ and $H\beta_2$ leads to the same results.

In earlier work, a priori reasoning was used for selecting the predominant rotamer between g^- and t. However, the assignment can be done by either stereoselective deuterium substitution of one of the β-protons, or by the pH effect on β-proton chemical shifts in certain cases of amino acids, e.g. Asp (Bystrov, 1976).

A more direct, general way of overcoming this ambiguity is by examining the vicinal β-proton coupling with the ^{13}C in the moiety H-Cβ-Cα-^{13}CO chain, and/or with the ^{15}N in the ^{15}N-Cα-Cβ-^{1}H chain. This information, along with the ^{1}H-Cα-Cβ-^{1}H coupling constants, permits the determination of various rotamer populations around the Cα-Cβ bond in amino acids. Recently, new techniques have been introduced which make the exact determination of $H\beta_1$ and $H\beta_2$ and their coupling to Hα much easier. The use of double-quantum spectroscopy (Bodenhausen, 1982) is one of those methods available. The main advantage is that the signals with mutual coupling are spread out in a different way in the ω_1 dimension than in COSY spectra. The separation between these protons will be according to their double-quantum frequencies (i.e., the sum of the frequencies of two coupling protons).

In our study, the assignment of the $H\beta_1$ and $H\beta_2$ protons was based on double resonance, COSY and long range COSY techniques. There was some difficulty in the assignment of β-protons of His^4 due to their overlap with Arg^6 δ CH_2. The values of $^{3}J_{H\alpha-H\beta}$ are listed in Table XI. Using certain emperical relationships, the various populations were calculated (deLeeuw and Altona, 1982; Haasnoot et al., 1980). As expected, the gauch (g^+, +60) rotamer was the least populated of the three possible rotamers (Table XI). However, one interesting features was the presence of an appreciable percent of g^+ in case of D-Phe residue. This suggests that this residue needs to relieve strain resulting from side-chain interaction between the benzyl side chain and the Arg

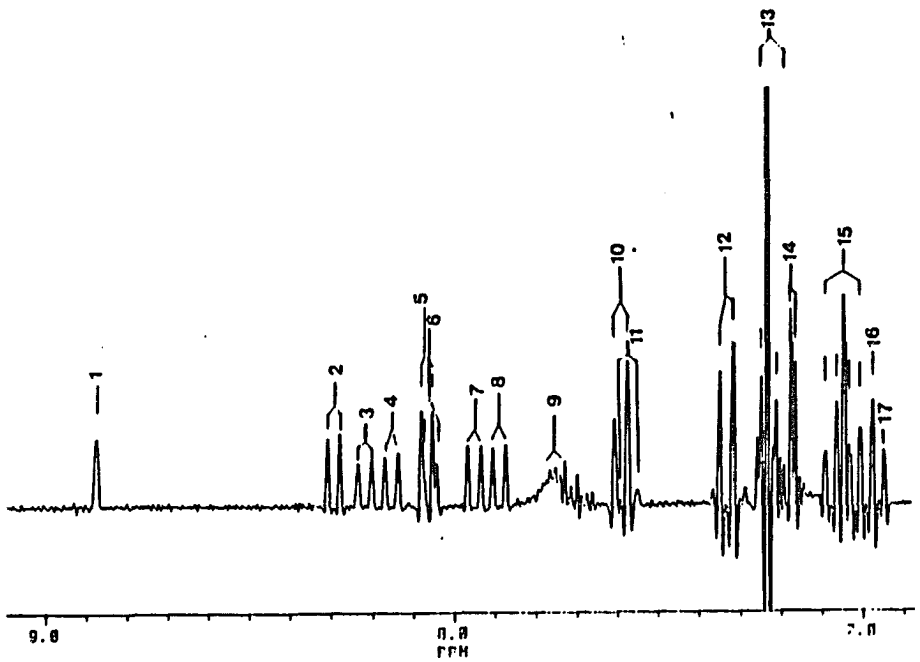

Fig. 6. 1D spectrum of the amide region of Ac-[Nle^4, Asp^5, D-Phe^7, Lys^{10}]-NH_2 in DMSO at 37°C with the following assigned peaks: 1, His 1H, 2; Asp, 3; Arg, 4; Trp, 5; D-Phe, 6; Lys, 7; His, 8; Nle, 9; Lys εNH_2, 10; Trp 4H, 11; Arg δNH, 12; Trp 7H, 13; D-Phe aromatic, 14; Trp 2H, 15; Trp 6H, 5H, 16; His 4H, 17; Arg εNH.

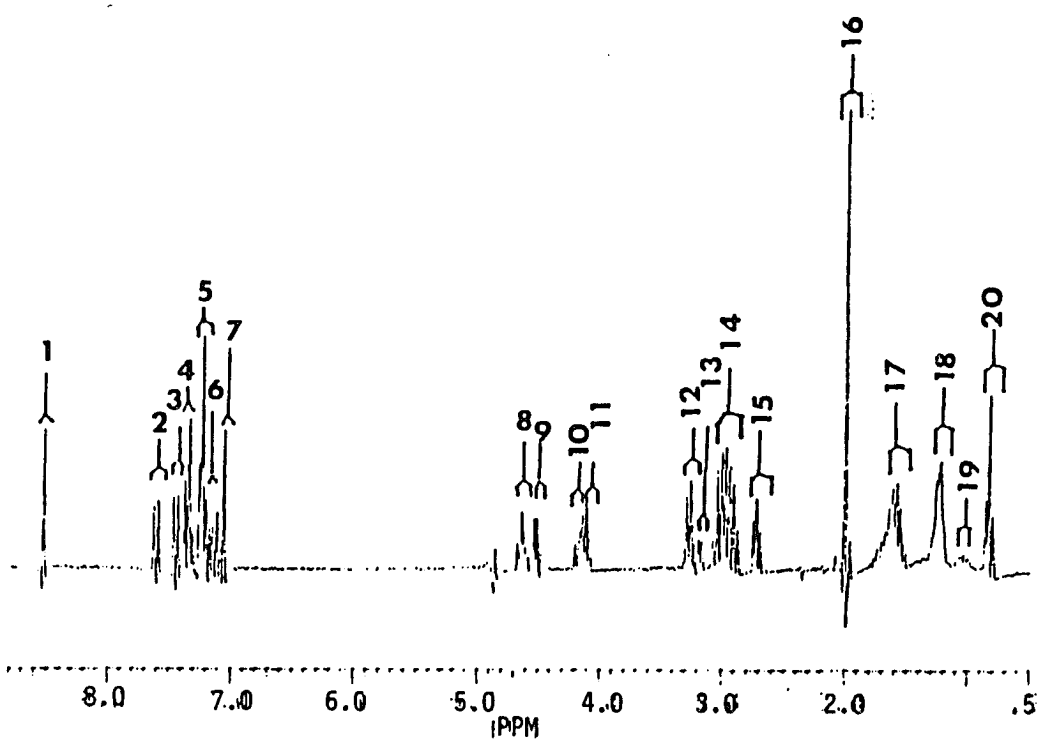

Fig. 7. 1D spectrum of Ac-[Nle^4, Asp^5, D-Phe^7, Lys^{10}]NH_2 in D_2O with HOD suppression. 1; His 4H, 2; Trp 4H, 3; Trp 7H, 4 and 5; D-Phe aromatic, 6; Trp 6H, 5H, 2H, 7; His 4H, 8, 9, Trp, D-Phe, His, Asp δHs, 10, 11; Arg, Lys, Nle δHs, 12; D-Phe βCH_2, 13; Trp βCH_2, 14; His βCH_2, 14; Arg δCH_2, Lys εCH_2, 15; Asp βCH_2, 16; Acetyl, 17; Arg βCH_2, Lys βCH_2, 18; Arg γCH_2, Lys δCH_2, Nle γCH_2, 19; Nle δCH_2, 20; Nle εCH_2.

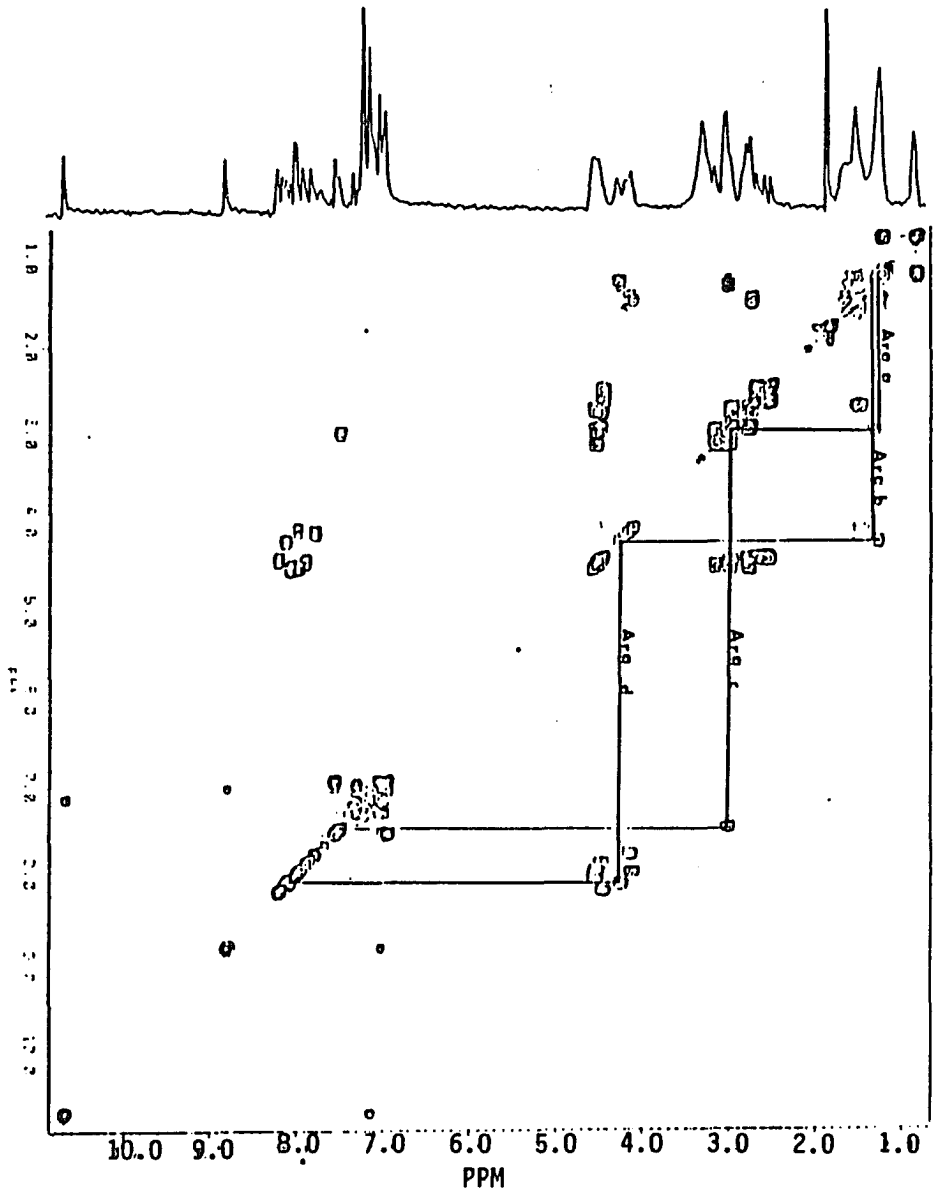

Fig. 8. COSY spectrum of Ac-[Nle^4, Asp^5, D-Phe^7, Lys^{10}]NH_2 in DMSO with the following connectivities: Arg a; CHγ-CHδ, b; CHβ-CHα, c; CHδ-NHδ, d; CHα-NHα.

side chain. This also affected behavior of the Arg side chain conformation which had more g^+ than the rest of the amino acids except D-Phe. The importance of this type of side-chain conformation on biological activity is not clear yet. However, it was reported that substitution of Phe^7 in melanotropin peptides with a 1,2,3,4-tetrahydroisoquinoline-3-carboxylic acid (Tic) caused a 100 fold reduction in the biological activity (Cody, 1985). The side chain conformation of Tic was found to be g^+, suggesting that this might contribute to the reduction in the biological potency of the tested analogue.

In conclusion, the possible secondary structure of peptide I contains a β-type turn with the presence of some g^+ side chain conformation in the D-Phe residue.

Peptide III: Ac-[Nle^4, Asp^5, D-Phe^7, Lys^{10}]α-MSH_{4-10}-NH_2.

In comparing the chemical shifts of the NH protons in peptide III to those in peptide I (Table XII and Table X) the following major differences were observed: (1) Nle^4, His^6, D-Phe^7, Trp^9 and Lys^{10} were shifted down field from 0.05 to 0.5 ppm; (2) Asp^5 and Arg^8 were shifted upfield from 0.2 to 0.8 ppm; the most highly affected amide was the Asp^5 NH proton which were shifted upfield about 0.8 ppm. This shift may be related to a change of side chain conformation such that one of the aromatic side chains is in close proximity to the Asp NH proton. From the computer modeling study (Ch. 5) the folding of the Trp indole ring over the peptide backbone and its proximity to the Asp NH may explain the high shift of the amide protons. Another factor

Table (XII). Proton NMR parameters in DMSO at 27°C for Ac-[Nle^4, Asp^5, D-Phe^7, Lys^{10}]α-MSH$_{4-10}$NH$_2$. Chemical Shifts Are Relative to TMS.

Amino Acid	Proton Chemical Shifts (ppm)						10^{-3} x δNH/ΔT	
	αCH	βCH$_2$	γCH$_2$	δCH$_2$	Others	NH	NH	Others
Ace	---	---	---	---	1.75			
Nle	4.0	1.44	1.25	1.25	εCH$_3$ 0.83	8.48	3.5	
Asp	4.33	2.81	---	---	---	7.49	0.22	
His	4.36	2.96	---	---	C$_2$H 8.8 C$_4$H 7.11	8.20	0.33	
D-Phe	4.42	3.15	---	---	φH 7.34	8.60	7.0	
Arg	4.20	1.64	---	---	δNH 7.87	8.07	5.3	
Trp	4.48	3.22			Indole	8.48	5.0	Indole
					NH 10.88 C$_4$H 7.65 C$_7$H 7.47 C$_2$H 7.24 C$_5$H 7.17 C$_6$H 7.24			NH3.0
Lys	4.13	1.54	1.26	1.65	εCH$_2$ 2.9	8.15	4.0	
Lactam					NH 7.48			lactam 1.77

which supports this possibility is the large change in the temperature coefficient ($\delta NH/\Delta T$) of the Asp NH from 4.0 ppb (in peptide I) to 0.22 ppb (in peptide III). This also may be related to either the shielding of the Asp NH from the solvent or to the involvement of this amide proton in intramolecular hydrogen bonding. In addition, the low $\delta NH/\Delta T$ for His is still maintained after cyclization. This result suggests that there is a turn structure in such types of peptide that the molecule tries to maintain even after the cyclization, while the D-Phe gets more exposed to the solvent. These results suggest that the cyclization does induce some changes in the backbone and the side chain orientations with maintenance of some general features that existed in the linear peptide.

Comparison of the coupling constants of amide protons to their corresponding CHα for the cyclic (Table XII) and linear (Table X) peptides indicates certain changes in the $^3J_{CH\alpha-NH}$ of some amino acids. The largest increase was for His^5 and the smallest change was for Trp^9. These changes indicate that these residues experienced the largest changes upon cyclization. Changes in the values for Asp^5 and Lys^{10} may be related to their involvement in the formation of the lactam bridge. The ϕ torsion angle estimates (Table XIII) did not suggest any major change in backbone conformation of the cyclic peptide relative to the linear analogue. In fact, the values of the ϕ torsion still are within the β-turn type of conformation, centered around the D-Phe^7.

Table ( ). Proton NMR Generated Conformational Parameters for Ac-[Nle^4, Asp^5, D-Phe^7, Lys^{10}]αMSH$_{4-10}$NH$_2$ in DMSO

Amino Acids	$^3J_{NH-CH\alpha}$ (Hz)	[a]Possible Torsione Angles (deg)				$^{a3}J_{CH\alpha-CH\beta1}$ $^3J_{CH\alpha-CH\beta2}$ (Hz)	[b]Possible Rotation States of χ^1 (deg)		
		φA	φB	φC	φD		g^+	t	g^-
Nle	6.9	60	60	-81	-159	7.6 8.0	0.0	0.50	0.50
Asp	7.9	60	60	-90	-150	11.0 11.9	0.0	1.0	0.0
[b]His	8.3	60	60	-93	-147	6.0 6.0	0.29	0.36	0.35
D-Phe	7.2	-60	-60	86	153	6.1 8.0	0.04	0.58	0.38
Arg	7.6	60	60	-87	-153	5.0 8.0	0.17	0.58	0.25
Trp	6.9	60	60	-83	-157	6.0 8.0	0.04	0.58	0.38
Lys	6.7	70	50	-80	-160	8.0 5.2	0.17	0.58	0.25

[a]These values are average numbers from D_20 and DMSO studies, with digital resolution of 0-36 Hzl point.

[b]There was difficulty in the assignment and the values are the average result

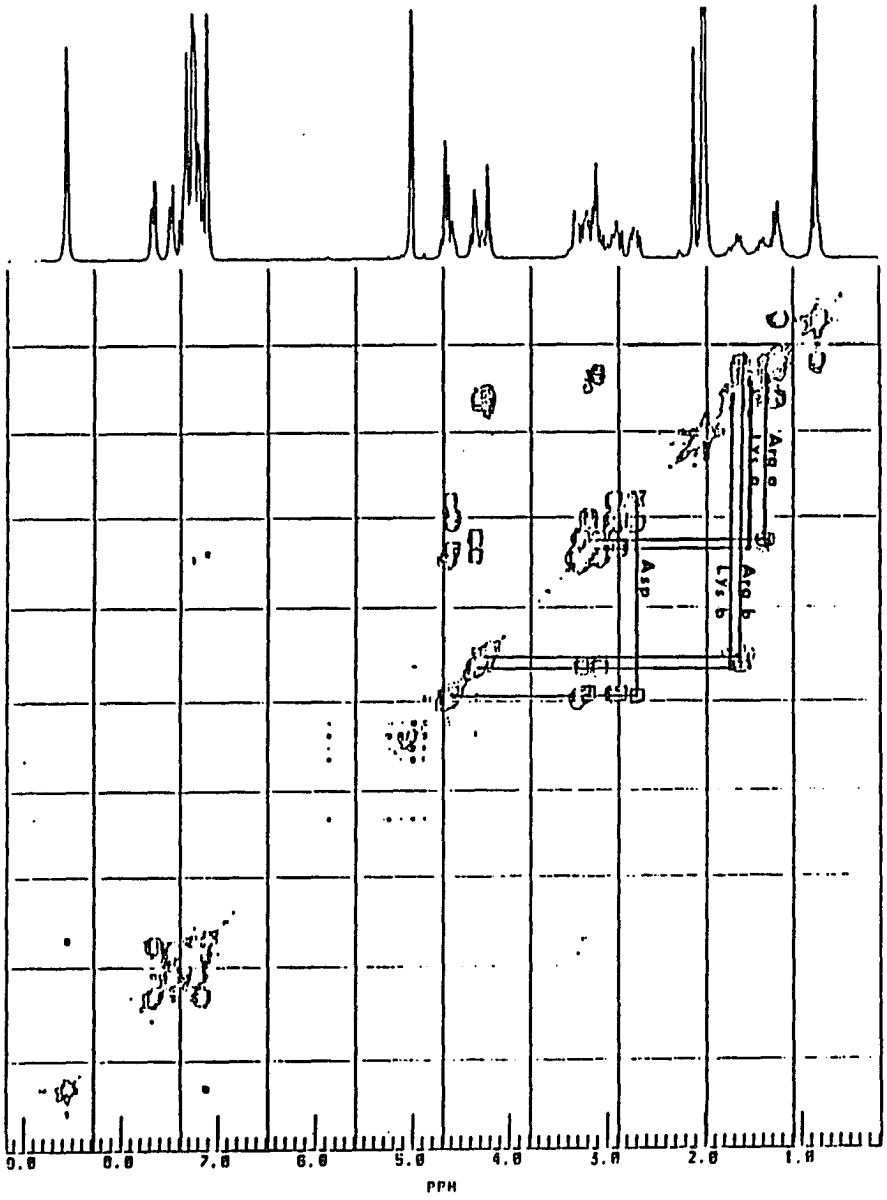

Fig. 9. COSY spectrum of Ac-[Nle^4, Asp^5, D-Phe^7, Lys^{10}]NH_2 in D_2O which illustrate the following connectivities: Arg a; CHγ - CHδ, b; CHα - CHβ, Lys a; CHδ - CHε, b; CHα - CHβ, Asp; CHα - CHβ.

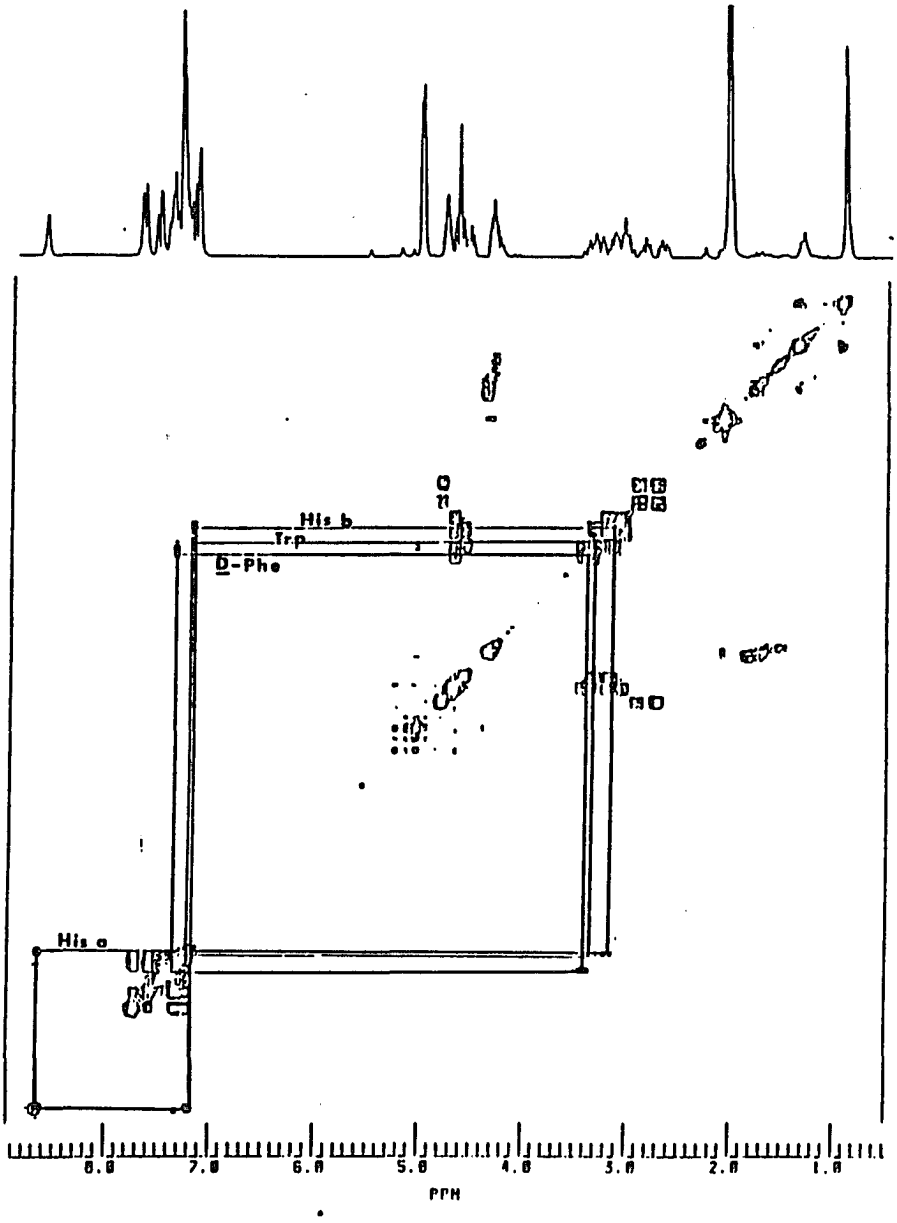

Fig. 10. Long range COSY spectrum of Ac-[Nle^4, Asp^5, D-Phe^7, Lys^{10}]NH_2 in D_2O which illustrate the following connectivities: His a; 4H-2H, b; 4H-CH β, Trp; 2H-CH β, D-_-Phe; 2, 6H-CH β.

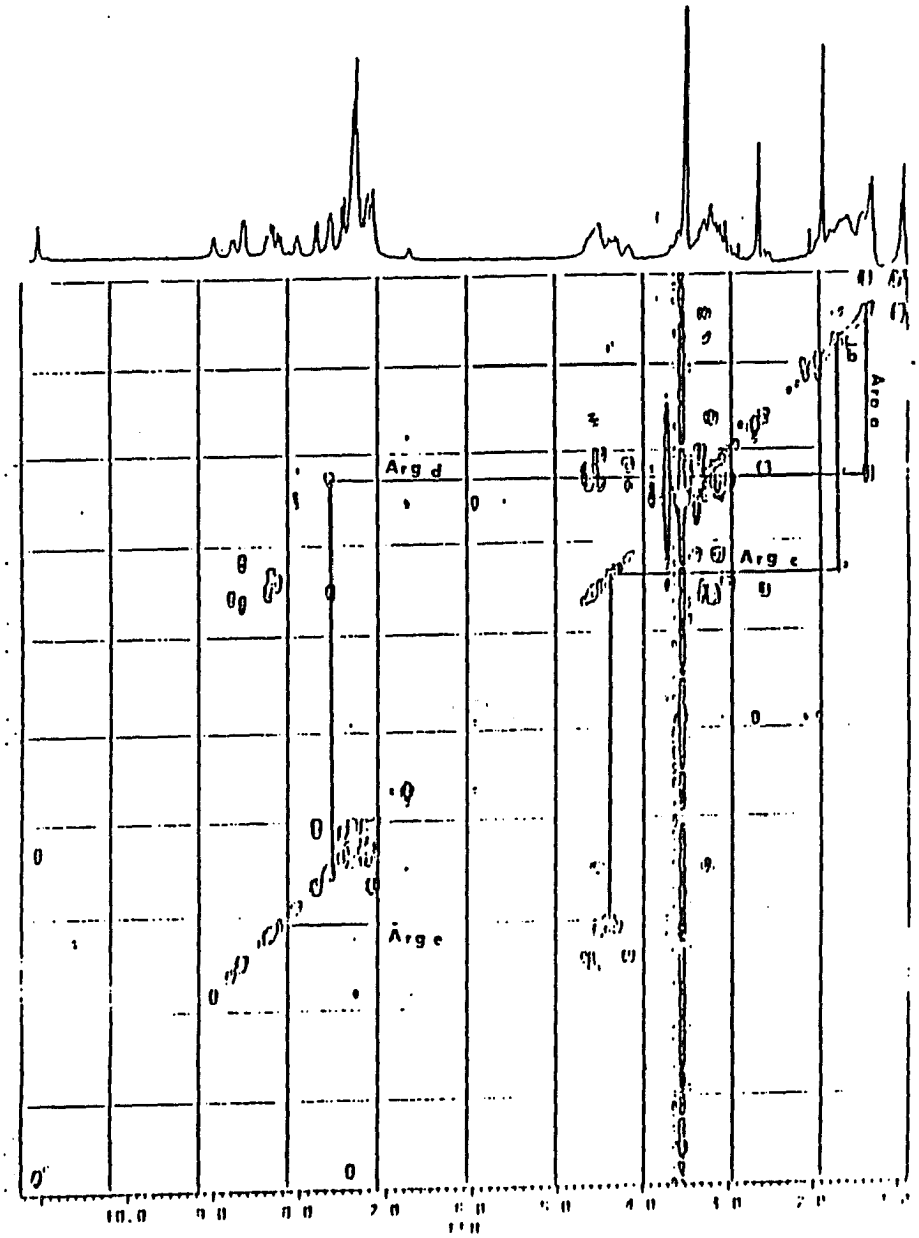

Fig. 11. COSY spectrum of Ac-[Nle^4, Asp^5, D-Phe^7, Lys^{10}]NH$_2$ in DMSO showing the following connectivities: Arg a; CHγ-CHβ, b; CHγ-CHβ, c; CHβ-CHα, d; CHδ-NHδ, e; CHα-NHα.

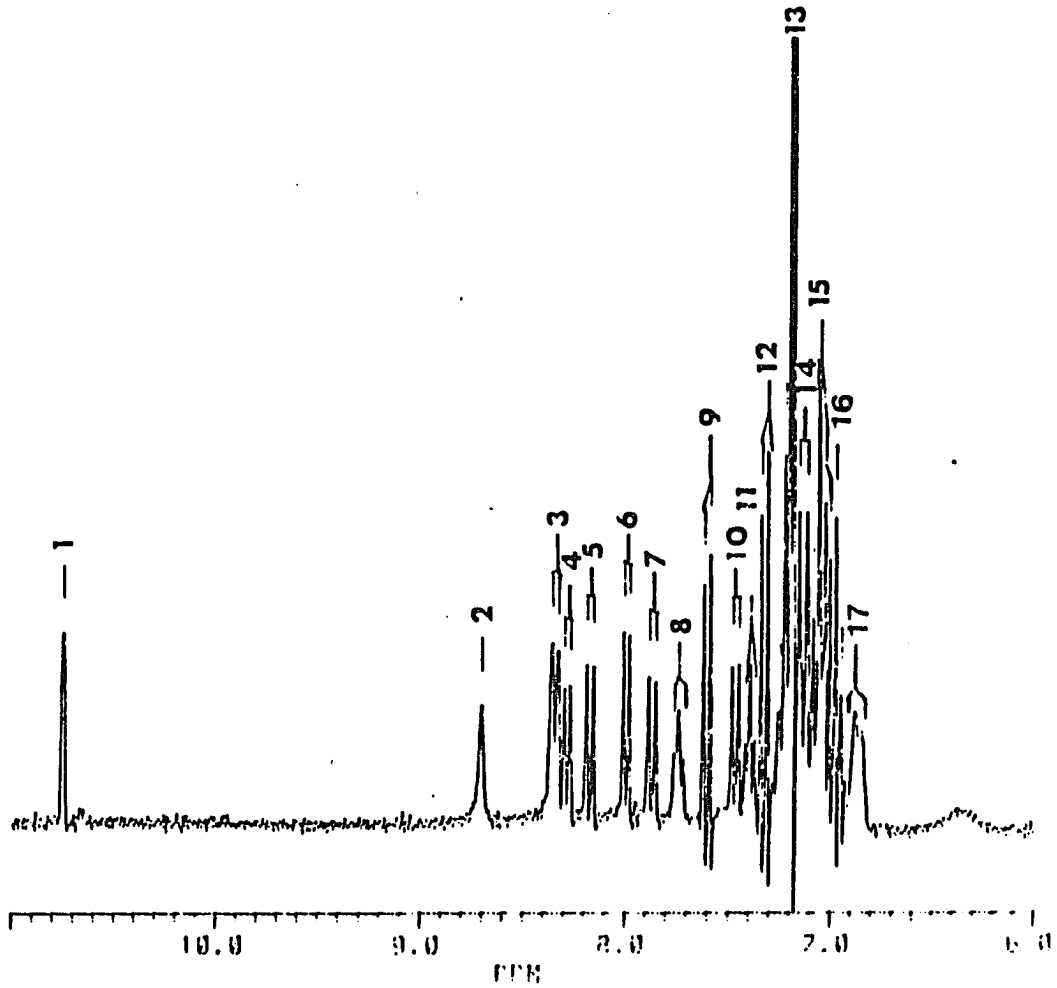

Fig. 12. 1D spectrum of the amide region of Ac-[Nle^4, Asp^5, D-Phe^7, Lys^{10}]NH_2 in DMSO at 61°C showing the following assigned peaks: 1; Trp 1H, 2; His 2H, 3; D-Phe, 4; Nle, 5; Trp, 6; His, 7; Lys, 8; Arg δNH, 9; Trp 7H, 10; Arg, 11; Lys εCH_2-εNH (Lactam), 12; Trp 4H, 13; D-Phe aromatic, 14; Trp 2H, 15; Trp 6H, 5H, 16; His 4H, 17; Arg εNH.

Furthermore, examination of the side chain populations based on the $^3J_{CH\alpha-CH\beta}$ did not indicate any major changes relative to the linear peptide (Table XIII and Table XI) except that there is a large change in the D-Phe^7 χ^1 from partially gauche + (g^+) in the linear case to mostly trans in the cyclic peptide. This result was consistent with the theoretical studies (Ch. 5).

In conclusion, these results suggest that cyclization induced some changes in the backbone as well as in the side chain conformations, with the changes centered around the His^5 and Trp^9 residues and to a certain extent D-Phe^7 and Arg^8. These changes may be correlated to the 100 fold increase in biological potency upon cyclization (Table V, Ch. 2 and Table IX, Ch. 3), and to the prolonged biological activity of the cyclic analogue.

Peptide II: Ac-[Nle^4, Asp^5, D-Phe^7, Dpr^{10}]α-MSH$_{4-10}$-NH$_2$.

Comparison of the chemical shift of the amide protons of peptide II and peptide I suggest that there is no difference between the two (Table X and Table XIV). This result is expected since the only difference between the two is the C-terminal substitution of Lys^{10} by 1,3-diaminopropionic acid (Dpr). There is a 0.18 ppm difference in chemical shift between the Lys^{10} amide NH and the Dpr amide NH which may result from the induction effect of β-NH$_2$ in the latter case. Other side chain and CHα chemical shifts are almost identical in the two peptides. However, the temperature effect of the amide protons on the two peptides is totally different. In the case of peptide II, the

Table (XIV). Proton NMR parameters in DMSO at 25°C for Ac-[Nle^4, Asp^5, D-Phe^7, Dpr^{10}]α-MSH$_{4-10}$-NH$_2$. Chemical Shifts Are Relative to TMS.

Amino Acid	Proton Chemical Shifts (ppm)						10^{-3} x$_{\delta NH/\Delta T}$	
	αCH	βCH$_2$	γCH$_2$	δCH$_2$	Others	NH	NH	Others
Ace	---	---	---	---	1.82			
Nle	4.10	1.42	1.22	1.20	εCH$_3$ 0.81	8.04	3.99	
Asp	4.42	2.76				8.28	3.86	
His	4.44	3.02			C$_2$H 8.53	8.15	3.86	
D-Phe	4.47	2.92 2.86			φH 7.21	8.08	4.16	
Arg	4.26	1.62			δNH 7.54	8.23	4.25	δNH6.11
Trp	4.52	3.18			Ind.	8.11	4.3	Ind.
		3.12			NH 10.73 C$_2$H 7.17 C$_4$H 7.55 C$_5$H 6.95 C$_6$H 7.03 C$_7$H 7.30			NH 3.75
Dpr	4.4	2.54 2.44			βNH$_2$ 7.39	7.92	1.77	βNH$_2$5.6

Table (XV). Proton NMR Generated Conformational Parameters for Ac-[Nle^4, Asp^5, D-Phe^7, Dpr^{10}]αMSH$_{4-10}$NH$_2$ in DMSO

Amino Acids	$^{a3}J_{NH-CH\alpha}$ (Hz)	Possible Torsion Angles (deg)				$^{a3}J_{CH\alpha-CH\beta1}$ $^{3}J_{CH\alpha-CH\beta2}$ (Hz)	Possible Rotation States of χ^1 (deg)		
		ϕA	ϕB	ϕC	ϕD		g^+	t	g^-
Nle	7.4	60	60	-87	-15	8.1 6.7	0.0	0.44	0.56
Asp	7.3	60	60	-85.5	-154.5	7.5 7.5	0.0	0.54	0.46
His	7.3	60	60	-85.5	-154.5	7.5 7.25	0.0	0.53	0.47
D-Phe	7.2	-60	-60	85	155	5.0 5.0	0.54	0.24	0.22
Arg	8.0	60	60	-91	-149	8.25 4.0	0.26	0.60	0.14
Trp	7.1	60	60	-85	-155	9.0 9.0	0.0	0.72	0.18
Dpr	8.2	60	60	-92	-148	7.25 7.25	0.0	0.51	0.49

[a]Digital resolution was 0.36 Hzl point.

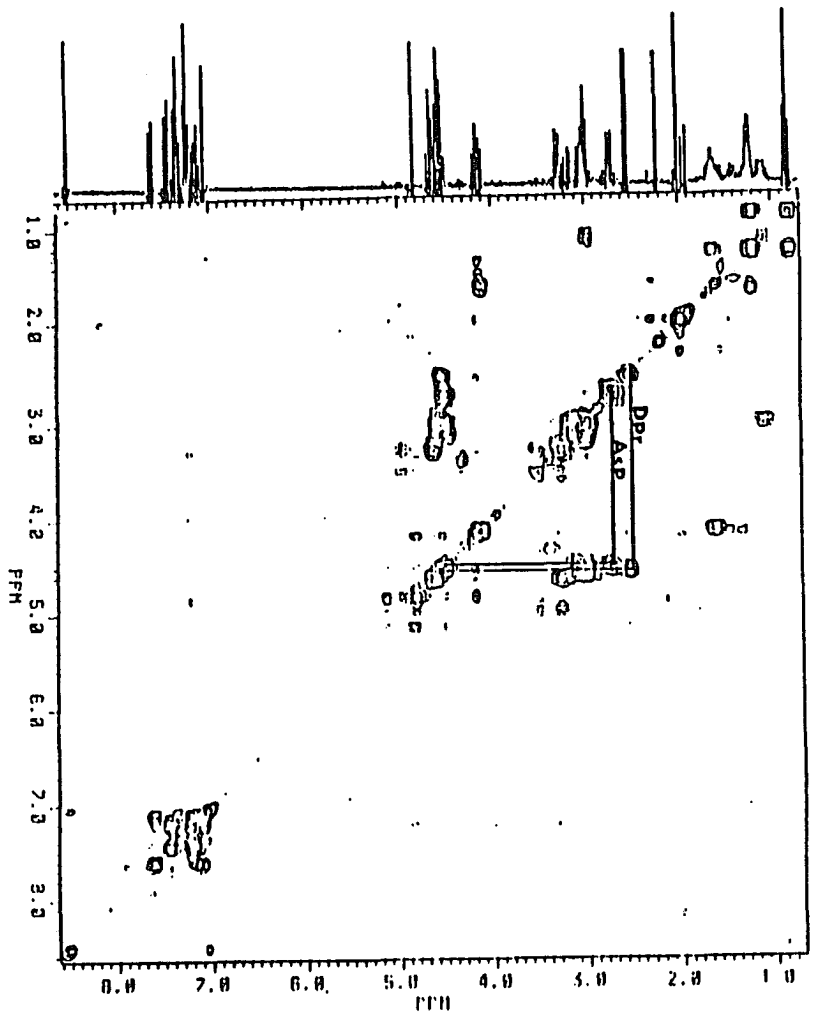

Fig. 13. COSY spectrum of Ac-[Nle^4, Asp^5, D-Phe^7, Dpr^{10}]NH_2 in D_2O showing the following connectivities: Dpr; CHβ-CHα, Asp; CHβ-CHα.

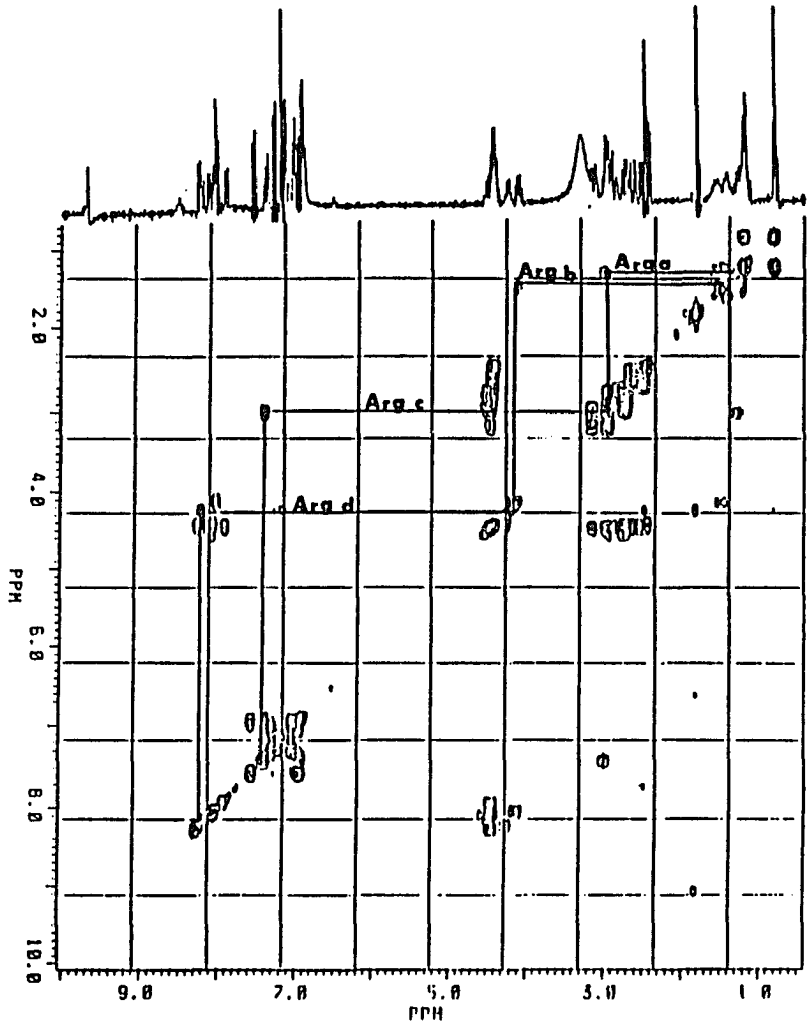

Fig. 14. COSY spectrum of Ac-[Nle^4, Asp^5, D-Phe^7, Dpr^{10}]NH_2, in DMSO showing the following connectivities: Arg a; CHγ-CHδ, b; CHβ-CHα, c; CHδ-NHδ, d; CHα-NHα.

only amide proton which showed a low $\delta NH/\Delta T$ was that of Dpr, while all the others appear to be exposed to the solvent. This result may be related to the difference in the topography of peptides as a result of the decreased length of the Lys^{10} side-chain ($4CH_2$) relative to the Dpr side-chain ($1CH_2$). Such an effect was not expected. Interestingly, the temperature coefficient $\delta NH/\Delta T$ of the Arg^{8} δNH suggested that the availability of this group to the solvent is more than that in the case of peptide I.

Generally, the backbone conformation of peptide II is closely related to that in peptide I with maintainance of the β-turn type of structure (Table XV and Table XI). However, the relationship in side-chains conformations of peptide I and II have some pronounced differences (Table XI and Table XV). The major differences are in χ^1_5 and χ^1_6 where both have much more g^+ in peptide II than in peptide I. These results, in general, are consistent with our theoretical study on these peptides (Ch. 5) in that χ^1_5 and χ^1_6 have more g^+ character over the molecular dynamic simulation time.

Peptide IV: Ac-[Nle^{4}, $\overline{Asp^{5}, \underline{D}\text{-}Phe^{7}, Dpr^{10}}$]αMSH$_{4-10}$-$NH_2$.

The cyclized peptide IV was chosen for a careful NMR and theoretical study since this cyclic 20-membered ring peptide had about a 100 fold reduction in potency relative to the linear analogue II (Table V, Ch. 2 and Table IX, Ch. 3). In this section the results of the NMR investigation will be presented. Examination of the CHα chemical shifts for various residues (Table XVI), indicated that the major

changes were an upfield shift for His^6 of 0.23 ppm and a downfield shift for Trp^8 of 0.12 ppm in peptide IV relative to peptide II. These changes clearly indicate that cyclization affected the overall conformation of this peptide. Furthermore, the aromatic protons of D-Phe^7 in peptide IV experience a low field shift of 0.29 ppm relative to that found for the same protons in peptide II. These effects can be related to the anisotropic effect between the imidazole ring of His^6 and the phenyl group of D-Phe^7.

The downfield shift in the N-terminal acetyl group chemical shift of 0.15 ppm relative to that in peptide II is an additional parameter indicating that the conformation of the cyclic peptide is different than its linear analogue.

Obviously, the amide sensitivity to temperature changes for peptide IV is slightly different from that in peptide II as is shown in Table XVI. The peptide NH of Nle^4 and His^6 and the Arg^8 δNH in peptide IV are much more solvent protected than in peptide II. Thus, certain conformational folding has resulted on cyclization of peptide II to give IV.

In comparing the backbone ϕ angles of peptides II and IV, as calculated from $^3J_{NH-CH\alpha}$ of those peptide (Table XV and Table XVII), a general conclusion can be drawn: there is an appreciable difference in the backbone conformations of these peptides. The major changes were centered around the D-Phe^7, Arg^8 and Trp^9 residues (Table XV and Table XVII). There is a clear β-turn of type II involving D-Phe^7 - Arg^8 in

Table (XVI). Proton NMR parameters in DMSO at 27°C for Ac-[Nle^4, Asp^5, D-Phe^7, Dpr^{10}]α-MSH$_{4-10}$-NH$_2$. Chemical Shifts Are Relative to TMS.

Amino Acid	Proton Chemical Shifts (ppm)						10^{-3} x δNH/ΔT	
	αCH	βCH$_2$	γCH$_2$	δCH$_2$	Others	NH	NH	Others
Ace	---	---	---	---	1.97			
Nle	4.19	1.45	1.60	1.30	εCH$_3$ 0.85	8.51	2.1	
Asp	4.57	2.77				8.62	5.7	
His	4.67	3.04			C$_4$H 7.14	7.91	3.0	
					C$_2$H 8.55			
D-Phe	4.48	3.30			φH 7.50	8.42	3.8	
Arg	4.27	1.66	1.27	3.04	δNH 7.52	8.20	4.0	δNH2.0
Trp	4.40	3.20			Ind.	8.10	5.2	
					NH 10.89 C$_4$H 7.63 C$_7$H 7.50 C$_6$H 7.22 C$_5$H 7.17		4.0	
Dpr	4.41	3.72	---	---				
Lactam	---	---	---	---	NH 7.16			lactam 4.3

Table (XVII). Proton NMR Generated Conformational Parameters for Ac-[Nle^4, Asp^5, D-Phe^7, Dpr^{10}]α-MSH$_{4-10}$-NH$_2$ in DMSO

Amino Acids	$^{a}3J_{NH-CH\alpha}$ (Hz)	Possible Torsion Angles (deg)				$^{a}3J_{CH\alpha-CH\beta1}$ $^{3}J_{CH\alpha-CH\beta2}$ (Hz)	Possible Rotation States of χ^1 (deg)		
		φA	φB	φC	φD		g^+	t	g^-
Nle	7.2	60	60	-84	-156	7.00 7.25	0.02	0.50	0.48
Asp	7.2	60	60	-84	-156	7.5 9.0	0.0	0.70	0.30
His	8.2	60	60	-93	-147	6.8 7.8	0.0	0.57	0.43
D-Phe	4.7	-21	-99	64	176	5.0 5.0	0.48	0.29	0.23
Arg	5.5	90	30	-70	-170	7.0 7.5	0.0	0.53	0.47
Trp	9.0	60	60	-102	-138	5.0 10.2	0.0	0.83	0.17
Dpr	8.2	60	60	-93	-147	5.0 7.50	0.23	0.52	0.25

[a]Digital resolution was 0.36 Hz/ point.

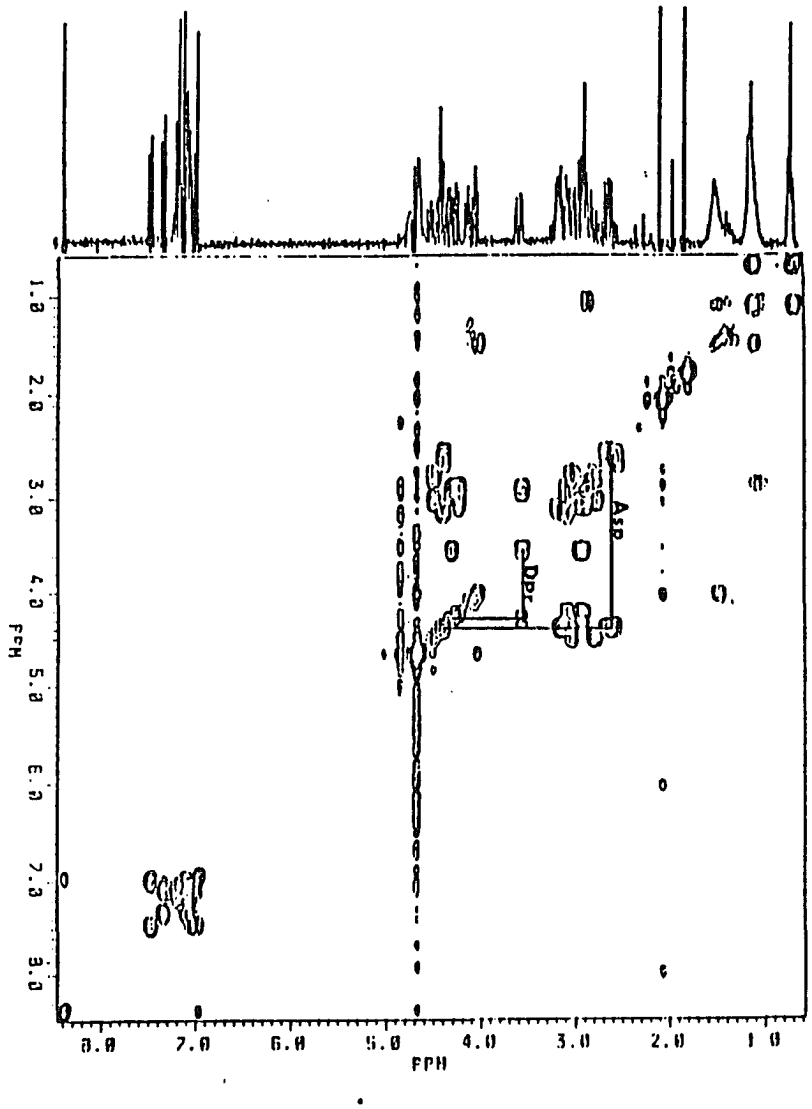

Fig. 15. COSY spectrum in D_2O of Ac-[Nle^4, Asp^5, D-Phe^7, Dpr^{10}]NH_2 in D_2O showing the following connectivities: Asp; CHβ-CHα, Dpr; CHβ-CHα.

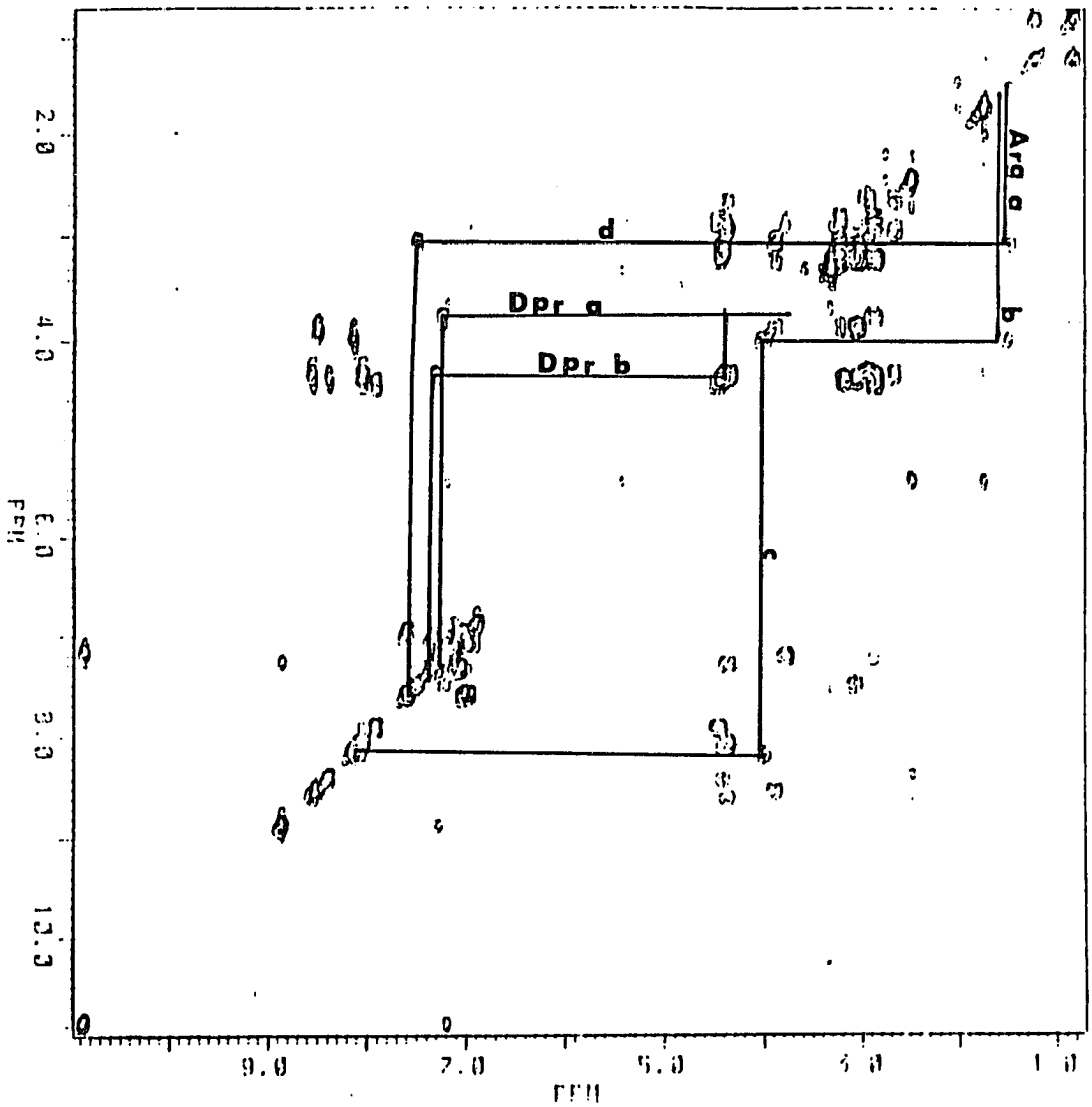

Fig. 16. COSY spectrum of Ac-[Nle^4, Asp^5, D-Phe^7, Dpr^{10}]NH_2 in DMSO showing the following connectivities: Arg a; CHγ-CHδ, b; CHβ-CHα, c; CHα-CHα, d; CHδ-NHδ, Dpr a; NHβ-CHβ (Lactam), b; CHα-NHα.

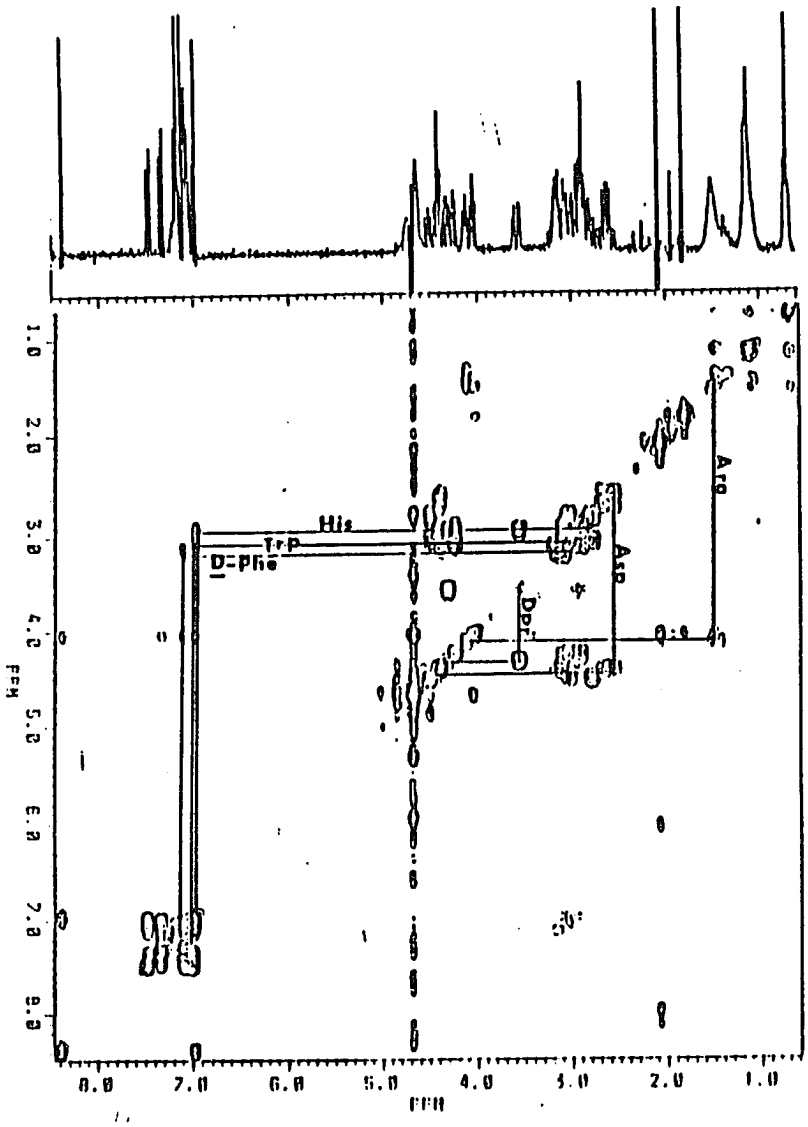

Fig. 17. Long range COSY spectrum of Ac-[Nle^4, Asp^5, D-Phe^7, Dpr^{10}]NH_2 in D_2O showing the following connectivities: Arg; CHβ-CHα, Asp; CHβ-CHα, Dpr; CHβ-CHα, His; 4H-CHβ, Trp; 2H-CHβ, D-Phe; 2, 6H-CHβ.

peptide IV which is not so clear in peptide II. In addition, a much greater contribution of the g^+ conformation of the D-Phe^7 side-chain is observed in peptide IV relative to II. Also there is more of the g^+ in the χ^1_8 in peptide IV relative to II. These results, again, are consistent with our theoretical studies (Ch. 5).

In conclusion, from all the NMR studies the following conclusion can be made: (1) the cyclization through side-chain lactam bridge induces an appreciable change in the topography of the molecules, and the effect increases relative to the ring size; (2) different ring sizes have different conformational features; (3) the most sensitive conformational parameters affected by cyclization were the side-chain conformations; (4) the maintainance of D-Phe side chain in g^+ conformation resulted in a lowering of the biological potency, while the trans conformation is favored for highly potent analogues; (5) ring constraint may lead to more backbone exposure to the solvent; (6) most of the NMR results are consistent with the theoretical studies with a tendency of the NMR to give an average structure with respect to the theoretically generated structures.

CHAPTER FIVE

DYNAMICS AND CONFORMATIONAL ENERGETICS OF LINEAR AND CYCLIC ANALOGUES OF α-MSH$_{4-10}$-NH$_2$.

Melanotropin stimulating hormone is a tridecapeptide secreted by the pars intermedia lobe of the pituitary gland (see Chapter 2). Since 1981 several attempts have been made to study the available conformational space for this peptide hormone and its fragment analogues (Nikiforovich et al., 1981). In addition, several different physical methods have been used, to elucidate the most probable three-dimensional structure of α-MSH and its fragments analogues (Cody et al., 1987, Ch. 4). The heptapeptide Met-Glu-His-Phe-Arg-Trp-Gly is a common fragment of α-MSH and ACTH. In our study of the modified form of this heptapeptide, Ac-Nle-Xxx-His-D-Phe-Arg-Trp-Yyy-NH$_2$, we were interested in correlating the theoretical structure of some of these heptapeptide fragments with their biological activity. The following peptides were selected as prototypes for this study.

I. Ac-Nle-Asp-His-D-Phe-Arg-Trp-Lys-NH$_2$.

II. Ac-Nle-Asp-His-D-Phe-Arg-Trp-Dpr-NH$_2$.

III. Ac-Nle-Asp-His-D-Phe-Arg-Trp-Lys-NH$_2$.

IV. Ac-Nle-Asp-His-D-Phe-Arg-Trp-Dpr-NH$_2$.

These peptides were chosen on the basis of their possessing the highest and the lowest biological potencies (see Table V, Ch. 2, and Table IX, Ch. 3).

Investigations of such peptides can provide answers to many

questions that can be asked in an attempt to understand the correlation between biological activity and the topographical structure or structures that are available to these peptides (Hruby et al., 1982; Strothers et al., 1984). Questions such as what are the conformations accessible to these peptide molecules, what kind of relationship(s) exists between these conformations and the amino acid sequence of the peptides, what are the major intramolecular forces that determine these structural characteristics and the dynamic properties of these peptide fragments, etc. can be asked. In order to answer some of these questions, we report in this chapter on the results obtained from a molecular mechanical analysis of peptides I, II, III and IV.

Methodology

As an initial hypothesis, these peptides are thought to have conformations in solution which are a time average of various low-energy molecular conformations in equilibrium (Glickson, 1975). Thus, in this study, as in the liquid state, we must account for an ensemble of potential conformations accessible to these peptides. One of the computer simulation methods which can be used to explore the configuration space of such a non-ordered system is molecular dynamics (Karplus and McCammon, 1981; McCammon and Karplus, 1980). In molecular dynamics, we express the potential energy, V, of the molecule in terms of an analytical representation of all internal degrees of freedom and interatomic distances of the system (Eq. 1).

$$V = \sum\{D_b[1-e^{-\alpha(b-b_o)^2}]-D_b\} + 1/2\ \sum H_\theta\ (\theta-\theta_o)^2$$
$$+ 1/2\ \sum H_\phi\ (1+s\ \cos n\phi) + 1/2\ \sum H_\chi \chi^2$$
$$+ \sum\sum F_{bb}\ (b-b_o)(b-b_o)$$
$$+ \sum\sum F_{\theta\theta}\ (\theta-\theta_o)(\theta-\theta_{oo})$$
$$+ \sum\sum F_{b\theta}\ (b-b_o)(\theta-\theta_o) \qquad (1)$$
$$+ \sum\sum\sum F_{\phi\theta\theta}\ \cos\phi(\theta-\theta_o)(\theta-\theta_o)$$
$$+ \sum\sum F_{\chi\chi}\ \chi\chi$$
$$+ \sum\varepsilon[2(r^*/r)^{12}-3(r^*/r)^6]+\Sigma\ q_i q_j/r$$

This expression reflects the energy necessary to stretch bonds from their unstrained geometries, and to generate strain in torsions (ϕ) by twisting atoms about the bond axis determining the torsional angle. Here D_b, α, H_θ, H_ϕ, H_χ, F_{bb} , $F_{\theta\theta}$, $F_{b\theta}$, $F_{\phi\theta\theta}$, and $F_{\chi\chi}$ are force constants for the corresponding deformations; s defines the phase of the torsion potential; b_o and θ_o are the unstrained values of bonds and angles, respectively; and r, ε, and q are the van der Waals radii, depth of the van der Waals potential, and partial atomic charges, respectively (Hagler, 1986). As a result of vibrational spectroscopy and normal mode analysis, it has been shown that these internal deformations are coupled, and this is represented by the cross terms in eq. 1., e.g. b and b or b and θ. Finally, the nonbonded and Coulomb interactions, representing steric replusions, attractions, and electrostatic interations, are represented by the last three terms in eq. 1, respectively.

After specifying the potential energy of the molecule, the initial conditions can be defined by selecting a set of initial velocities

for each of the atoms. Once the initial conditions are given, Newton's equation of motion is integrated forward in time (Eqs. 2 & 3).

$$F_i = ma_i \quad (2)$$

$$-\frac{\partial V(r_i \ldots r_n)}{\partial r_i} = F(r_i \ldots r_n) = m_i \frac{d^2 r_i}{dt^2} \quad (3)$$

Where F_i is the force on atom i, r_i represents the (x,y,z) coordinates of atom i, m_i is its mass, and a_i is its acceleration. By integrating Newton's equation, the trajectory of the atom as a function of time can be estimated. In this way, the concerted motions of the individual atoms of the peptide molecule can be traced as their velocities fluctuate in response to the forces exerted on them by the other atoms in the molecule. This can be done by calculating the forces F_i, through the integration of the potential energy, V, which is given in Eq. 1. Then, upon taking a small time step of 10^{-15} seconds (fs), and applying the acceleration, $a_i(t)$, as calculated from Newton's equation over this time interval, we update the velocity and position of each atom in the peptide by using an algorithim called the predictor-corrector procedure (Gear, 1971). Then, by repeating the estimation of the forces and accelerations at the new position, a tracing of the trajectories of the atoms and the associated conformations and transitions can be followed over the specified time period of the dynamic simulation. Upon analysing the dynamic trajectories, the conformational motion of the peptide can be viewed on an interactive graphics system. In addition, the different conformations

that the peptide hormone can undergo become amenable to analysis and comparison with the experimentally derived structure (Hagler et al., 1985, Dauber et al., 1981). In order to run a dynamic simulation, we have used the CHARMM program developed by Karplus' group at Harvard (Brooks, et al., 1983). The following steps were used to study each of the four peptides mentioned at the beginning of this chapter.

1. Energy Minimization:

By using the extended conformation, the structure of the peptide under study was built using the CHARMM program. The generated structure was then minimized using ABNR algorithim (Adapted Basis of Newton Raphson Method) until convergence of the structure to a minimum. The minimized structure coordinates can be stored in PDB format (Protein Data Bank format) to be used in the next step.

2. Thermalization:

After generation of the minimized structure, its PDB can be subjected to dynamic simulation (for 2000-3000 femtoseconds, in our case) at the specified temperature (300° K in our study). By this thermalization step, the initial conformation can be generated. The small residual forces in the molecule induce acceleration to each of the atoms, and thus give rise to atomic motion. The velocities are scaled until they correspond approximately to room temperature. The peptide then continues in constant motion, a result of the thermal energy possessed by the atoms. The trajectory is determined by the temperature (or kinetic energy) and the interatomic forces.

3. Production:

In this step we used the thermalized structure conformation as our starting point. Then, upon dynamic simulations for a specified time interval (20 ps in our study) and analyzing the resultant trajectories, we can derive information regarding the structure of the peptides under study.

4. Analysis of The Dynamic Trajectories:

Using the analysis facility in CHARMM, we were able to analyze the trajectories of each of the four peptides (vide supra). The analysis was carried out at 1 ps intervals, and the corresponding energy and PDB coordinates along the time interval of the dynamic simulation were generated and studied. The valence, total and the nonbonded energy component of each peptide are tabulated in tables (XVIII, XXII, XXVI, XXX). Using the total energy as an indicator for the comparison, we were able to group the possible structures of each peptide into several subgroups with 5 Kcal/Mol energy difference between each group. Then, selecting a prototypical structure of each subgroup, and energy minimizing it, we obtained a minimized structure that represents a particular class of possible structures that are available for the peptide under investigation. In all the cases we studied, the generated structures were grouped into four main groups. Then, each prototypical structure was minimized and its coordinates and energies were extracted and analyzed to get the torsion angles and the contribution of each energy term to the total energy of the peptide structure (Tables XIX, XXIII, XXVII, XXXI). In

addition, the four minimized structures of each peptide were compared to the possible structure(s) generated by the NMR for each of the four peptides studied. The comparison to the NMR based structure was done by comparing the calculated coupling constants for the torsion angles, ϕ (Pardi et al., 1984) of the energy minimized structures of each peptide from the dynamic study to the coupling constants of the corresponding peptide obtained in DMSO solvent in the NMR study. Then, the theoretical torsion angle ϕ and the one obtained from NMR were compared (Table XXI). The selection of the best representative structures from the theoretical study to that from the NMR study was made following multiple regression analysis (Jurs, 1986) of the coupling constants of the theoretical and NMR-derived structures, using R^2 as the indicator of the closest similarity between the theoretical and NMR-derived conformation. The summarized results from these studies are given in Tables XXI, XXV, XXIX, XXXIII. To better understand the conformational-biological activity relationships, we examined and compared the linear and cyclic peptide having the same structural components with the only difference being the lactam side chain bridging between the linear and the cyclic peptide.

Results and Discussion

1. Ac-[Nle^4, Asp^5, D-Phe^7, Lys^{10}]α-MSH$_{4-10}$-NH$_2$

Linear (I) and Cyclic Lactam (III).

A. Peptide I: Ac-[Nle^4, Asp^5, D-Phe^7, Lys^{10}]α-MSH$_{4-10}$-NH$_2$.

The molecular dynamic simulation and energy minimization of the generated prototype structures will be discussed in comparison with the results obtained from the NMR study of this peptide.

Conformer I (0 ps):

The peptide was still in a fully extended conformation with weak hydrogen bonding between the His^4(Nδ)..D-Phe^5(NH) and Arg^6(δNH)..Lys^8(CO). The differences between the minimized and dynamic structure are mostly reflected in the torsion angles ϕ and ψ, with little change in the side chain torsion angles (χ^1). The generated stereo-structures of this peptide after minimization are shown in Fig. 18. One observation about this structure is that the χ^1 of the side chain of all amino acids of this peptide were in the trans conformation. This result is consistent with the NMR results which indicated that the predominant side chain conformation of the amino acid components of this peptide are the trans types. In addition, the changes in the backbone conformation upon minimization of the dynamic generated structure are most rather minor. There is no characteristic turn structure, but the most possible is the extended type of strucutre with a γ-turn at the N-terminal Ac-Nle^4. Also, there is a distorted β-turn around D-Phe^7 with stabilization of that turn by a His^6 side chain to backbone interaction, His^6 ($^\delta$N) to D-Phe^7 (NH). This type

of hydrogen bonding persists after the minimization which indicates that this arrangement is a low energy conformation. A further side chain to backbone interaction which remained after minimization is an $Arg^6(N^9H)$ to $Lys^8(CO)$ bond, which forms a 16 membered hydrogen bonded ring structure.

Conformer II (4 ps).

This conformer has the same type of N-terminal conformation as that reported above for conformer I. In addition, a Type II β-turn at His^4-D-Phe^5 is observed. The side chain topology described by the χ^1 angle is the same as that of conformer I. The difference between the dynamic and the minimized structure is mostly in the torsion angles ϕ and ψ but not in the χ^1 angles. This suggests that changes in the backbone are more common than in the side chain. It is reported that side chain conformation is more closely related to the biological activity requirements than the backbone (Manavalan and Momany, 1981). The backbone side chain interaction of $His^4(\delta N)....$D-$Phe^5(NH)$ also appeared in the minimized structure. Some of the hydrogen bondings which are present in the dynamic structure are $Asp^3(NH)....Ac^1$, $Arg^6(N^9H_2)....Arg^6$ and $Lys^8(NH_2$ amide$)....Asp^3$ were replaced by $Lys^8(NH)....Asp^3$ with persistance of $Lys^8(NH_2$ amide$)....Asp^3$. This type of interaction is very important since it shows clearly that the interaction between Lys^8 side chain and Asp^3 side chain is one of the most stable. This kind of interaction led us to examine whether the cyclization via lactam bridging between ε-NH_2 of Lys^8 and β-COOH of Asp^3 will stabilize this type of conformation and also enhance the biological activity vide infra. The stereoview

structure of this conformer is shown in Fig. (19).

Conformer III (5 ps):

There are no major changes in the backbone conformation of this conformer relative to conformer II; one interesting feature is related to the change in the side chain conformation of Nle^4 which shifted from trans to g^-. This change in the side chain topology may be important for binding of the hormone to its receptor. The change in the Nle^4 side chain was reflected in a big change in ϕ and ψ angles of the proceeding residue Asp^5. This suggests that changes in side chain topology may affect the backbone of the peptide in certain cases, but the opposite is not true as is clearly shown from a study of Table XX. In addition, the pattern of hydrogen bonding in conformer III resulted from the interaction between the Asp^5 and Lys^8 side chains. Also, the following hydrogen bonds were present in the dynamic structure: D-Phe^5(NH)....Asp^3, Lys^8(NH)....Asp^3, and Lys^8(NH_2 amide)....Asp^5 (βCO) which were replaced by Lys^8(NH)....Asp^3 and Lys^8(NH_2 amide)....Asp^5 (βCO) upon minimization. The total energy of conformer III is about 5Kcal/Mol lower than that of conformer II. The difference in energy may be due to the conversion of some of the potential energy into kinetic energy. The stereoview structure of conformer III is shown in Fig. 19, and the energy is listed in Table XVIII.

Conformer IV (11 ps):

This conformer is about 2Kcal/Mol away from the dynamically generated minimal structure, and is characterized by further changes in the side chain topography of Asp^5 and D-Phe^7 residues. The χ^1_5 of Asp^5 changed from a trans to g^-, while the D-Phe χ^1_7 went to g^+ from trans. A g^+ conformation is rare in peptides and proteins (Richarson, 1981). This may not be related to the enhanced biological activity of these melanotropin peptide hormone related fragments upon D-Phe substitution for L-Phe in position 7 (Sawyer et al., 1981). The changes of χ^1_4 of Nle^4 to its preferred trans form, with movement of the Asp^5 side chain toward g^- with a concomitant change of D-Phe^7 χ^1_5 from trans to g^+ suggests that the changes in side chain topography in a residue further down in a peptide chain may be reflected on a change in the side chain conformation of another residue 1 to 3 residues away. However, the pattern in hydrogen bonding of conformer IV is characterized with the a number which also existed in other conformers, e.g. Lys^{10}(NH)....Asp^5(βCO), Lys^{10}(NH_2 amide)....Asp^5(βCO) and Lys^{10}($N^{\varepsilon}H_2$)....Asp^5(βCO) in the dynamic structure, which were replaced by Lys^{10}(NH)....Asp^5(βCO), Lys^{10}(NH_2 amide)....Asp^5(βCO) and Arg^8(NH)....His^6(OC) in the minimized structure.

Correlation Between the Theoretical and NMR Based Conformational Structures of Ac-[Nle^4, Asp^5, D-Phe^7, Lys^{10}]α-MSH_{4-10}-NH_2:

A correlation between the theoretical and NMR based conformational structure of Ac-[Nle^4, Asp^5, D-Phe^7, Lys^{10}]α-MSH_{4-10}-NH_2 was examined in an effort to correlate the structure and the biological activity.

TABLE (XVIII). Total Energy and Energy Components of the Minimum Energy Structures Underlying the Dynamic Trajectory of Ac-[Nle^4, Asp^5, D-Phe^7, Lys^{10}]α-MSH$_{4-10}$-NH$_2$

Time (ps)	Potential Energy		
	Valence[a]	Nonbonded[b]	Total (Δ_{min})[c]
0	97.52	-35.22	62.30(20.96)
1	100.00	-36.89	64.12(22.78)
2	93.92	-35.03	58.88(17.54)
3	85.71	-32.58	53.13(11.79)
4	93.54	-38.65	54.89(13.55)
5	88.09	-37.48	50.62(09.28)
6	109.61	-48.38	61.23(19.89)
7	98.76	-44.76	54.03(12.69)
8	96.28	-51.69	44.59(03.25)
9	103.09	-48.42	54.67(13.33)
10	111.37	-51.41	59.96(18.62)
11	97.83	-54.11	43.72(02.38)
12	99.98	-44.14	55.84(14.50)
13	99.70	-50.58	49.12(07.78)
14	98.43	-41.84	56.59(15.25)
15	92.32	-50.98	41.34(00.00)
16	99.32	-54.33	44.99(03.65)
17	91.00	-45.63	45.37(04.03)
18	96.74	-48.33	48.41(07.07)
19	111.53	-49.26	62.27(20.93)
20	115.01	-54.02	60.99(19.65)

[a]The valence term represents deformations of the internal coordinates with respect to the minimized starting structure.

[b]The nonbonded refers to the van der Waals, electrostatic potential and hydrogen bonds energies.

[c]Δ_{min} represents the difference in energy between any structure and the minimum structure.

Table (XIX). Energy and Energy Components of Dynamic Generated Conformers of Ac-[Nle^4, Asp^5, D-Phe^7, Lys^{10}]α-MSH$_{4-10}$-NH$_2$.

Energy Components (Kcal/Mol)	Conformer I 0 PS Dyn (Min)	Conformer II 4 PS Dyn (Min)	Conformer III 5 PS Dyn (Min)	Conformer IV 11 PS Dyn (Min)
[a]E Total	62.2(-13.7)	55.0(-18.1)	50.7(-23.4)	43.8(-26.4)
E Bonds	25.2(1.2)	28.7(1.1)	23.1(1.1)	21.6(1.2)
E Angles	46.9(15.6)	42.2(15.8)	39.1(15.7)	41.6(17.2)
E Dihedrals	25.2(6.7)	22.7(9.3)	25.9(6.2)	24.6(6.6)
E VDW	--34.4(-36.7)	-38.2(-44.7)	-37.3(-46.5)	--50.9(-56.4)
E Elec	-0.22(0.3)	-0.5(0.31)	-0.2(0.10)	-1.1(-1.3)
E HB	-0.7(-0.9)	-0.001(-.007)	-0.02(-0.01)	-2.1(-3.9)

[a]E represents the term energy

Total = total potential energy (Valence energy + Nonbonded energy)

Bonds = energy term which describes the bond strain

Angles = energy term which describes the angle strain

Dihedrals = energy term which describes the torsion angles strain

VDW = energy term which describes Van der Waals energy

Ele = energy term which describes Columbic energy

HB = energy term which describes the hydrogen bonding energy

Table (XX). Conformational Parameters for Selected Conformers of Ac-[Nle^4, Asp^5, D-Phe^7, Lys^{10}]α-MSH$_{4-10}$-NH$_2$. Dynamic and Minimized Parameters are Listed.

Residue	Angle (deg.)	Conformer I 0 PS Dyn (Min)	Conformer II 4 PS Dyn (Min)	Conformer III 5 PS Dyn (Min)	Conformer IV 11 PS Dyn (Min)
	φ	-92.1(-84.3)	-128.7(-83.1)	-84.1(-81.0)	-117.6(-71.6)
Nle	ψ	119.5(125.2)	150.7(122.1)	111.9(128.0)	-40.7(-47.8)
	χ^1	172.2(-174.8)	-178.6(-170.4)	-67.0(-64.4)	-172.9(179.9)
	φ	-83.6(-83.8)	-102.7(-89.9)	-171.9(-152.6)	-117.5(-116.1)
Asp	ψ	114.1(118.2)	125.7(115.9)	162.9(140.8)	157.6(148.3)
	χ^1	-176.2(-174.2)	-161.8(-172.7)	-154.5(-176.1)	-60.8(-52.7)
	φ	-127.2(-136.7)	-99.7(-89.3)	-95.2(-78.6)	-103.3(-87.3)
His	ψ	159.6(162.1)	108.4(102.7)	119.7(114.4)	82.2(128.6)
	χ^1	-162.7(-166.3)	-159.3(-170.7)	-161.7(-174.2)	-160.0(-169.7)
	φ	155.2(152.1)	132.4(127.3)	86.4(94.6)	99.7(76.2)
D-Phe	ψ	-139.6(-149.0)	-123.9(-142.6)	-109.5(-142.5)	-61.7(-103.4)
	χ^1	-176.9(173.4)	176.7(172.2)	174.6(173.4)	40.0(62.3)
	φ	-164.4(-158.6)	-123.9(-94.78)	-89.6(-84.7)	-94.2(-73.1)
Arg	ψ	133.7(134.5)	113.5(120.5)	119.9(116.2)	140.1(122.3)
	χ^1	-162.6(-176.0)	-174.7(-176.3)	-167.4(-177.6)	-165.3(-175.3)
	φ	-84.4(-88.0)	-109.1(-99.8)	-117.9(-87.4)	-105.6(-93.9)
Trp	ψ	126.0(133.0)	122.2(131.9)	131.4(130.0)	149.1(144.7)
	χ^1	-177.5(-176.2)	-175.9(-171.1)	176.3(-174.8)	-159.7(-153.9)
	φ	-80.2(-93.7)	-102.3(-101.8)	-105.3(-95.2)	-130.3(-126.5)
Lys	ψ	-36.7(-51.9)	-53.3(-44.2)	-50.7(-45.5)	-30.3(-43.9)
	χ^1	-164.9(-170.4)	-177.7(-167.6)	-172.0(-168.2)	-139.8(-173.3)

Thus, an NMR investigation (see Ch. 4) of peptide I was carried out. A comparison of the calculated and observed coupling constants for various amino acids of peptide I (Table XXI) in conjunction with regression analysis suggested that conformer III is the one which corresponds mostly closely to the possible conformer generated by the NMR. Since conformer I and II also are somewhat related to the NMR structure but mostly to a highly energetic form (dynamic structure), their contribution should be negligible. In conformer III the corresponding ϕ angles can be fit to values based on the $^{3}J_{NH-CH\alpha}$ values from the NMR study of I in DMSO (Table XI, Ch. 4). In general the ϕ values are not related to those for parallel β-sheets (ϕ = -119°), the α-helix (ϕ = -57°), or the anti-parallel β-sheet (ϕ = -139°). Examination of the backbone torsion angles of conformer III, clearly suggest a slightly distorted type II or II β-turn structure centered around D-Phe residue while the N-terminal amino acids. Asp^{5} and Nle^{4}, and the acetyl group exist as a distorted C_7 turn. Usually in protein turns are distorted from their standard values (Richardson, 1981). From the study of the energy components of the various conformers (Table XIX), it appears that the favored conformer III is slightly higher in energy relative to the lower energy but less favored conformer IV.

From our studies and others (Hruby et al., 1987), it has been shown that the active segment (message sequence) of α-MSH in the central tetrapeptide His-Phe-Arg-Trp. In order to further understand the beha-

[a]Table (XXI). Theoretical and Experimental Determined Coupling Constants for Different Residues of Ac-[Nle^4, Asp^5, D-Phe^7, Lys^{10}]α-MSH$_{4-10}$-NH$_2$. The R^2 of the Regression Analysis is also listed.

Residue	$^3J_{NH-CH\alpha}$(Hz) Conformer I Dyn (Min)	Conformer II Dyn (Min)	Conformer III Dyn (Min)	Conformer IV Dyn (Min)	NMR[b]
Nle	8.1 (7.3)	9.5 (7.1)	7.2 (6.9)	9.7 (5.6)	6.9
Asp	7.2 (7.2)	9.1 (7.9)	5.2 (7.6)	9.7 (9.7)	7.90
His	9.6 (9.1)	8.8 (7.8)	8.4 (6.5)	9.1 (7.6)	8.30
D-Phe	7.3 (7.7)	9.4 (9.6)	7.5 (8.4)	8.8 (6.20)	7.20
Arg	6.2 (6.9)	9.7 (8.4)	7.9 (7.3)	8.3 (5.8)	7.6
Trp	7.3 (7.7)	9.4 (8.8)	9.7 (7.6)	9.3 (8.3)	7.10
Lys	6.7 (8.3)	9.0 (9.0)	9.2 (8.4)	9.1 (9.6)	6.70
[b]R^2 Dyn (Min)	0.2 (0.07)	0.2 (0.10)	0.1 (0.32)	0.0 (0.00)	

[a]Values generated by using Eq. 1 (p. 73) and values in Table XX.

[b]Values obtained from NMR study.

[c]R^2 calculated via the following equation:

$$R^2 = 1-\sum (Yi-Yi)^2/\sum(Yi-Yi)^2$$

where yi = Dependent variable

yi = Estimated value of yi

yi = Mean value of i $y = \frac{1}{n} \sum_{k=1}^{n} y_k$

where n is the number of observables.

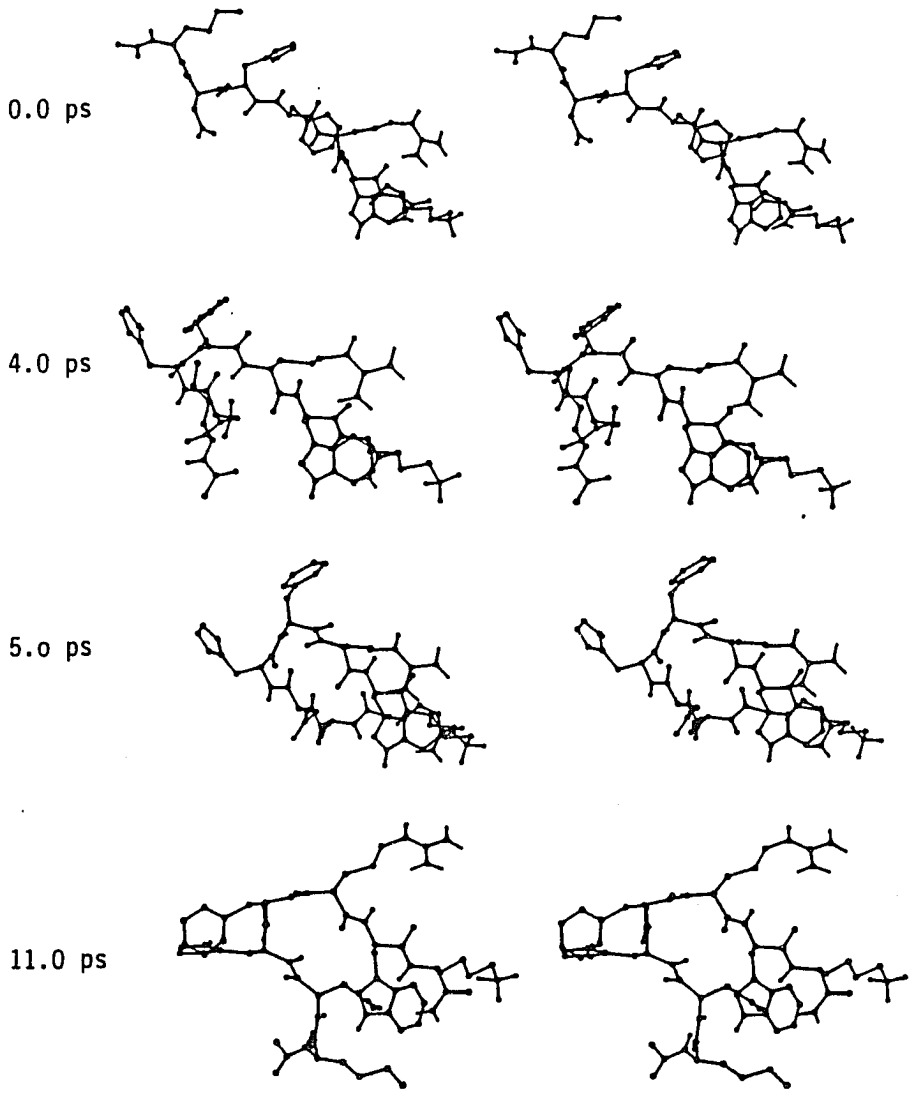

Fig. 18. Stereoviews of Ac-[Nle^4, Asp^5, D-Phe^7, Lys^{10}]α-MSH$_{4-10}$-NH$_2$ in four conformations generated in a molecular dynamics simulation (time along molecular dynamics trajectory given in picoseconds).

vior of the peptide I during the dynamic run, we investigated the behavior of the backbone torsion angles ϕ and ψ for the residues His^6, D-Phe^7, Arg^8 and Trp^9 together with the side chain torsion angle χ^1 for these amino acid residues. The results of these studies are given in Figs. 19a and 19b). The His^6 ϕ and ψ angles stabilize during the first four ps of the simulation and remain around the values which are characteristic of β-turns (ϕ = -60, ψ = 120). The close relationship between the ϕ and ψ angle of a particular residue is very clear in Fig. 19a. Any changes in the value of ϕ will be associated with a change of ψ. In addition, the fluctuation of the side chain χ^1_6 is parallel to the fluctuation in the ϕ torsion angle for the same residue. Also, the χ^1_6 angle stays within the range of trans (±180) to g^- (g^- = -60°). This type of conformation was identical to that found in the NMR of His^6 in DMSO. The trans and g^- conformations are the most probable types of conformations of the side chain in peptides and proteins (Richardson, 1981).

In the plot of the torsion angles for D-Phe we noticed a transition in the side chain torsion angle χ^1_7 from trans to g^+ (g^+ = +60°). Although g^+ is generally a less favored conformation, its behavior may explain the enhancement in the biological activity of the melanotropin related peptides upon substitution of Phe^7 by its enantiomer D-Phe^7 (Sawyer et al., 1981). The transition in D-Phe of χ^1 was accompanied in movement of the ψ angle from -180 to about -90 and this angle fluctuated around that value. The change in ϕ angle happened before the change in χ^1_7 angle of D-Phe. However, upon investigation the orientation of the aromatic side chain of Phe^7 using interactive graphics,

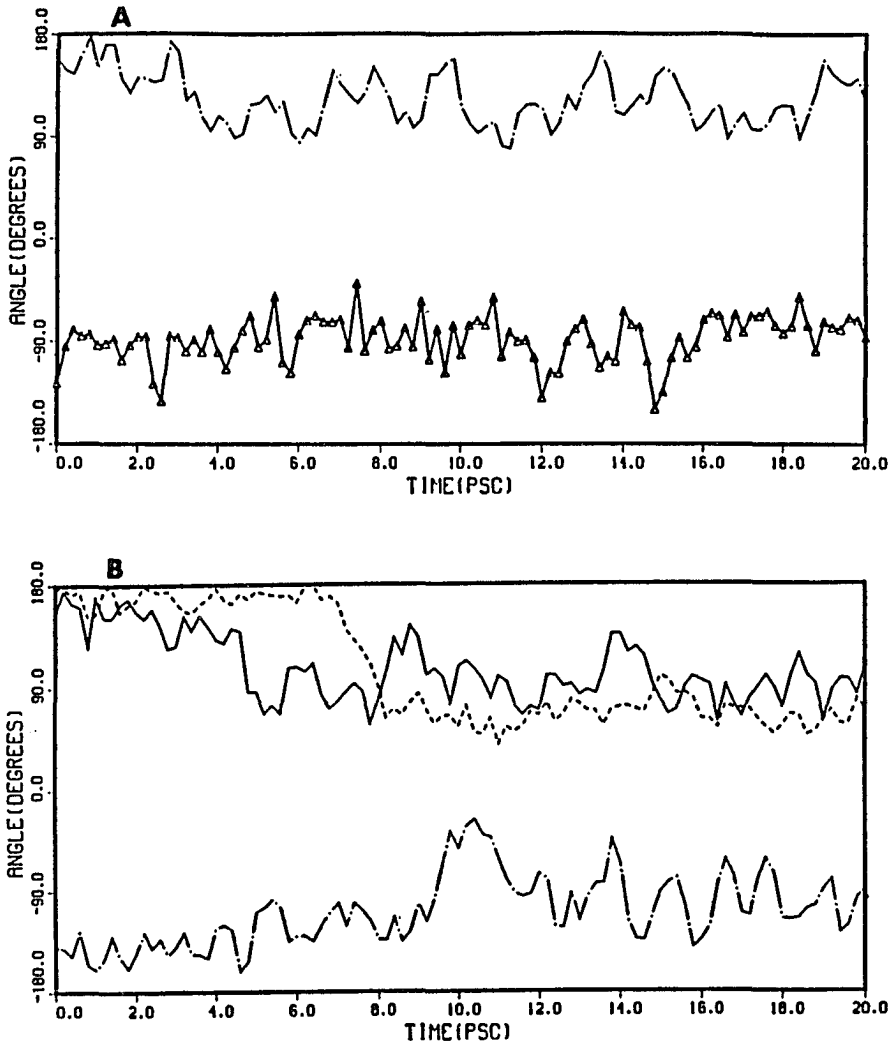

Fig. 19a Plot of the torsion angles χ^1---, ϕ____, and ψ_._, as functions of the time elapsed in the dynamic simulations for A; His^6, and B; D-Phe^7 in Ac-[Nle^4, Asp^5, D-Phe^7, Lys^{10}]α-MSH_{4-10}-NH_2.

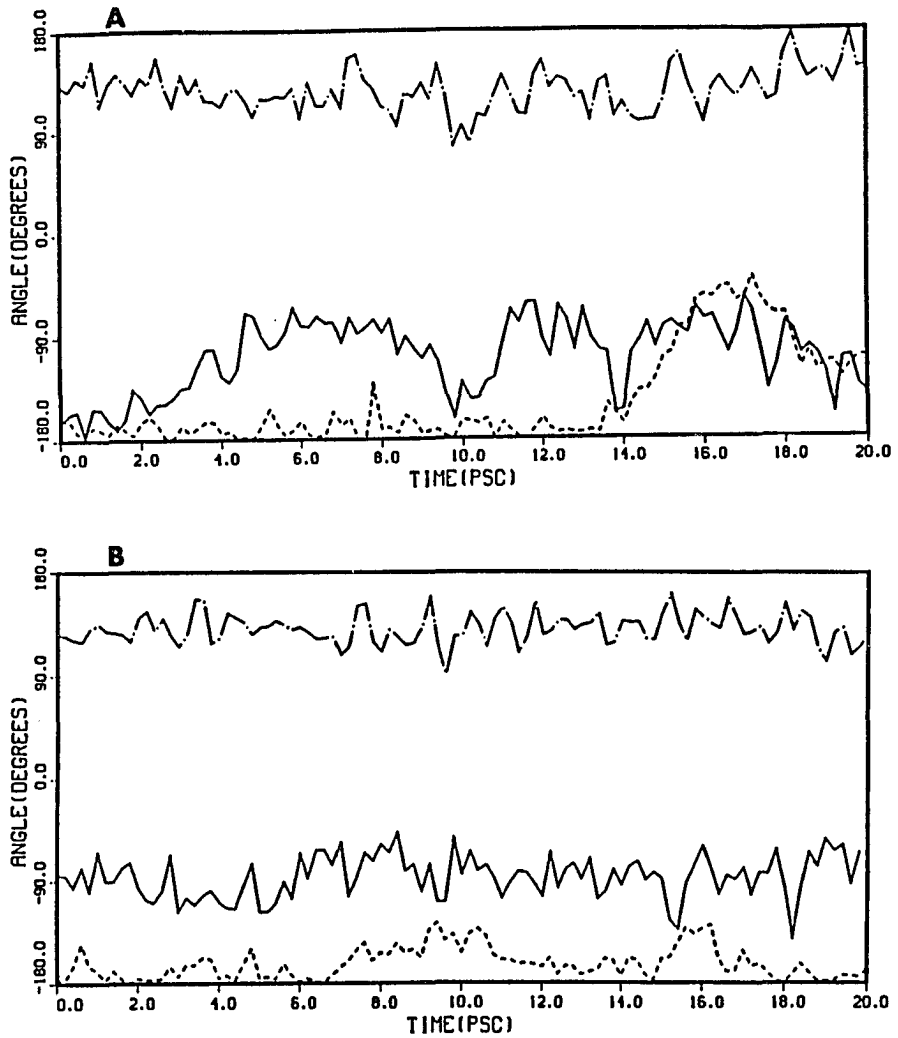

Fig. 19b. Plot of the torsion angles χ^1---, ϕ____, and ψ_._, as functions of the time elapsed in the dynamic simulations for A; Arg^8, and B; Trp^9 in Ac-[Nle^4, Asp^5, D-Phe^7, Lys^{10}]α-MSH_{4-10}-NH_2.

it appeared that in the g^+ conformation it first has a pseudo equatorial orientation, and then went to an axial conformation for the rest of the dynamic run. The changes in the side-chain conformation of Phe^7 was accompanied by changes in ϕ and χ^1_8 of the neighboring residue Arg^8. But the changes in the Arg conformation were transient since the molecule tried to restore the original conformation after the first four picoseconds of the simulation. In addition, at around 14 ps the χ^1_8 angle changed from trans to g^- for a short period of time and then tried to return to the trans form.

These major changes in the conformation of D-Phe^7 and Arg^8 can be determined from the NMR studies of melanotropin peptides with D-Phe^7 substituted for L-Phe^7. It has been shown that the ^{13}C relaxation time for Arg side chain (δ carbon) was very short in D-Phe^7-containing compounds compared to the L-Phe^7-containing ones. This result was interpreted as an indication of steric hindrance in the environment of Arg^8 due to the D-Phe^7 substitution. Thus, the effort of D-Phe to stay in a g^+ conformation may be related to a relief of strain due to side chain interactions with Arg^8.

Investigation of the trajectory of the Trp^9 residue in the dynamic studies does not seem to involve any major changes in its backbone or side-chain conformation. The backbone conformation of Trp^9 is almost identical to that of His^6. In addition, the χ^1_6 and χ^1_9 are locked in a trans conformation most of the time, although χ^1_6 has a higher population of g^-. This result is well correlated with the NMR results (Table XI, Ch. 4).

B. Peptide III: Ac-[Nle^4, Asp^5, D-Phe^7, Lys^{10}]α-MSH$_{4-10}$-NH$_2$:

Conformer I (0 ps):

This peptide initially has extended structure with a total potential energy of about 63 Kcal/mole. The contribution of the non-bonded energy term is about 30% of the total energy (Table XXII). The major contributing factor in the nonbonded energy was the Van der Waals component (Table XXIII). Energy minimization causes 10-35° changes in the backbone torsion angle (ϕ and ψ) but little change in the side chain torsion χ^1 (Table XXIV). The backbone conformation is locked mostly in β turn of type II (Asp^5, His^6) or type II′ (D-Phe^7, Arg^8). The major turn is located around the D-Phe residue. Side chain torsions range between g$^-$ for Nle^4, His^6 and Lys^8 to trans for Asp^5, His^6, D-Phe^7, Arg^8 and Trp^9. Hydrogen bonds range between weak (0.0/Kcal/M) to strong (-2.38 Kcal/M). The main ones Arg^6(N$^{\eta}$H)....Lys^{10}(CO), Arg^8(N$^{\eta}$H$_2$)....Lys^{10}(CO). These two hydrogen bonds persisted after energy minimization of this conformer. The stereoview structures of this conformer is shown in Fig. 20.

Conformer II (8 ps):

There are no major changes in the side chain conformation of this conformer relative to those reported for conformer I. In addition, the backbone conformation is almost identical to that of conformer I with more ordered β turn of Type II for Arg^8, Trp^9. The major hydrogen bonds in the dynamic form are: Arg^8(N$^{\eta}$H$_2$)....Lys^{10}(OC) and Trp^9(N^{in}H).... His^6(OC). Upon energy minimization additional hydrogen bond are

TABLE (XXII). Total Energy and Energy Components of the Minimum Energy Structures Underlying the Dynamic Trajectory of Ac-[Nle^4, $\overline{\text{Asp}^5}$, $\overline{\underline{\text{D}}\text{-Phe}^7, \text{Lys}^{10}}$]$\alpha$-MSH$_{4-10}$-NH$_2$

Time (ps)	Potential Energy		
	Valence[a]	Nonbonded[b]	Total (Δ_{min})[c]
0	94.14	-31.48	62.66(16.21)
1	96.56	-34.19	62.37(15.92)
2	97.88	-35.99	61.89(15.44)
3	87.26	-39.39	47.87(01.42)
4	99.09	-38.85	60.24(13.79)
5	99.73	-34.92	64.81(18.36)
6	94.51	-40.36	54.15(07.70)
7	97.76	-40.97	56.79(10.34)
8	103.54	-43.86	59.68(13.23)
9	93.34	-40.55	52.79(06.34)
10	110.98	-53.20	57.78(11.33)
11	101.03	-50.80	50.23(03.78)
12	99.48	-53.03	46.45(00.00)
13	93.54	-45.78	47.76(01.31)
14	118.00	-48.09	69.91(23.46)
15	104.09	-46.34	57.75(11.30)
16	104.86	-53.38	51.48(05.03)
17	104.52	-54.48	50.04(03.59)
18	108.28	-51.90	56.38(09.93)
19	100.44	-53.30	47.14(00.69)
20	101.01	-49.92	51.09(04.64)

[a]The valence term represents deformations of the internal coordinates with respect to the minimized starting structure.

[b]The nonbonded refers to the van der Waals, electrostatic potential and hydrogen bonds energies.

[c]Δ_{min} represents the difference in energy between any structure and the minimum structure.

Table (XXIII). Energy and Energy Components of Dynamic Generated Conformers of Cyclic Ac-[Nle^4, $\overline{\text{Asp}^5, \underline{\text{D}}\text{-Phe}^7, \text{Lys}^{10}}$]$\alpha$-MSH$_{4-10}$-NH$_2$.

Energy Components (Kcal/Mol)	Conformer I 0 PS Dyn (Min)	Conformer II 8 PS Dyn (Min)	Conformer III 11 PS Dyn (Min)	Conformer IV 14 PS Dyn (Min)
[a]E Total	62.7(-12.1)	59.8(-18.6)	50.3(-28.5)	69.7(-26.7)
E Bonds	24.1(1.3)	24.0(1.4)	27.0(1.4)	25.4(1.3)
E Angles	44.8(19.5)	49.5(18.3)	46.7(20.1)	58.7(19.2)
E Dihedrals	25.1(8.7)	30.1(13.2)	27.3(15.0)	23.6(13.5)
E VDW	-28.2(-37.5)	-41.2(-45.0)	-46.1(-58.2)	-44.6(-54.0)
E Elec	-0.6(-0.62)	-0.6(-0.7)	-0.7(-1.0)	-0.5(-0.8)
E HB	-2.7(-3.4)	-1.9(-6.0)	-3.9(-5.8)	-3.0(-6.0)

[a]For notations see Table XIX.

Table (XXIV). Conformational Parameters for Selected Conformers of Cyclic Ac-[Nle^4, Asp^5, D-Phe^7, Lys^{10}]α-MSH$_{4-10}$-NH$_2$. Dynamic and Minimized Parameters are Listed.

Residue	Angle (deg.)	Conformer I 0 PS Dyn (Min)	Conformer II 8 PS Dyn (Min)	Conformer III 11 PS Dyn (Min)	Conformer IV 14 PS Dyn (Min)
	φ	-101.9(-82.4)	-106.3(-85.5)	-80.8(-87.0)	-95.8(-77.9)
Nle	ψ	104.2(109.3)	157.9(138.7)	89.2(107.5)	130.9(96.2)
	χ^1	-62.5(-64.4)	-41.0(-64.2)	-57.2(-63.3)	-45.2(-64.6)
	φ	-94.2(-86.8)	-95.4(-78.5)	-99.5(-69.0)	-109.9(-78.6)
Asp	ψ	115.7(93.8)	98.6(105.4)	104.1(95.5)	129.2(99.2)
	χ^1	162.6(-176.0)	-175.6(-171.5)	-80.3(-80.2)	-92.75(-88.4)
	φ	-100.4(-86.9)	-76.3(-84.8)	-108.7(-99.2)	-62.7(-95.4)
His	ψ	149.7(140.4)	112.2(86.1)	58.1(78.5)	-178.1(85.2)
	χ^1	-76.5(-63.1)	-51.1(-69.3)	-65.9(-59.0)	-67.2(-57.8)
	φ	86.7(84.7)	70.2(88.6)	124.5(95.4)	112.1(94.0)
D-Phe	ψ	82.0(68.0)	135.1(139.2)	-132.3(-129.4)	-146.4(-132.9)
	χ^1	177.3(-178.7)	117.1(143.8)	167.9(177.6)	172.5(176.2)
	φ	-89.5(-77.9)	-81.4(-86.7)	-116.5(-118.9)	-102.3(-136.2)
Arg	ψ	118.8(105.7)	118.4(109.5)	102.4(100.1)	92.5(111.8)
	χ^1	-166.4(-172.9)	-176.8(-173.8)	-130.6(-154.8)	-178.9(-169.5)
	φ	-148.0(-127.8)	-117.8(-125.6)	-111.9(-97.40)	-101.9(-96.8)
Trp	ψ	69.6(50.7)	-8.8(10.8)	-21.2(-32.5)	-3.6(-34.2)
	χ^1	-165.8(-162.3)	-49.0(-40.2)	-63.0(-69.3)	-61.1(-45.1)
	φ	-125.7(-117.5)	-95.9(-104.2)	-90.0(-90.2)	-90.0(-78.9)
Lys	ψ	116.2(107.3)	74.4(101.7)	-55.7(-47.2)	-93.3(-39.9)
	χ^1	-56.7(-56.5)	-54.6(-54.10)	-60.0(49.0)	-54.0(-48.9)

$His^4(N^{im}H)....Nle^2(OC)$. The total energy of this conformer is not very far from that for conformer I (59 vs. 63), but upon minimization these conformers converged to different structures as reflected by their total energy (Table XXIII). The stereoview structure of this conformer is shown in Fig. 20.

Conformer III (11 ps):

This conformer still maintained the general backbone conformation of conformer II with some changes in χ^1 angles. The total energy of the dynamic structure is about 50 Kcal/Mole which minimized to -29 Kcal/Mol with major contributions from the nonbonded energy term. The hydrogen bonding pattern is still about the same as reported for conformer II with strong hydrogen bonding for $Trp^9(NH)....Asp^5$, $Arg^8(N^gH_2)...\underline{D}\text{-}Phe^5$ and $Lys^{10}(NH)...Asp^5$. The minimized structure has some additional hydrogen bonds including $His^6(N^{im}H)....Nle^4$, $Arg^8(N^gH_2)....Asp^5$, and $Lys^{10}(NH)....Asp^5$ with loss of the $Arg^8(N^gH_2)....\underline{D}\text{-}Phe^7(OC)$ H-bond. The stereoview of this structure with the hydrogen bonds is shown in Fig. 20.

Conformer IV (14 ps):

This conformer is close to conformer III based on its structure after minimization, with the only major changes being the ψ angles of the Nle^4 and His^6 residues. These changes may be reflected through the cooperative effect between residues via the backbone or through side chains interaction. The major hydrogen bond was $Trp^9(NH)....Asp^5(\beta CO)$

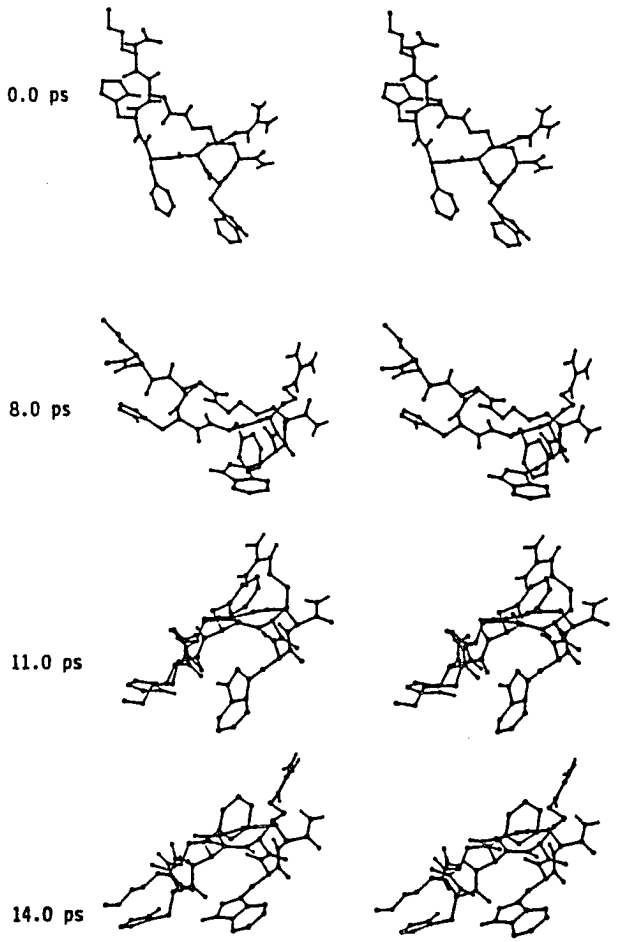

Fig. 20. Stereoviews of Ac-[Nle^4, Asp^5, D-Phe^7, Lys^{10}]α-MSH$_{4-10}$-NH$_2$ in four conformations generated in a molecular dynamics simulation (time along molecular dynamics trajectory given in picoseconds).

which gets stronger after minimization. The minimized structure has additional hydrogen bonds including $Trp^{9}(N^{in}H)....Nle^{4}$ and $His^{6}(N^{im}H)....Nle^{4}$. The folding over of the C-terminal and N-terminal part of the molecule is reflected through the $Lys^{10}(N^{\epsilon}H)....Ac^{1}(OC)$ hydrogen bond which is present in both dynamic and minimized structures of conformers III and IV. The stereoview structure of this conformer is given in Fig. 20.

Correlation Between The Theoretical and NMR Based Conformational Structures of Ac-[Nle^{4}, $\overline{Asp^{5}, \underline{D}\text{-}Phe^{7}, Lys^{10}}$]$\alpha$-$MSH_{4-10}$-$NH_2$:

A comparative study of the NMR results from both water and DMSO with the theoretical results using molecular dynamic simulation, indicates that some of the dynamic conformers are closer to the NMR model than others. In Table XXV, we summarize the theoretical and experimental coupling constants for peptide III. The regression analysis indicated that the dynamic structure for conformers II, III and IV are close to the NMR structure with the closest resemblance being the energy minimized conformer II. Based on the energy of these conformers in Table XXIII, we see that there are considerable differences in the total energy for the various minimized and dynamic structures. Examination of the backbone changes of conformers I, II, III and IV by interactive graphics and by examination of Table XXIV, showed that major changes occured in ϕ and ψ angles with much less change in the side chain torsion angles. Thus, various backbone arrangements can have the same side chain topography which is important for the biological activity of the peptide hormone.

[a]Table (XXIX). Theoretical and Experimental Determined Coupling Constants for Different Residues of Ac-[Nle^4, Asp^5, D-Phe^7, Lys^{10}]α-MSH$_{4-10}$-NH$_2$. The R^2 of Regression Analysis is also listed.

Residue	$^3J_{NH\alpha-CH\alpha}$(Hz)				
	Conformer I [a]Dyn (Min)	Conformer II Dyn (Min)	Conformer III Dyn (Min)	Conformer IV Dyn (Min)	[b]NMR
Nle	2.0 (6.3)	9.2 (7.4)	6.8 (7.5)	8.5 (6.5)	6.9
Asp	8.3 (7.5)	8.4 (6.5)	8.8 (5.4)	9.5 (6.6)	7.9
His	8.6 (7.6)	6.3 (7.4)	9.4 (8.7)	4.5 (8.5)	8.3
D-Phe	7.3 (7.3)	5.4 (7.6)	9.5 (7.9)	9.2 (8.0)	7.2
Arg	7.8 (6.5)	7.0 (7.5)	9.6 (9.7)	9.0 (9.1)	7.6
Trp	8.1 (9.5)	9.6 (9.6)	9.5 (8.6)	9.0 (8.6)	7.1
Lys	9.6 (9.6)	8.5 (9.0)	7.9 (7.9)	7.9 (6.6)	6.7
[c]R^2 Dyn (Min)	0.1 (0.11)	0.21 (0.36)	0.29 (0.0)	0.24 (0.15)	

[a]Values generated by using Eq. 1 (p. 73) and values in Table XXIV.

[b]Values obtained from NMR Study.

[c]R^2 calculated via the linear regression analysis using LOTUS 1-2-3 software (for definition of R^2 see Table XXI).

The differences between NMR deduced models and the theoretical ones may be related to either ambiguities in the measurement of NMR parameters or due to the differences between the two techniques. In NMR study one uses solvent as the media which is not the case in the theoretical study which is based on in vacuo environment. Furthermore, the theoretical structure is generated for a fragment is derived using parameters from X-ray as a major source of informations. Thus the presence of solvent is implicit in the structures produced by the theoretical simulations. One possible way to bring a closer correlation between the experimental and theoretical results is to do more elaborated NMR studies and to explicitly including the solvent effect in the theoretical study. Of course, the major NMR parameter correlated to conformation is the torsion angles estimated from coupling constants which are difficult to obtain exactly. In addition, the ϕ angle can be affected by changes in the ψ or χ angles. Thus all of these parameters have to be determined before we can come to a firm conclusion about the correlation between theoretical and experimental results.

In studying the trajectory of the torsion angles ϕ, ψ and χ^1 for the core residues His^6, D-Phe^7, Arg^8 and Trp^9 over the dynamic simulation time many important conformational features can be obtained. In Figs. 21a, 21b the plots of the torsion angles as functions of the time are reported. In the case of His^6 there are no major changes in either its backbone or side chain dihedral angles. Also, the probable backbone conformation for His is the Type II β-turn and gauche(-) (g^-) side chain

arrangement. There are some fluctuations in the ψ angle after the 1st 8 ps of the run. The cooperative effect between ϕ and ψ angles is very clear along the trajectory. These results are in agreement to a certain extent with the NMR determinations shown in Table XIII of Ch. 4. However, since the NMR results are usually represented as an average value, we don't see the predominance of one conformational type as is the theoretical study.

In case of the D-Phe^7 residue, more pronounced changes occurred during the simulation. The major transition in ψ angle from about 90° to -180° after the first 8 ps may reflect the high conformational preference for this residue. In comparison to peptide I the conformation for D-Phe^7 in peptide III is more specific. The ϕ and ψ angles remained in their preferred conformation after the first 8 ps of the study in the case of the cyclic peptide, while they continued to fluctuate in the linear one. The most drastic difference between the linear and cyclic peptide is that the χ^1_7 in the cyclic analogue is locked in the trans conformation, but it goes to gauche(+) (g^+) in the linear. This side chain may be the important factor in causing about 100 fold enhancement in biological activity after cyclization (Table V, Ch. 2 and Table IX, Ch. 3). Further testing of this hypothesis is under study in our laboratory.

There is not much change in the conformation of the Arg^8 residue. From Fig. 21b, it is clear that the fluctuations in backbone and side chain conformation is much less in the cyclic peptide than in the linear (Figs. 19 vs. 21). The transition of ϕ angle in Arg from about -90 to more extended form after the first 8 ps of the simulation may be related to

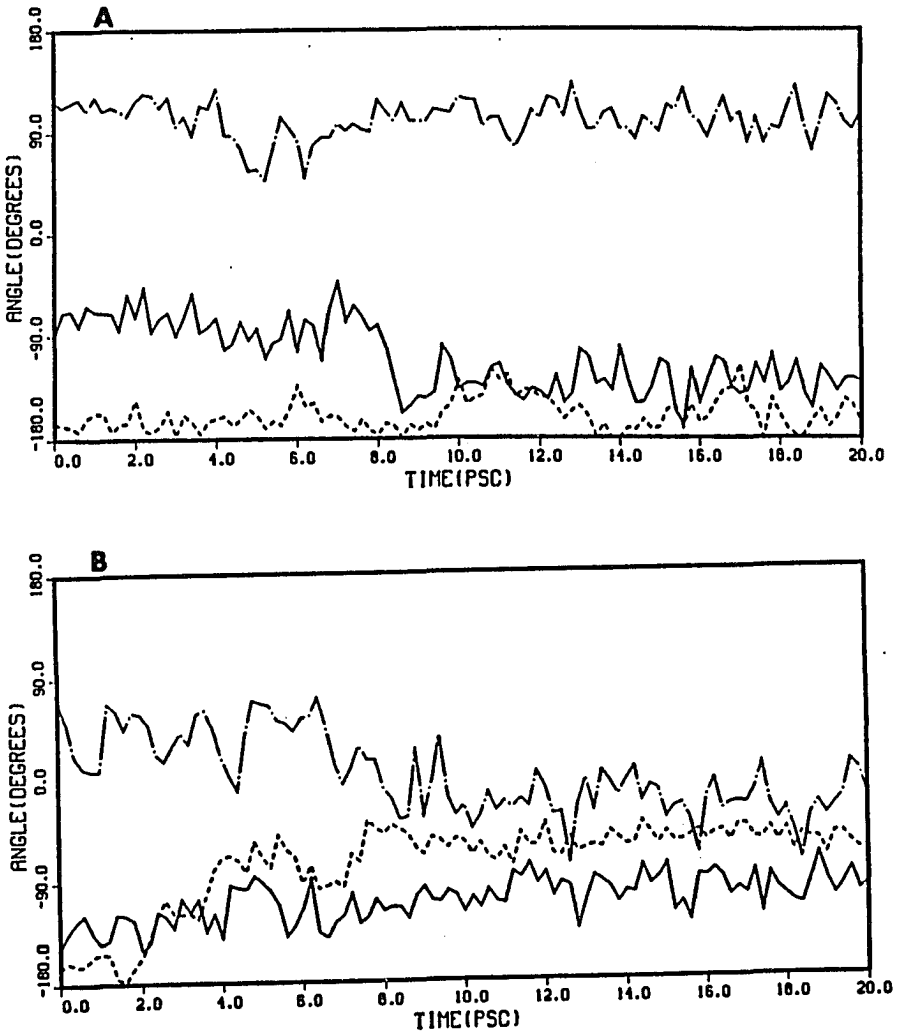

Fig. 21a. Plot of the torsion angles χ^1 ---, ϕ ____, and ψ _._._, as functions of the time elapsed in the dynamic simulations for A; His^6, and B; D-Phe^7 in Ac-[Nle^4, Asp^5, D-Phe^7, Lys^{10}]α-MSH$_{4-10}$-NH$_2$.

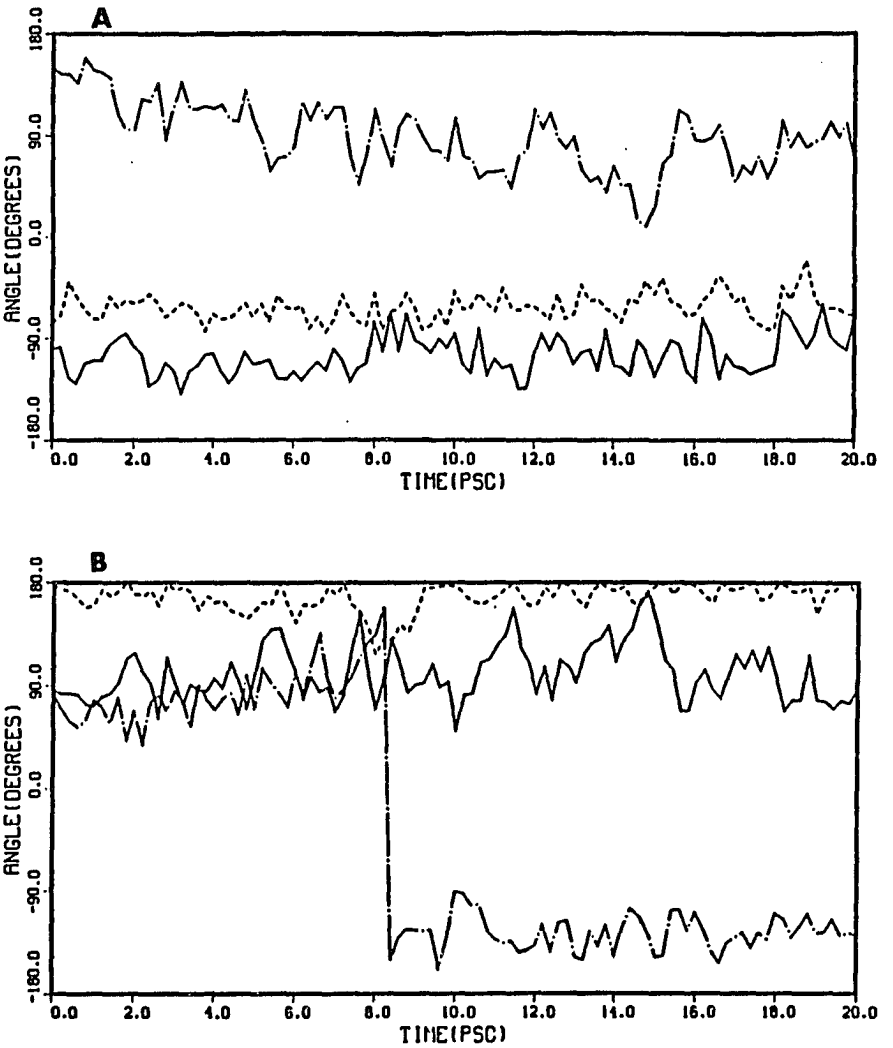

Fig. 21b. Plot of the torsion angles χ^1---, ϕ____, ψ_._, as functions of the time elapsed in the dynamic simulations for A; Arg^8, and B; Trp^9 in Ac-[Nle^4, Asp^5, D-Phe^7, Lys^{10}]α-MSH_{4-10}-NH_2.

the transition in the backbone of the D-Phe^7 residue.

Another crucial change occured in the Trp^9 residue which also may play a major role in the enhancement of the biological potency of the cyclic analogue. The transition in the backbone and side chain conformation started after the first 4 ps, and transform both ϕ and ψ to the β-turn Type II conformation ($\phi \simeq -80$, $\psi \simeq 10$ to 70). This conformational locking may be a result of the limited space available to this residue due to the restriction introduced by the cyclization. In addition to that, χ^1_7 is locked in gauche (g^-) most of the time. This side chain conformation is different from the one in the linear analogue. These results are consistent with the NMR results (Table XIII, Ch. 4).

2. Ac-[Nle^4, Asp^5, D-Phe^7, Dpr^{10}]α-MSH$_{4-10}$-NH$_2$
   Linear (II) and Cyclic Lactam (IV).
   A. Peptide II: Ac-[Nle^4, Asp^5, D-Phe^7, Dpr^{10}]α-MSH$_{4-10}$NH$_2$.

Dynamic simulation of the minimized structure of Peptide II for 20 ps, leads to several substructures. Analysis of the dynamic trajectory at each picosecond and gathering the conformers within 5 Kcal/Mol differences in their total energy lead to four major conformers. The energy analysis of the dynamic simulation and the energy and its components for each conformer are listed in Table XXVI and Table XXVII. In addition, the backbone and side chain torsions for each residue in peptide II are tabulated in Table XXVIII. To further investigate the detailed properties of each conformer, we will describe each conformer separately.

Conformer I (0 ps):

The peptide was a fully extended structure with all χ^1 angles in the trans form except for the C-terminal residue, Dpr, which was in gauche (g^-) conformation. The major changes in the energy minimized structure were in the backbone ϕ and ψ angles of each residue, though it appears that the ψ angle is much less affected by minimization than the ϕ angle. The cooperativity between ϕ and ψ is not very strong for some of the residues e.g. His^6, D-Phe^7 and Asp^5. This may indicate that the molecule maintains a preferred type of conformation at the sites occupied by those residues. The general type of backbone arrangement seems to be a distorted type of β-turn type II or II centered around the D-Phe^7 residue. The major contributing component for the energy of this conformer is again the nonbonded term described by the van der Waals energy. Also, there is an appreciable hydrogen bond contribution in both the dynamic and the energy minimized structures. Several hydrogen bonds exist in conformer I. The major ones are D-Phe^7(NH)....$His^6(N^{im})$, $Trp^9(NH^{in})$....$His^5(N^{im})$, Dpr^{10}(NH)....Asp^5, $Dpr^{10}(NH_2$ amide).... Asp^5 and $Dp^{10}(\beta NH_2)$....Arg^8. Some of these hydrogen bonds are lost after minimization but others are retained, including the D-Phe^7(NH)....$His^6(N^{im})$, $Trp^9(NH^{in})$....$His^6(N^{im})$, $Dpr^{10}(NH_2$ amide).... Asp^5 and $Dpr(\beta NH_2)$....Arg^6(OC). The latter was the strongest in both structures, which may be related to the observed temperature effect on the amide proton NMR chemical shifts in DMSO (Table XIV, Ch. 4).

Also the His^{6} residue is involved in hydrogen bonding in both structures which may explain the small temperature coefficient for its amide proton.

Conformer II (4 ps).

In this structure several changes occured in the backbone and side chains conformation relative to Conformer I. The predominance of a distorted β-turn around the tetrapeptide His-D-Phe-Arg-Trp is still evident. The change in χ^{1}_{7} from trans to the gauche (g^{+}) conformation was observed for this conformer. The change in the D-Phe^{7} side chain conformation was accompanied with changes in its ψ angle and also in the adjact Arg^{8} φ and ψ angles. These changes may be related to the fact that side chain groups need to change in order to accomodate the change in the D-Phe^{7} side chain conformation. Several hydrogen bonds exist in this conformer with the major ones being $Trp^{9}(N^{in}H)$.... $His^{6}(N^{im})$, $Drp^{10}(NH)$....$Asp^{5}(\beta OC)$ and $Dpr^{10}(\beta NH_2)$....$Asp^{5}(\beta OC)$. This result was consistent with the NMR result. From the energy point of view, there is about 10 Kcal/Mol difference between conformer I and II, but both of them converged to the same energy upon energy minimization calculations. This result may be related to the fact that small peptides are flexible molecules in their structural conformation (Richardson, 1981). Also, the substitution of certain amino acids with their specific side chain may introduce more flexibility in the peptide backbone conformation (Hruby, 1981).

Conformer III (9 ps):

There are no major changes in this conformer with respect to Conformer II, though some changes in ϕ and ψ angles for some of the amino acids occurred. The β-turn type II is more pronounced in D-Phe^7-Arg^8 with the locking of χ^1_7 into a gauche (g^+) conformation. A new H-bond appeared between Arg^8(NH)....Asp^5, and Dpr^{10}(NH)....Asp^5 and Dpr^{10}(βNH)....Arg^8(OC) are still present. Upon energy minimization, the Arg^8(NH)....Asp^5 hydrogen bonds disappeared while the others remained. The minimized structure has lower energy than the other two conformers discussed above (Table XXVII), which is parallel to the total energies of their dynamic structures.

Conformer IV (17 ps):

This structure represents another group of substructures. The backbone conformation, as described by the ϕ and ψ dihedral angles, has a more extended form at the N-terminal amino acids Nle^4 and Asp^5. The type II β-turn conformation of the distorted kind is found for the Nle^4, Asp^5, His^6 and D-Phe^7 residues. The turn conformation centered around D-Phe residue is still of the β type II kind. The type II turn is highly distorted, and can be described for the D-Phe-Arg site. The hydrogen bonding pattern for conformer IV was as follows: In the dynamic structure there were very weak hydrogen bonds between Nle^4(NH)... His^6 (γ-turn), Arg^8(NH)...Asp^5 (β-turn), and Dpr^{10}(NH amide)...Trp^9. Upon minimization, the following hydrogen bonds were present:

TABLE . (XXVI). Total Energy and Energy Components of the Minimum Energy Structures Underlying the Dynamic Trajectory of Ac-[Nle^4, Asp^5, D-Phe^7, Dpr^{10}]α-MSH$_{4-10}$-NH$_2$.

Time (ps)	Potential Energy		
	Valence[a]	Nonbonded[b]	Total (Δ_{min})[c]
0	113.31	-53.54	59.77(08.76)
1	111.15	-53.73	57.42(06.41)
2	112.28	-46.73	65.55(06.41)
3	112.35	-51.42	60.93(09.92)
4	115.61	-48.75	66.86(15.85)
5	121.62	-55.87	65.75(14.74)
6	105.04	-45.41	59.63(08.62)
7	108.82	-46.36	62.45(11.45)
8	120.51	-54.15	66.36(15.35)
9	104.96	-53.95	51.01(00.00)
10	106.44	-53.43	53.01(02.00)
11	107.97	-46.50	61.47(10.46)
12	108.71	-46.89	61.82(10.81)
13	120.33	-48.71	71.62(20.61)
14	117.59	-50.90	66.69(15.68)
15	118.10	-47.93	70.17(19.16)
16	110.04	-47.37	62.67(11.66)
17	114.30	-47.21	67.09(16.08)
18	107.94	-49.42	58.52(07.51)
19	112.30	-46.02	66.28(15.27)
20	111.69	-52.17	59.52(08.51)

[a]The valence term represents deformations of the internal coordinates with respect to the minimized starting structure.

[b]The nonbonded term refers to the van der Waals, electrostatic hydrogen bond energies.

[c]Δ_{min} represents the difference in energy between any structure and the minimum structure.

Table (XXVII). Energy and Energy Components of Dynamic Generated Conformers of Ac-[Nle^4, Asp^5, D-Phe^7, Dpr^{10}]α-MSH_{4-10}-NH_2.

Energy Components (Kcal/Mol)	Conformer I 0 PS Dyn (Min)	Conformer II 4 PS Dyn (Min)	Conformer III 9 PS Dyn (Min)	Conformer IV 17 PS Dyn (Min)
E Total	59.6(-10.3)	66.8(-10.0)	51.0(-14.2)	66.9(-13.2)
E Bonds	25.0(1.2)	22.1(1.2)	26.3(1.5)	19.9(1.1)
E Angles	49.2(21.3)	41.9(23.4)	35.5(23.8)	47.7(21.3)
E Dihedrals	39.1(24.5)	42.5(25.4)	42.9(25.5)	46.5(24.7)
E VDW	-45.7(-50.2)	-45.0(-53.0)	-48.3(-58.2)	-44.8(-51.6)
E Elec	-1.1(-0.9)	-1.0(-1.2)	-1.3(-1.3)	-0.4(0.8)
E HB	-6.7(-8.1)	-2.6(-6.1)	-4.3(-6.0)	-2.8(-8.1)

[a]See Table XIX for notations.

Table (XXVIII). Conformational Parameters for Selected Conformers of Ac-[Nle^4, Asp^5, D-Phe^7, Dpr^{10}]α-MSH$_{4-10}$-NH$_2$. Dynamic and Minimized Parameters are Listed.

Residue	Angle (deg.)	Conformer I 0 PS Dyn (Min)	Conformer II 4 PS Dyn (Min)	Conformer III 9 PS Dyn (Min)	Conformer IV 17 PS Dyn (Min)
	φ	-151.0(-129.6)	-106.2(-83.3)	-115.1(-88.7)	-84.2(-151.6)
Nle	ψ	130.2(124.1)	127.1(110.6)	-169.5(171.1)	137.2(129.4)
	χ^1	-167.5(-169.4)	-79.3(-65.9)	-82.0(-61.2)	175.4(-173.2)
	φ	-103.6(-96.6)	-151.3(-142.9)	-95.9(-105.8)	-138.4(-91.7)
Asp	ψ	58.8(60.9)	59.3(52.4)	-60.1(-44.5)	-35.2(-79.1)
	χ^1	-173.2(-173.9)	-171.2(-173.3)	-174.6(-179.7)	-150.93(-173.40)
	φ	-71.1(-79.2)	-85.4(-72.0)	-60.2(-77.6)	-75.9(-62.30)
His	ψ	157.2(157.3)	167.8(137.2)	107.1(95.2)	136.6(127.10)
	χ^1	-166.6(-163.2)	-55.2(-65.8)	-62.8(-65.9)	-60.0(-77.2)
	φ	89.8(88.9)	89.7(104.1)	111.1(121.8)	77.8(100.6)
D-Phe	ψ	-93.0(-97.5)	-119.3(-87.1)	-19.2(-52.5)	-95.7(-92.7)
	χ^1	171.9(172.5)	55.4(57.9)	62.1(57.40)	63.6(61.3)
	φ	-99.3(-83.9)	-80.3(-93.3)	-117.9(-103.4)	-81.9(-95.4)
Arg	ψ	83.7(102.3)	108.6(85.5)	36.0(69.5)	142.4(100.2)
	χ^1	-177.0(-173.5)	-163.6(-152.1)	-46.2(-52.1)	-48.6(-57.4)
	φ	-69.4(-86.9)	-71.7(-71.8)	-53.6(-61.2)	-106.3(-75.6)
Trp	ψ	99.3(105.1)	146.7(108.7)	122.2(114.3)	77.9(94.8)
	χ^1	-66.2(-76.4)	-86.3(-72.2)	-63.2(-66.3)	-63.3(-69.7)
	φ	110.0(-127.8)	-93.3(-101.7)	-142.9(-106.2)	-114.6(144.1)
Dpr	ψ	-31.5(-33.4)	-78.6(-45.0)	119.2(127.4)	139.8(121.1)
	χ^1	-51.2(-63.2)	-61.3(-53.4)	-67.6(-61.0)	-71.6(-62.2)

$His^6(N^{im}H)...Arg^8(OC)$, $Arg^8...Asp^5$, $Arg^8(N^{\eta}H_2)...Asp^5$, Dpr^{10}(NH amide)...$His^6(N^{im})$ and $Dpr^{10}(\beta NH)...His^6(N^{im})$. The persistance of the $Arg^8(NH)...Asp^5$ hydrogen bond is an indication of the involvement of this part of the molecule in a type II β-turn conformation. Most of these results are consistent with the NMR results described in Ch. 4 of this work. The stereoview structures of various conformers are shown in Fig. 22.

Correlation Between the Theoretical and NMR Based Conformational Structures of Ac-[Nle^4, Asp^5, D-Phe^7, Dpr^{10}]α-MSH_{4-10}-NH_2:

Comparison of the calculated NMR coupling constants (based on the φ angles of various residues (Table XXVIII)) in the dynamic and the energy minimized structure were made through multiple regression analysis (Table XXIX), and the best fit was with conformer III. Although conformer III is the structure which has the minimal energy in both dynamic and minimized studies, it also has the highest value of the nonbonded energy term (van der Waals). This may indicate that the minimal dynamic structure is the one which has the closest resemblance to the NMR structure. This fact will be very important for future search to determine the best structure generated by theoretical calculation which corresponds to the one determined experimentally. In addition, conformer III has a permanent hydrogen bonding between $Arg^8....Dpr^{10}(\beta NH_2)$ and $Dpr^{10}(NH)....Asp^5$. The latter may explain the involvement of Dpr amide hydrogen in an intramolecular hydrogen bond (Table XIV, Ch. 4). The formation of a Type II β-turn is also represented by the $Arg^8(NH)....Asp^5$ hydrogen bonding which is present in this conformer.

The correlation between the ϕ angles of conformer III residues and the NMR generated values are in close agreement, with the highest difference being about 20° (Table XV, Ch. 2 and Table XXVIII). However, there is still more resemblance between the minimized structures of conformers II and IV and the NMR-based structure (Table XXIX). This result may result because the NMR generated conformation usually represents an average structure in case of peptides (Rose et al., 1985). Thus, the theoretical based structure will represent the finally tuned one in comparison to the NMR structure. This fact has to be kept in mind during any correlation between theoretical and experimental results.

To look deeply into the details of changes in the structure of the peptide along the trajectory in the dynamic simulation, the history of the backbone and side chain torsion angles were plotted in Figs. 23a, 23b. The residues His^6, D-Phe^7, Arg^8 and Trp^9 were the ones selected for the study since these are the message sequence amino acids of melanotropin hormone (Hruby et al., 1987). In Fig. 23a the ϕ angle for His^6 is locked at around -90° with some transitions at around 6 to 8 ps. These fluctuations in the ϕ angles were accompanied by slight changes in the ψ angles which started at around 4 ps to go from about -180° to -90° and stayed around that value. These values for the backbone angles are in the range for a type II β-turn conformation (Rose et al., 1985). In addition, the χ^1_6 is changed from trans (-180°) to gauche (g^- -60°) and spent all the time in that form. This type of behaviour in the peptide backbone and side chain conformation may indicate that although this

is a linear peptide, which we expected to be highly flexible, it still has an ordered structure. The arrangement of the peptide in its order structure might be directly related to the biological activity of that peptide (Rose et al., 1985, Hruby, 1982).

In case of D-Phe^7 the major characteristics are in the transition of the χ^1_7 from a trans to a gauche(+) (g^+) conformation where it spends all the rest of the time. The other backbones dihedrals are similar in their conformation to that observed in case of peptide I. One major difference is that the χ^1_7 in case of peptide II went to gauche(+) (g^+) earlier than that by peptide I. This fast conversion in side chain conformation may be related to the substitution of an amino acid with a shorter side chain group (Lys^{10} to Dpr^{10}) which has appreciable effect on the side chain conformation of D-Phe^7. This result may be related to the reduction in the biological activity of peptide II relative to peptide I (Tab. V, Ch. 2), and it may be possible to use this finding to design an antagonist to melanotropin. Thus, by proper substitution for certain amino acids, the χ^1_7 can be locked in its gauche (g^+) conformation which will bind to the receptor but without transduction.

The conformation along the dynamic trajectories for Arg^8 is characterized by a transition in the ϕ and ψ angles toward a more β-turn type of conformation. Further changes in the ψ angle started around 4 ps and were accompanied by the transition of χ^1_8 from trans to gauche(-) (g^-). In addition, the ψ angle tries to return to a distorted β-turn type of conformation. Both ϕ and χ angles stayed at the same range of values after the first 5 ps of the dynamic run.

[a]Table (XXIX). Theoretical and Experimental Determined Coupling Constants for Different Residues of Ac-[Nle^4, Asp^5, D-Phe^7, Dpr^{10}]α-MSH$_{4-10}$-NH$_2$. The R^2 of Regression Analysis is also listed.

Residue	$^3J_{NH\alpha-CH\alpha}$(Hz)				
	Conformer I Dyn (Min)	Conformer II Dyn (Min)	Conformer III Dyn (Min)	Conformer IV Dyn (Min)	NMR
Nle	7.8 (9.5)	9.3 (7.1)	9.6 (7.8)	7.2 (7.7)	7.40
Asp	9.1 (8.6)	7.8 (8.6)	8.5 (9.3)	9.0 (8.1)	7.30
His	5.6 (6.6)	7.4 (5.7)	4.2 (6.4)	6.2 (4.5)	7.30
D-Phe	7.9 (7.8)	7.9 (9.2)	9.5 (9.7)	6.4 (8.9)	7.20
Arg	8.8 (7.2)	6.8 (8.3)	9.7 (9.1)	7.0 (8.5)	8.00
Trp	5.4 (7.6)	5.7 (5.7)	3.5 (4.3)	9.3 (6.2)	7.10
Dpr	3.6 (9.6)	8.3 (9.0)	8.6 (9.3)	9.6 (1.8)	8.20
R^2 Dyn (Min)	0.1 (0.11)	0.0 (0.23)	0.2 (0.25)	0.0 (0.20)	

[a]see Table XXI for notations.

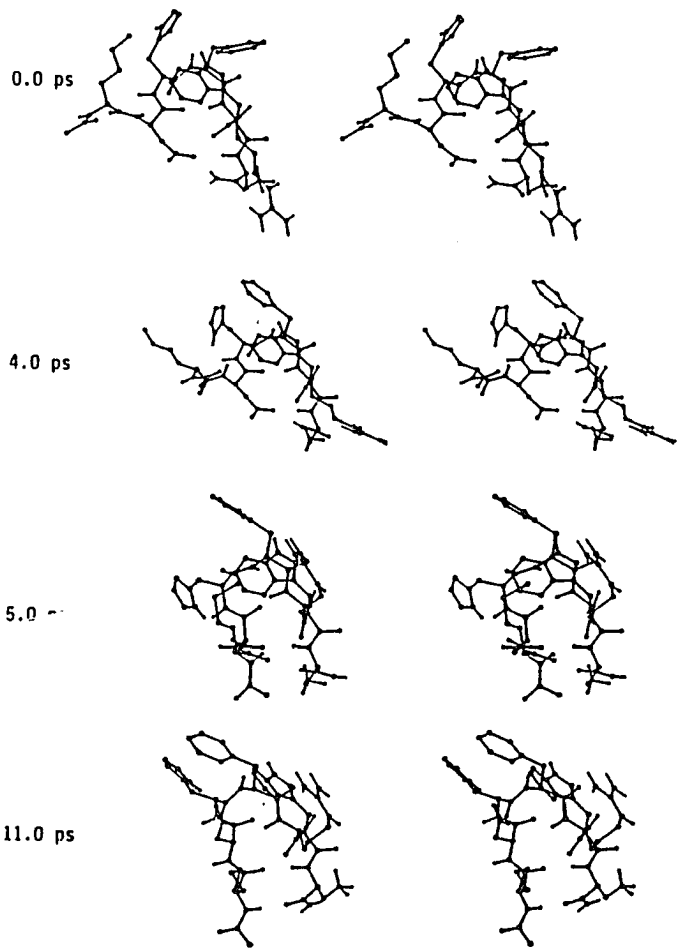

Fig. 22. Stereoviews of Ac-[Nle^4, Asp^5, D-Phe^7, Dpr^{10}]α-MSH$_{4-10}$-NH$_2$ in four conformations generated in a molecular dynamics simulation (time along molecular dynamics trajectory given in picoseconds).

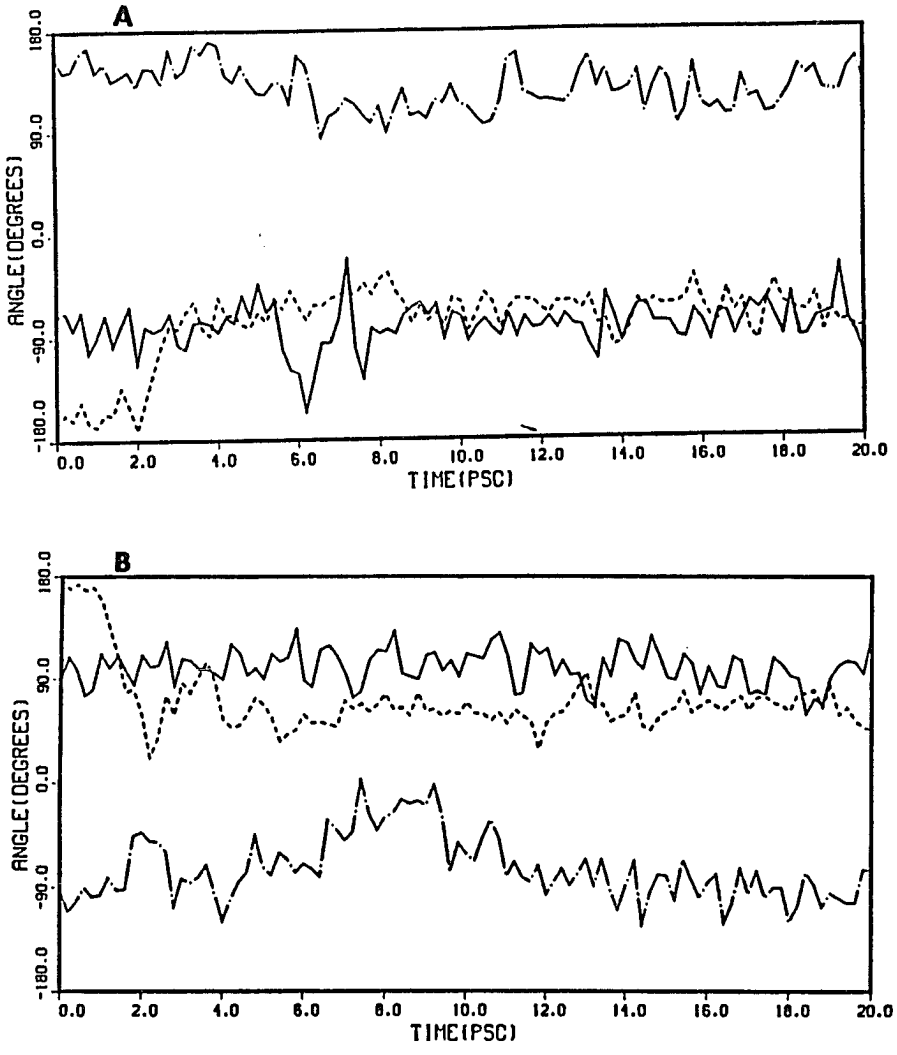

Fig. 23a. Plot of the torsion angles χ^1---, ϕ____, and ψ_._, as functions of the time elapsed in the dynamic simulations for A; His^6, B; D-Phe^7 in Ac-[Nle^4, Asp^5, D-Phe^7, Dpr^{10}]α-MSH$_{4-10}$-NH$_2$.

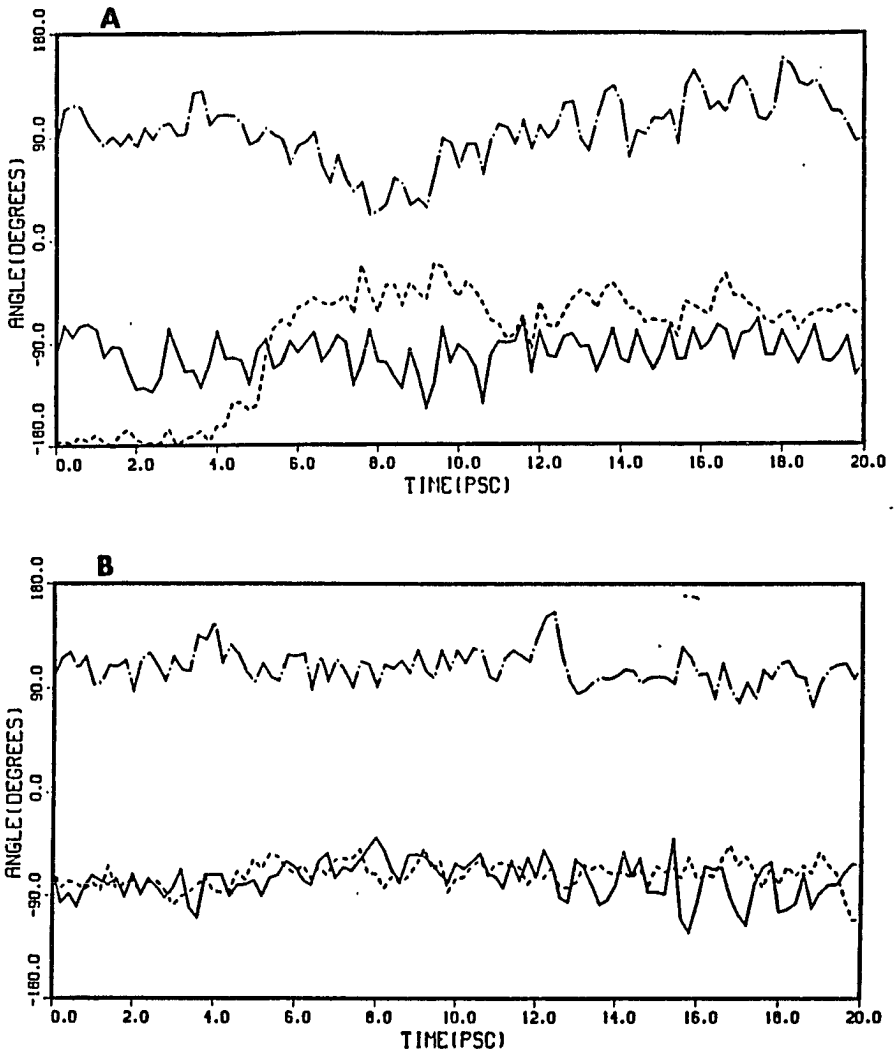

Fig. 23b. Plot of the torsion angles χ^1---, ϕ____, ψ_._, as functions of the time elapsed in the dynamic simulations for A; Arg^8, B; Trp^9 in Ac-[Nle^4, Asp^5, D-Phe^7, Dpr^{10}]α-MSH_{4-10}-NH_2.

Thus, an ordered conformation of this peptide was observed over most of the dynamic simulation. The arrangement of the Arg^8 side chain in gauche(-) (g^-) place it away from the backbone of the peptide. This arrangement is in parallel to the result obtained by the effect of temperature on the chemical shift of the guanidino δNH group (Table XIV, Ch.4).

For Trp^9, the ϕ and ψ angles were fixed at around -90° and +90°, respectively. This conformation was comparable to that observed for Trp^9 in peptide I. The χ^1_9 in case of peptide II is fixed at gauche(-) (g^-) which is different in peptide I, where it was fixed in a trans form. The perferred gauche (g^-) for Trp^9 over the more stable trans may be related to a preferred arrangement of the C-terminal amino acid, Dpr in such a way as to favor this conformation for the Trp^9 residue.

B. Peptide IV: Ac-[Nle^4, $\overline{Asp^5, \underline{D}\text{-}Phe^7, Dpr^{10}}$]α-$MSH_{4-10}$-$NH_2$.

In analyzing the dynamic simulation for Ac-[Nle^4, Asp^5, $\underline{D}$-Phe^7, Dpr^{10}]α-MSH_{4-10}-NH_2, four substructures were selected. The general characters and major factors related to the conformation of this peptide will be explained in the following paragraphs.

Conformer I (0 ps).

This conformer is about 12 Kcal/Mol above the minimal energy in the dynamic simulation (Table XXX). Energy minimization gave a conformer with an energy of about -20 Kcal/mol. The difference in backbone dihedral angles was about 2 to 20° for the dynamic and the energy minimized structure. The conformation for acids His^6, Phe^7, Arg^8, and Trp^9

was that of a distorted type II or type II β-turn, depending on the residues under consideration. Two major properties of this conformer can be seen by looking at the χ^1_7 which is g^+ and that which is in a cis conformation. These conformational changes are the opposite of those in peptide II, which may explain the 100 fold reduction in the biological activity of peptide IV relative to peptide II. The g^+ conformation of χ^1_7 were confirmed by the NMR study, but the ω_4 conformation is still under investigation. This pattern of arrangements were noticed in all the conformers of peptide IV. The only hydrogen bonding in conformer I was $Arg^8(NH)...Asp^5$ which persisted during the minimization. The stereoview structure of conformer I is shown in Figure 24.

Conformer II (5 ps).

This conformer has a lower energy than conformer I (Table XXXI), with conformational changes leading to the β-turn structure, and there is more hydrogen bonding in this conformer than conformer I. The major hydrogen bonds were $Dpr^{10}(NH)...His^6(N^{im})$, Dpr^{10}(C-terminal NH_2)... $His^6(N^{im})$, and $Dpr^{10}(\beta NH)...His^6(N^{im})$ in the dynamic structure, which were maintained in the minimized structure with an additional hydrogen bond between $Arg^8(N^{\eta}H)...Nle^4$. This latter hydrogen bond may be related to the NMR result which showed the involvement of δNH of guanidino group in Arg in intramolecule hydrogen bonding (Table XVI, Ch.4). The stereoview of this conformer is given in Figure 24.

TABLE (XXX). Total Energy and Energy Components of the Minimum Energy Structures Underlying the Dynamic Trajectory of Ac-[Nle^4, Asp^5, D-Phe^7, Dpr^{10}]α-MSH$_{4-10}$-NH$_2$.

Time (ps)	Potential Energy		
	Valence[a]	Nonbonded[b]	Total (Δ_{min})[c]
0	82.50	-37.72	44.78(12.29)
1	91.00	-44.14	46.86(14.37)
2	85.18	-50.04	35.14(02.65)
3	86.75	-41.81	44.94(12.45)
4	95.51	-49.32	46.19(13.70)
5	94.20	-50.82	43.38(10.89)
6	90.42	-46.85	43.57(11.08)
7	91.74	-48.65	43.09(10.60)
8	106.47	-54.02	52.45(19.96)
9	89.98	-49.29	40.69(08.20)
10	91.75	-50.34	41.41(08.92)
11	90.02	-48.54	41.48(08.99)
12	85.55	-53.06	32.49(00.00)
13	90.94	-56.80	34.15(01.66)
14	85.96	-48.00	37.96(05.47)
15	83.48	-48.25	35.23(02.74)
16	92.04	-48.61	43.43(10.94)
17	94.79	-45.43	49.36(16.87)
18	86.34	-50.58	34.76(03.27)
19	96.39	-48.47	47.92(15.43)
20	94.07	-43.36	50.71(18.22)

[a]The valence term represents deformations of the internal coordinates with respect to the minimized starting structure.

[b]The nonbonded refers to the van der Waals, electrostatic potential and hydrogen bonds energies.

[c]Δ_{min} represents the difference in energy between any structure and the minimum structure.

Table (XXXI). Energy and Energy Components of Dynamic Generated Conformers of Cyclic Ac-[Nle^4, Asp^5, D-Phe^7, Dpr^{10}]α-MSH$_{4-10}$-NH$_2$.

[a]Energy Components (Kcal/Mol)	Conformer I 0 PS Dyn (Min)	Conformer II 5 PS Dyn (Min)	Conformer III 12 PS Dyn (Min)	Conformer IV 17 PS Dyn (Min)
E Total	44.8(-19.5)	43.3(-28.1)	32.6(-30.5)	49.4(-28.0)
E Bonds	20.9(1.1)	20.8(1.5)	16.7(1.5)	21.3(1.3)
E Angles	34.2(18.7)	39.4(18.5)	42.1(20.4)	42.3(20.0)
E Dihedrals	27.3(9.0)	33.8(11.7)	26.8(10.0)	30.9(10.1)
E VDW	-37.2(-47.5)	-46.5(-53.2)	-48.0(-55.1)	-44.0(-54.0)
E Elec	-0.5(-0.8)	-0.5(-0.7)	-0.5(-0.4)	-0.3(-0.7)
E HB	-0.04(-0.05)	-3.9(-5.9)	-4.6(-7.2)	-1.3(-4.8)

[a]See Table XIX for notation.

Conformer III (12 ps):

This conformer has the lowest total energy compared to the other substructures which resulted in the dynamic simulation of peptide IV (Table XXXI). In addition, conformer III minimized to the lowest energy. The involvement of Dpr^{10} in several hydrogen bonds through its amide NH or C-terminal amide with the His^{4} imidazole nitrogen is related to the adaptation of this peptide in an order structure during the dynamic simulation. Also, an additional hydrogen bond (Arg^{8}(NH)...Nle^{4}) is involved in stabilizing this conformer. The Dpr^{10}(NH)...His^{6}(N^{im}) hydrogen bonding is related to a side chain backbone interaction which introduces a stabilization of the peptide conformation (Rose, et al., 1985). The stereoview of this conformer is listed in Fig. 24.

Conformer IV (17 ps):

Although this conformer has about 10 to 7 Kcal/Mol more potential energy than conformers II and III, it minimized to the same energy as the other two conformers. The hydrogen bonding in this conformer is similar to the one we noticed in conformers III and II. In conformer IV, several hydrogen bonds exist: Arg^{8}(NH)...Asp^{5}, Dpr^{10}(C-terminal NH_2)...Trp^{9} and Nle^{4}(NH)...His^{6}(OC). The latter hydrogen bond may be related to the NMR result (Table XVI, Ch. 4) which showed the involvement of the Nle^{4} amide in intramolecular hydrogen bonding. The minimized

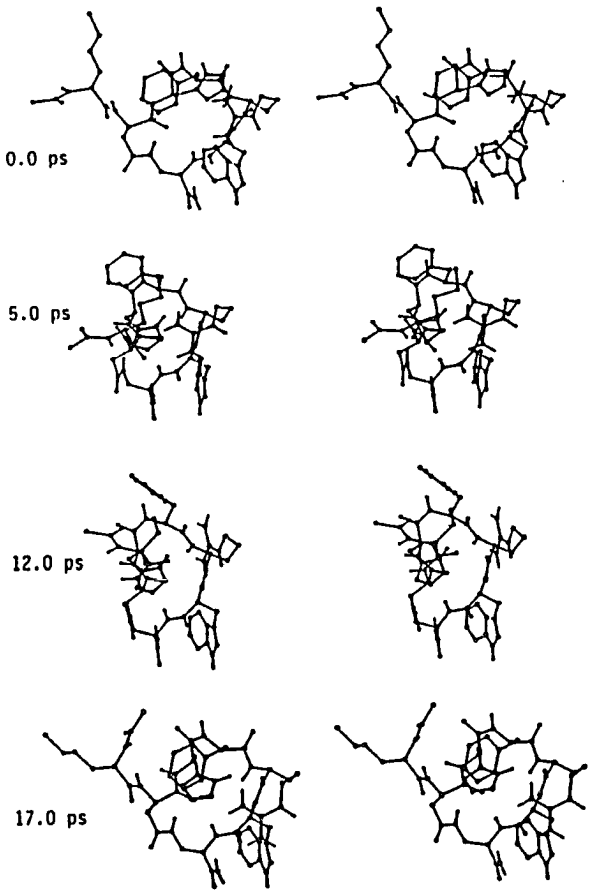

Fig. 24. Stereoviews of Ac-[Nle^4, Asp^5, D-Phe^7, Dpr^{10}]α-MSH$_{4-10}$-NH$_2$ in four conformations generated in a molecular dynamics simulation (time along molecular dynamics trajectory given in picoseconds).

structure of conformer IV has several new hydrogen bonds, e.g. $His^{6}(N^{im})...Arg^{8}$, $Arg^{8}(NH)...Asp^{5}$, $Arg^{8}(NHg_{2})...Asp^{5}$, $Dpr^{10}(NH_2$ amide)... $His^{6}(N^{im})$ and $Dpr^{10}(\beta NH)...His^{6}(N^{im})$. These hydrogen bonds were in the range of -0.2 to -1.6 Kcal/Mol. The NMR study showed that the Nle^{4}, Dpr^{10} and His^{6} residues are involved in intramolecular hydrogen bonds (Table XVI, Ch. 4). The stereo-structure of conformer IV is shown in Fig. 24.

Correlations Between the Theoretical and the NMR Based Conformational Structures of Ac-[Nle^{4}, Asp^{5}, D-Phe^{7}, Dpr^{10}]α-MSH_{4-10}-NH_2:

A comparison of the observed and calculated coupling constants for the ϕ angles in Table XXXIII, and the results were analyzed by multiple regression analysis. They showed that the NMR structure represents an average structure of the four major conformers. The closest conformer to the NMR structure is conformer III (Table XXXIII). This conformer is the lowest in its potential energy relative to the other structures (Table XXXI). Also, this conformer showed the same pattern of hydrogen bonding as was indicated by the NMR results (Table XVI, Ch. 4). A comparison of the ϕ angles of conformer III and the χ angles of its side chain groups indicated that the conformations from the calculations and from the NMR analysis of peptide IV (Table XVI and Table XVII, Ch. 4) are similar. Thus, this theoretically deduced structure is in a close relationship to that determined by the experimental approach using ^{1}H NMR. However, the NMR structure doesn't resemble only one type of conformer, but rather an average.

Table (XXXII). Conformational Parameters of Cyclic Ac-[Nle^4, Asp^5, D-Phe^7, Dpr^{10}]α-MSH$_{4-10}$-NH$_2$.

Residue	Angle (deg.)	Conformer I Dyn ^{0} PS (Min)	Conformer II Dyn ^{5} PS (Min)	Conformer III Dyn ^{12} PS (Min)	Conformer IV Dyn ^{17} PS (Min)
	φ	-83.1(-81.3)	-112.1(-83.0)	-82.3(-63.0)	-102.4(-112.9)
Nle	ψ	97.9(119.9)	103.4(104.9)	-15.3(-35.2)	-46.7(-50.0)
	χ^1	-65.1(-65.6)	-92.0(-69.5)	-75.2(-64.6)	-122.1(-64.1)
	φ	-94.9(-105.9)	-136.6(-125.7)	-66.8(-62.2)	-153.7(-118.0)
Asp	ψ	21.2(-42.9)	-59.4(-69.0)	-46.3(-51.3)	-30.0(-42.4)
	χ^1	-128.8(-167.3)	-114.9(-157.4)	-163.4(-162.5)	-144.3(-161.5)
	φ	-110.9(-117.1)	-130.4(-122.6)	-131.9(-133.6)	-118.3(-110.6)
His	ψ	100.1(112.2)	60.5(77.3)	89.3(84.8)	117.2(108.2)
	χ^1	-175.9(-169.6)	-80.7(-98.3)	-95.4(-94.5)	-71.8(-62.0)
	φ	91.2(90.7)	85.1(87.0)	76.5(68.0)	96.0(85.0)
D-Phe	ψ	-161.5(-151.7)	-139.4(-134.4)	-139.8(-141.57)	-129.3(-131.2)
	χ^1	106.9(78.0)	55.8(57.4)	76.9(64.2)	67.2(72.8)
	φ	-134.5(-99.4)	-101.1(-107.5)	-78.9(-85.3)	-130.3(-131.0)
Arg	ψ	53.8(-50.9)	-119.1(-69.4)	-76.0(-78.4)	-63.1(-58.3)
	χ^1	-69.6(-66.6)	-57.4(-60.9)	-72.0(-68.6)	-61.3(-44.0)
	φ	-147.5(-170.4)	-137.6(-152.0)	-167.7(-149.0)	-160.3(-158.5)
Trp	ψ	133.9(142.2)	121.0(130.7)	146.2(123.7)	144.0(126.8)
	χ^1	178.9(-177.6)	-130.2(-168.9)	-175.4(-179.3)	175.3(179.1)
	φ	65.5(-79.0)	-81.4(-109.6)	-140.8(-112.6)	-111.9(-76.0)
Dpr	ψ	-29.2(-57.3)	-28.8(-46.0)	-57.4(-45.1)	-36.0(-53.1)
	χ^1	-55.3(-66.8)	-46.2(-58.4)	-52.0(-54.8)	-53.2(-60.6)

Table (XXXIII)[a]. Theoretical and Experimental Determined Coupling Constants for Different Residues of Cyclic Ac-[Nle^4, Asp^5, D-Phe^7, Dpr^{10}]α-MSH$_{4-10}$-NH$_2$. The R^2 of Regression Analysis is also listed.

Residue	Conformer I	Conformer II	Conformer III	Conformer IV	NMR
Nle	7.1 (6.9)	9.6 (7.1)	7.0 (4.6)	9.0 (6.6)	7.20
Asp	8.4 (9.3)	9.1 (9.6)	5.0 (4.5)	7.5 (9.7)	7.20
His	9.5 (9.7)	9.5 (9.7)	9.4 (9.3)	9.7 (9.5)	8.2
D-Phe	8.0 (8.0)	7.4 (7.6)	6.3 (5.2)	8.5 (7.3)	5.0
Arg	9.3 (8.8)	9.0 (9.4)	6.6 (7.4)	9.5 (9.4)	5.5
Trp	8.2 (5.4)	9.1 (7.1)	5.7 (8.0)	6.7 (6.9)	9.0
Dpr	4.9 (6.6)	6.9 (9.5)	8.8 (9.6)	9.6 (6.2)	8.20
R^2 Dyn (Min)	0.1 (0.17)	0.1 (0.02)	0.1 (0.27)	0.1 (0.06)	

[a]See Table XXI for notation

Close examination of the backbone and side-chain torsion angles of the four residues, His^6, D-Phe^7, Arg^8 and Trp^9 provided much insight into the behavior of this peptide along the dynamic trajectory. The results of this study are shown in Fig. 25a, 25b. The comparison of the behavior of the ϕ, ψ and χ angles of peptides II and IV can help explain the changes in biological activity of these peptides (Table V, Ch. 2 and Table IX, Ch. 3).

The ψ angle of the His^6 experienced the least change of any major transition along the dynamic trajectory (Figure 25a). This angle is mostly locked in one type of conformation which is related to a β-turn structure (+120 to 0). The same thing is noticed for the ϕ angle which fluctuated around -90°. This value also is in close approximation to the β-turn conformation (-60 or -90). The major change in the conformation of this residue was in the fluctuation of the χ^1_6 angle between trans and gauche(-) (g^-), and the cis arrangement of ω_6 dihedral angle. These changes in the side chain and backbone may have a tremendous effect on the biological activity of the peptide hormone. It has been noticed that several backbone conformations of single peptide hormone may have only one type of side chain conformation (Manavalan and Momany, 1981). Studies of several peptide hormones have shown that the correlation between side chain conformation and biological activity is more reliable than the relationship between backbone and biological response (Rose et al., 1985, Hruby, 1982).

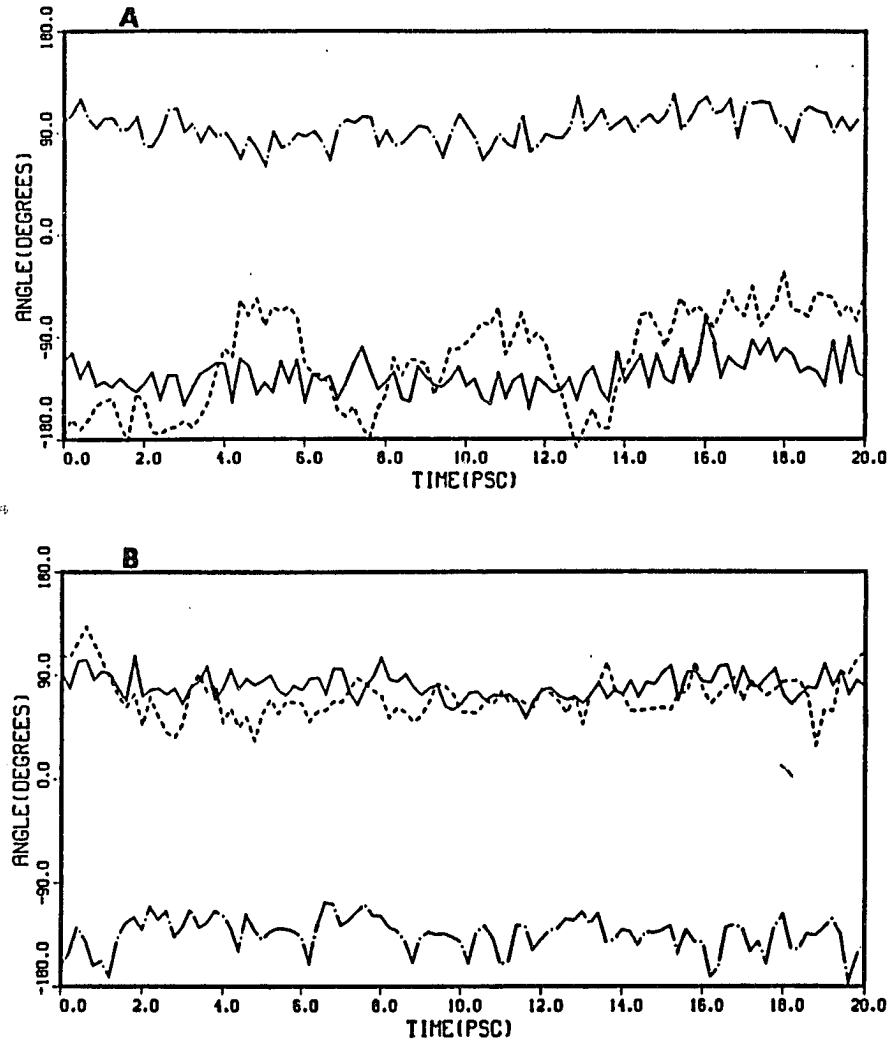

Fig. 25a. Plot of the torsion angles χ^1---, ϕ____, ψ_._, as functions of the time elapsed in the dynamic simulations for A; His^6, B; D-Phe^7 in Ac-[Nle^4, Asp^5, D-Phe^7, Dpr^{10}]α-MSH$_{4-10}$-NH$_2$.

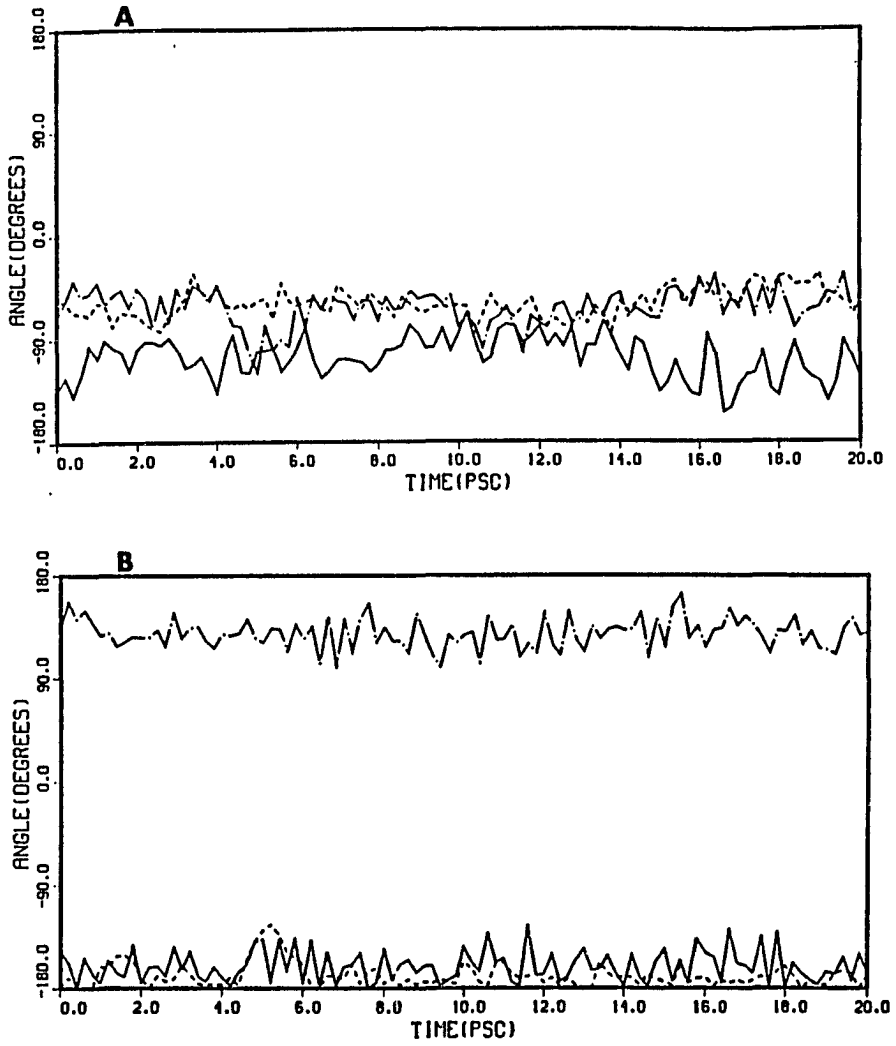

Fig. 25b. Plot of the torsion angles χ^1---, ϕ____, ψ_._, as functions of the time elapsed in the dynamic simulations for A; Arg^8, B; Trp^9 in Ac-[Nle^4, Asp^5, D-Phe^7, Dpr^{10}]α-MSH_{4-10}-NH_2.

In the case of His^6 in peptide IV, the story is different since the backbone conformation is stable relative to the side-chain conformations. The change in conformation of this peptide is due to the ring constraint (20 membered ring) which brings the His^6 and Trp^9 side-chain groups close to each other (Fig. 24). Thus the molecule tries to relieve the strain by changing the side chain conformation of one of the interacting amino acids. This is not the case for peptide II, which has no constraint due to cyclization (it is a linear peptide), and where the His^6 side-chain and ω_4 angle are locked in a trans form throughout the dynamic simulation. The large change in biological activity between the linear and cyclic peptide may be attributed to these kinds of conformational changes. The D-Phe^7 residue is also locked in one type of conformation for both its ϕ and ψ angles. The side chain χ^1_7 is locked into a gauche(+) (g^+) conformation. This type of side chain conformation appears to be related to a reduction in the biological activity of this peptide relative to the linear peptide which has a mixture of trans and gauche(+) (g^+) conformations. Again, the presence of only one type of conformation in peptide IV also is related to the constraint experienced by the molecule due to the side-chain to side-chain cyclization. This technique of using the constraint as a way to fix the molecule in one type of conformation over the other is well documented in the literature (Sakikibara, 1986; Kopple et al., 1984; Mosberg et al., 1982; Kessler et al., 1985; Kazmierski and Hruby, 1987).

The conformation of Arg^8 is again different from that of the linear analogue (peptide II). The ψ angle is transformed from 90° to

about -70° with transitions of χ^1_8 from its fluctuation value between trans (-180°) and gauche(-) (g^- 60°) to only a gauche(-) (g^-) type of conformation. There is no change in the ϕ angle for the linear and the cyclic structure. There is another factor which may be related to the effect of cyclization on the biological response of peptide IV. The Trp^9 residue has no change in its ψ angle in the linear and cyclic peptides, but does have transitions of its ϕ and χ^1_9 conformation from -90° in the linear peptide to -180° in the cyclic peptide. This latter conformation is also favored in most peptide structures (Rose et al., 1985). The locking of Trp in this extended conformation is in parallel with the NMR result which showed that Trp residue is highly exposed to solvent with $\Delta\delta/\Delta T$ of 5.2×10^{-3} in DMSO (Table XVI, Ch. 4). This again may be related to an unfavorable conformation of this peptide which reduces its biological activity by a factor of about 100 (Table V, Ch. 2 and Table IX, Ch. 3).

Conclusions:

From the preceeding studies, the following points can be made:

(1) The dynamic simulation of the conformational history of the four molecules over 20 picoseconds demonstrates a drastic reduction in flexibility of the constrained cyclic analogues relative to their linear analogues.

(2) Essentially one conformational family emerged for the cyclic analogues.

(3) Despite the variations in backbone conformation, the orientations of side chains were highly conserved from structure to structure except in the cases where a highly active molecule converted to a very inactive one upon cyclization or substitutions.

(4) High melanotropic activity with prolongation requires the locking of D-Phe side chain in a trans conformation; while the low activity is characterized by a gauche(+) (g^+) conformation of the D-Phe side chain.

(5) The correlation between the dynamic and the NMR structures is not very high because of the nature of the NMR technique which gives an average structure; many results from the NMR measurements are confirmed through the analysis of the dynamic simulation.

(6) To further correlate the theoretical structure with the experimental will require elaborate experiments.

(7) The search for a single bioactive peptide conformation is frustrated by the sensitivity of the peptide conformation to its environment and the likelihood that different active analogues have different backbone conformations while retaining

essentially the same side chain arrangements. In addition, the presence of multiple receptors or biological variation toward the same peptide can add another difficulty.

(8) Dynamic simulation and energy minimization is a powerful technique which can give a wealth of information necessary to understand the correlation between conformation and biological activity of peptide hormones.

REFERENCES

Allen, B. M. (1916). Science, 44, 755.

Akiyama, K., Yamamura, H. I., Wilkes, B. C., Cody, W. L., Hruby, V. J., Castrucci, A. M. L. and Hadley, M. E. (1984). Peptides, 5, 1191.

Arold, H. (1975). J. Prakt. Chem., 317, 682.

Aue, W. P., Bartholdi, E., and Ernst, R. R. (1976). J. Chem. Phys., 64, 2229.

Bats, J. W., Fuess, H., Kessler, H., and Schuck, K. (1980). Chem. Ber., 113, 520.

Bax, A. (1982). In "Two-Dimensional Nuclear Magnetic Resonance in Liquids." Delft University Press, Riedel, Dordrecht, Netherlands.

Bax, A. (1984). In "Topics in Carbon-13 NMR Spectroscopy," Vol. 4 (G. C. Levy, ed.), pp. 199. Wiely, New York.

Bax, A., and Lerner, L. (1986). Science, 232, 960.

Benfey, B. J., and Purvis, J. L. (1955). J. Amer. Chem. Soc., 77, 5167.

Benn, R., and Gunther, H. (1983). Angew. Chem. Int. Ed. Engl., 22, 350.

Bodenhausen, G. (1982). In "Progress in Nucl. Magn. Reson. Spectrosc." Vol. 14, pp. 137. Pergamon Press, London.

Bosch, C., Brown, L. R., and Wuthrich, K. (1980). Biochim. Biophys. Acta., 603, 298.

Bradley, S. F., Daleveda, W. J., Arison, B. H., Freidinger, R. M., Nutt, R. F. and Veber, D. F. (1983). In "Peptides: Synthesis, Structure and Function," (V. J. Hruby and D. H. Rich, eds.), pp. 127. Pierce Chemical Co., Rockford, Il.

Brady, S. I., Varga, L. S., Freidinger, M. R., Schwenk, A. D., Mendlowski, M., Holly, W. F. and Veber, F. D. (1979). J. Org. Chem., 18, 3101.

Brooks, B. R., Bruccoleri, R. E., Olafson, B. D., States, D. J. Swaminathan, S., and Karplus, M. (1983). J. Comp. Chem., 4, 187-217.

Bundi, A., and Wuthrich, K. (1979). Biopolymers, 18, 285.

Bystrov, V. F. (1976). in "Progress in Nucl. Magn. Reson. Spectrosc." Vol. 10, pp. 41. Pergamon Press, London.

Christensen, T. (1979). in "Peptides, Structure and Biological Function," (E. Gross and J. Meienhofer, eds.), pp. 385-388. Pierce Chemical Co., Rockford, Il.

Cody, W. L., Mahoney, M., Knittel, J. J., Hruby, V. J., Castrucci, A. M. de L. and Hadley, M. E. (1984). J. Med. Chem., 28, 583.

Cody, W. L. (1985). Ph.D. Dissertation. University of Arizona.

Cody, W. L., Wilkes, B. C., Muska, B. J., Hruby, V. J., Castrucci, A. M. de L. and Hadley, M. E. (1983). J. Med. Chem., 27, 1186.

Cody, L. W., Hadley, M. E. and Hruby, V. J. (1987). in "Melanotropin Peptides: Mechanisms of Actions and Biomedical Applications," Vol. (M. E. Hadley, ed.), pp. . CRC Press, (in press).

Dauber, P., Goodman, M., Hagler, A. T., Osguthorpe, D., Sharon, R. and Stern, p. (1981). in "ACS Symposium on Supercomputers in Chemistry," (P. Lykos and I. Shavitt, eds.) pp. 161. ACS Symp. Series 173.

de Leeuw, F. A. A. M., and Altona, C. (1982). Int. J. Pept. Protein Res., 20, 120.

Donzel, B., Rivier, J. and Goodman, M. (1977). Biopolymers, 16, 2587.

Elizabeth, E. S., Cody, W. L., Abdel-Malek, Z., Hadley, M. E., and Hruby, V. J. (1986). Biopolymers, 25, 2029.

Farmer, P. S. (1980). in "Drug Design," Vol. 10 (E. J. Ariens, ed.), pp. 1198. Academic Press, New York.

Ferretti, J. A. and Padillo, L. (1969). Biopolymers, 7, 155.

Freeman, R., and Morris, G. A. (1979). Bull. Magn. Reson., 1, 5.

Fujii, T. and Sakakibara, S. (1974). Bull. Chem. Soc. Japan., 47, 3146.

Gear, C. W. (1971). in "Numerical Initial Value Problems in Ordinary Differential Equations," pp. . Prentice-Hall, England Cliffs, N.J.

Glickson, J. D. (1975). in "Peptides: Chemistry, Structure and Biology," (R. Walter and J. Meienhofer, eds.), pp. 787. Ann Arbor Science, Ann Arbor, Mich.

Haasnoot, C. A. G., de Leeuw, F. A. A. M., and Altona, C. (1980). Tetrahedron, 36, 2783.

Hadley, M. E., Anderson, B., Heward, C. B., Sawyer, T. K., Hruby, V. J. (1981). Science, 213, 1025.

Hadley, M. E., and Bugnara, J. T. (1975). Amer. Zool., Suppl. 1, 15, 81.

Hadley, M. E. and Bagnara, J. T. (1969). Endocrinology, 84, 69.

Hadley, M. E., Wood, S. H., Lemus-Wilson, A. M., Dawson, B. V., Levine, N., Dorr, R. T., and Hruby, V. J. (1987). Life Sci., 40, 1889.

Hadley, M. E., Heward, C. B., Hruby, V. J., Sawyer, T. K., and Yang, Y. C. S. (1981). In "Peptides of the Pars Intermedia," Vol. 81 (D. Evered, and G. Lawrenson, ed.), pp. 242, Ciba Found. Symp., Pitman Medical, London.

Hagler, A. T. (1985). In "The Peptides: Conformation in Biology and Drug Design, Vol. 7 (V. J. Hruby, ed.), pp. 214. Academic Press, Inc. New York.

Halstrom, J. and Klostermeyer, H. (1968). Liebigs Ann. Chem., 715, 208.

Harris, J. I., and Lerner, A. B. (1957). Nature, 179, 1346.

Harris, J. I. (1959). Biochem. J., 71, 451.

Herbert, E., Budarf, M., Phillips, M., Rosa, P., Policustro, P., Oates, E., Roberts, J. L., Seidah, N. G., and Chretien, M. (1980). Ann. N.Y. Acad. Sci., 343, 79.

Higashijima, T., Wakamatsu, K., Milon, A., Okada, A., and Miyazawa, T. (1987). In "Japanese Peptide Symposium.?

Higuchi, N., and Kyogoku, Y. (1981). Biopolymers, 20, 2203.

Hofmann, K. (1974). Hanb. Physiol., Sect. 7, Endocrinol., 2, 29.

Hruby, V. J. and Hadley, M. E. (1986). In "Design and Synthesis of Organic Molecules Based on Molecular Recognition," (G. van Binst, ed.), pp. 269. Proceedings of the XVIIIth Solway Conference on Chemistry. Springer-Verlay, Heidelberg.

Hruby, V. J., Sawyer, T. K., Yang, Y. C. S., Bergman, M. D., Hadley, M. E. and Heward, C. B. (1980). J. Med. Chem., 23, 1432.

Hruby, V. J., Muscio, F., Groginsky, C. M., Gitu, P. M., Saba, D., and Chan, W. Y. (1973). J. Med. Chem., 16, 624.

Hruby, V. J., Upson, D. A., and Agarwal, N. S. (1977). J. Org. Chem., 42, 3552.

Hruby, V. J. (1982). Life Sci., 31, 189.

Hruby, V. J. (1985). Trends Pharm. Sci., 6, 259.

Hruby, V. J. in "Conformationally Directed Drug Design," (J.A. Vida and M. Gordon, eds.), pp. 9-27. ACS Symposium Series, No. 251, Washington, D.C.

Hruby, V. J., Wilkes, B. C., Cody, W. L., Sawyer, T. K., and Hadley, M. E. (1984). Peptide and Protein Reveiws, 3, 1.

Hruby, V. J. (1981). in "Perspectives in Peptide Chemistry," (A. Eberle, R. Geiger, and T. Wieland, eds.), pp. 207. Karger, Basel.

Hruby, V. J. and Mosberg, H. (1982). Peptides, 3, 329. New York.

Huntington, T., and Hadley, M. E. (1970). Endocrinology, 66, 599.

Ikeda, K. W., Hamuguchi, K., Kubo, K., and Yajima, H. (1971). Chem. Pharm. Bull. JPN., 19, 1815.

Jackman, L. M. (1975). in "Dynamic Nuclear Magnetic Resonance Spectroscopy," (L. M. Jackman and F. A. Cotton, eds.), pp. 203. Academic Press, New York.

Jardetzky, O. (1980). Biochim. Biophys. Acta, 621, 227-232.

Kaiser, E., Colescott, R. L., Bossinger, C. D., and Cook, P. I. (1970). Anal. Biochem., 34, 595.

Karplus, M. and McCammon, J. A. (1981). CRC Crit. Rev. Biochem., 9, 293.

Kessler, H. (1985). in "The Peptides: Conformation in Biology and Drug Design," Vol. 7 (V. J. Hruby, ed.), pp. 438. Academic Press Inc., New York.

Kessler, H. (1970). Angew. Chem. Int. Ed. Engl., 9, 219.

Kessler, H., and Bermel, W. (1985). in "Methods in Stereochemical Analysis. Applications of NMR Spectroscopy to Problems in Stereochemistry and Conformational Analysis," Vol. 6 (A. PO. Marchand and Y. Takeuchi, eds.), pp. 179-205.

Kessler, H. (1982). Angew. Chem. Int. Ed. Engl., 21, 512.

Kessler, H., Zimmermann, G., Forster, H., Oepen, E. J., and Sheldrick, W. S. (1981). Angew. Chem. Int. Ed. Eng., 20, 1053.

Knittel, J. J., Sawyer, T. K., Hruby, V. J., and Hadley, M. E. (1983). J. Med. Chem., 28, 125.

Kopple, K. D. (1972). J. Pharm. Sci., 61, 1345.

Kopple, K. D., Parameswaran, K. N., and Yonan, J. P. (1984). J. Am. Chem. Soc., 106, 7212.

Kurithara, T., and Suzuki, K. (1955). J. Pharm. Soc. Japan, 75, 1269.

Lebl, M., Cody, W. L., Wilkes, B. C., Hruby, V. J., Castrucci, A. M. de L. and Hadley, M. E. (1984). Int. J. Peptide Protein Res., 24, 472.

Lee, T. H., and Lerner, A. B. (1956). J. Biol. Chem., 221, 943.

Lerner, A. B., and Lee, J. L. (1955). J. Amer. Chem. Soc., 77, 1066.

Lerner, A. B., Wright, M. R. (1960). Methods Biochem. Analy., 8, 295.

Liepkaula, I., Skujina, A., Romanovskii, P. Ya., Porunkevich, E. A., Ratkevich, M. P., Vosekalna, I., Gailite, E. and Cipens, G. (1985). Bioorg. Khim., 11, 1157.

Liepkaula, I., Skujins, A., Romanovskii, P. Ya., Porunkevich, E. A., Ratkevich, M. P. and Cipens, G. (1984). Bioorg. Khim., 10, 1326.

Liepkaula, I., Skujins, A., Romanovskii, P. Ya., Porunkevich, E. A., Ratkevich, M. P. and Cipens, G. (1984). Bioorg. Khim., 10, 807.

Loudon, G. M., Radhakrishna, A. S., Almon, M.R., Blodgett, J. K., and Boutin, H. R. (1984). J. Org. Chem., 49, 4272.

Mains, R. E., and Eipper, B. A. (1980). Ann. N.Y. Acad. Sci., 343, 94.

Manavalan, P., and Momany, F. A. (1981). Int. J. Pept. Protein Res., 18, 256.

Matsueda, G. R. (1982). Int. J. Peptide Protein Res., 20, 26.

McCammon, and Karplus, M. (1980). Ann. Rev. Phys. Chem., 31, 29.

Medzihradszky, K. (1982). Medicinal Res. Rev., 2, 274.

Medzihradszky, K. (1976). Recent Dev. Chem. Nat. Carbon. Compd., 7, 203.

Mosberg, H. I., Hurst, R., Hruby, V. J., Gee, K., Yamamura, H. I., Galligan, J. J., and Burks, T. F. (1983). Proc. Natl. Acad. Sci. USA, 80, 5871.

Mosberg, H. I., Hurst, R., Hruby, V. J., Gallegan, J. J., Burks, T. F., Ges, K., and Yamamura, H. I. (1982). Biochem. Biophys. Res. Commun., 106, 506.

Nikiforovich, G. V., Rozenblit, S. A., Shenderovich, M.D., and Cipens, G. I. (1984). FEBS, 170, 315.

O'Donohue, T. L. and Jacobowitz, D. M. (1980). In "Polypeptide Hormone," (R. F. Beers, and E. G. Bassett, eds.), pp. 203. Raven, New York.

Opella, S. J., and Gierasch, L. M. (1985). In "The Peptides: Conformation in Biology and Drug Design," Vol. 7, (V. J. Hruby, ed.), pp. 405, Academic Press, Inc. New York.

Porath, J. Roos, P. Landgreb, F. W., and Mitchell, G. M. (1955). Biochim. Biophys. Acta., 17, 598.

Rawson, B. J., Feeney, J., and Kimber, B. J. (1982). J. Chem. Soc. Perkin Trans., 11, 1471.

Richardson, J. S. (1981). Adv. Protein. Chem., 34, 167-339.

Roos, P. (1956). Acta. Chem. Scand., 10, 1061.

Sawyer, T. K. (1981). Ph.D. Dissertation. University of Arizona.

Sawyer, T. K., Hruby, V. J., Wilkes, B. C., Draelos, M. T., Hadley, M. E., and Bregsneider, J. (1982). J. Med. Chem., 25, 1022.

Sawyer, T. K., Hruby, V. J., Darman, P. S. and Hadley, M. E. (1982). Proc. Natl. Acad. Sci. U.S.A., 73, 1751.

Sawyer, T. K., Sanfilippo, P. J., Hruby, V. J., Engel, M. H., Heward, C. B., Burnet, J. B., and Hadley, M. E. (1980). Proc. Natl. Acad. Sci. U.S.A., 77, 5754.

Sewart, J. M., Pena, C., Matsueda, G. P., and Harris, K. (1976). In "Peptides, Proceedings of the European Peptide Symposium," (A. Loffet, ed.), 14th, Wepron, Belgium, Apr. 11-17, pp. 285-290 Editions de l'Universite de Bruxelles, Brussels.

Shizume, A. B., Lerner, A. B., and Fitzpatrick, T. B. (1954). Endocrinology, 54, 553.

Smith, J. A., and Pease, L. G. (1980). CRC Crit. Rev. in Biochem., 8, 315.

Smith, P. E. (1916). Science, 44, 280.

Spatola, A. F. (1983). In "Chemistry and Biochemistry of Amino Acids, Peptides and Proteins," Vol. 7 pp. 167.

Stewart, J. M. and Young, J. D. (1984). "Solid Phase Peptide Synthesis," (2nd. Ed.). Pierce Chemical Co., Rockford, Il.

Strothers, R. S., River, J. and Hagler, A. T. (1984). In "Conformationally Directed Drug Design," (J. Vida and M. Gordon, eds.), pp. . ACS, Washington, D.C.

Swaab, D. F. and Visser, M. (1977). In (Frontiers in Hormone Research," Vol. 4 (J.H. Tilders, D.F. Swaab and T.B. van Wimersma eds.), pp. 179. S. Karger, Bassel.

Thompson, K. F., and Gierasch, L. M. (1984). J. Am. Chem. Soc., 106, 3648.

Tonelli, A. E., and Bovey, F. A. (1970). Macromolecules, 3, 410.

Upson, D. A. and Hruby, V. J. (1976). J. Org. Chem., 41, 1353.

van Nipson, J. W., and Greven, H. M. (1982). Pharmac. Ther., 16, 67.

Vida, J. A., and Gordon, M. (1984). "Conformationally Directed Drug Design. Peptides and Nucleic Acids as Templates or Targets,". ACS Symposium SEries 251, Washington, D.C. pp. 1.

Waki, M., Kitajima, Y., and Izumiya, N. (1981). Synthesis, 266.

Wieland, T. H. and Birr, C. H. (1972). Liebigs Ann. Chem. 715, 136.

Wilkes, B. C. (1985). Ph.D. Dissertation. University of Arizona.

Wilkes, B. C., Sawyer, T. K., Hruby, V. J., and Hadley, M. E. (1983). Int. J. Peptide Protein Res., 22, 313-324.

Yajima, H., and Kawatani, H. (1974). In "Chemistry and Biochemistry of Amino Acids, Peptides and Proteins," Vol. 2 (B. Weinstein, ed.), pp. 39-143. Marcel Dekker, New York.

Yamashiro, D. (1964). Nature (London), 201, 76.

Yang, Y. C. S., Heward, C. B., Hadley, M. E., and Hruby, V. J. (1980). Int. J. Peptide Protein Res., 15, 130.